

**UNIVERSITY OF MODENA AND REGGIO EMILIA**

**PhD Program of Clinical and Experimental Medicine  
(CEM)**

**XXXIII Doctorate Cycle**

**Director of the PhD Program: Prof. Giuseppe Biagini**

***Post-status epilepticus* models of mesial temporal  
lobe epilepsy: newly reported aspects of brain  
injury, remodeling and neuroprotection**

**Supervisor:**

**Prof. Giuseppe Biagini**

**Co-supervisor**

**Prof. Nikolai V. Lukoyanov**

**PhD candidate**

**Ítalo Rosal Lustosa**

# Table of Contents

	Abbreviations.....	3
Chapter 1.....		6
	Abstract (English version).....	6
	Abstract (Italian version).....	8
Chapter 2.....		10
	General Introduction.....	10
	1. Epilepsy.....	10
	1.1. Definition of epilepsy.....	10
	1.2. Classification of epilepsy types.....	11
	1.3. Pathology of the mesial temporal lobe epilepsy.....	12
	2. Pharmacoresistance.....	14
	2.1. Hypothesis of the molecular drug target alteration.....	16
	2.2. Hypothesis of the efflux transporters.....	17
	3. In vivo models of epilepsy.....	18
	4. Drug development.....	23
	5. The basolateral nuclear complex of the amygdala and its cholinergic innervation.....	23
Chapter 3.....		29
	Aims and thesis overview.....	29
Chapter 4.....		31
	Neuroplasticity in cholinergic projections from the basal forebrain to the basolateral nucleus of the amygdala in the kainic acid model of temporal lobe epilepsy.....	31
Chapter 5.....		45
	A proline derivative-enriched fraction from <i>Sideroxylon obtusifolium</i> protects the hippocampus from intracerebroventricular pilocarpine-induced injury associated with status epilepticus in mice.....	45
Chapter 6.....		70
	Status epilepticus dynamics predicts latency to spontaneous seizures in the kainic acid model.....	70
Chapter 7.....		89
	Summary, conclusion and future perspectives.....	89
	References.....	90
	Acknowledgements.....	118

## Abbreviations

6-OHDA	6-Hydroxydopamine
aCSF	Artificial cerebrospinal fluid
AED	Antiepileptic drug
BBB	Blood-brain barrier
BF	Basal forebrain
BL	Basolateral nucleus of the amygdala
CA	Cornu Ammonis
CAE	Childhood absence epilepsy
CPu	Caudate-putamen, striatum
CSE	Convulsive status epilepticus
CSF	Cerebrospinal fluid
DAB	3,3-Diaminobenzidine tetrahydrochloride
DAPI	4',6'-diamine-2-phenyl-indol
DB	Diagonal band (of Broca)
DEn	Dorsal endopiriform nucleus
DG	Dentate gyrus
DH	Dentate hilus, hilus of the dentate gyrus
DRE	Drug resistant epilepsy
ECoG	Electrocorticogram
EEG	Electroencephalogram
GABA	Gamma-aminobutyric acid
GAD	Glutamic acid decarboxylase
GAT-1	GABA transporter-1
GFAP	Glial fibrillary acidic protein
HDB	Horizontal limb of the diagonal band (of Broca)
HS	Hippocampal sclerosis
I	Intercalate nucleus of the amygdala
ILAE	International League Against Epilepsy
IPI	Initial precipitating injury
IL-1	Interleukin 1
IL-6	Interleukin 6
i.c.v.	Intracerebroventricular
i.p.	Intraperitoneal

IR	Immunoreactive
i.v.	Intravenous
JME	Juvenile myoclonic epilepsy
KA	Kainic acid
MCPO	Magnocellular preoptic nucleus
MDR	Multidrug resistance-associated protein
MFB	Medial forebrain bundle
MS	Medial septum
MTLE	Mesial temporal lobe epilepsy
NCSE	Non-convulsive status epilepticus
NeuN	Neuron-specific nuclear protein
NMDA	N-methyl-D-aspartate
NMP	N-methyl-(2S,4R)-trans-4-hydroxy-L-proline
PBS	Phosphate-buffered saline
PET	Positron emission tomography
Pgp	P-glycoprotein
Pilo	pilocarpine
PTZ	Pentylentetrazole
Pir	Piriform cortex
qPCR	Quantitative polymerase chain reaction
Re	Nucleus reuniens of the thalamus
Sal	Saline
s.c.	Subcutaneous
SD	Standard deviation
SE	Status epilepticus
SEM	Standard error of the mean
SERT	Serotonin transporter
SI	<i>Substantia innominata</i>
SRS	Spontaneous recurrent seizures
st.	Stage
Sub	Subiculum
SUDEP	Sudden unexpected death in epilepsy
SV2A	Synaptic vesicle protein 2A
SWD	Spike-Wave discharge

TBI	Traumatic brain injury
TBS	Tris-buffered saline
TLE	Temporal lobe epilepsy
TNF- $\alpha$	Tumoral necrosis factor alpha
VACht	Vesicular acetylcholine transporter
VDB	Vertical limb of the diagonal band (of Broca)
v-ECOG	Video-electrocorticogram
VP	Ventral <i>pallidum</i>

## Chapter 1

### **Abstract (English version)**

The mesial temporal lobe epilepsy (MTLE) represents about  $\frac{3}{4}$  of epilepsy cases in adults. MTLE is associated with a well-defined pattern of injury, being among the “structural” etiologic group of epilepsies. About  $\frac{2}{3}$  of people with MTLE do not achieve satisfying control of seizures with the standard therapy which, at least regarding the odds ratio of SUDEP, is considered  $\leq 1$  generalized seizure per year. People with MTLE show a higher incidence of cognitive and psychiatric comorbidities. In recent years, plastic alterations ranging from system to molecular levels have driven attention of researchers. Deeper knowledge of mechanisms associated to epileptogenesis is hoped to shorten the way to more effective prognostic and therapeutic approaches to MTLE and its comorbidities. In this thesis, I aimed to 1) investigate plastic alterations in the amygdalopetal cholinergic fibers from the basal forebrain (BF) after *status epilepticus* (SE); 2) test the effect of a proline derivative, N-methyl-(2S,4R)-trans-4-hydroxy-L-proline (NMP) in counteracting the neuronal death (that is, neuroprotective effect) after SE. I carried out morphometric analysis of neurons and axon terminals in specific divisions of amygdala and BF in rats after kainic acid- (KA) induced SE and sham controls. I analyzed behavior, neuronal death and glial activation in mice that undergone intracerebroventricular (i.c.v.) pilocarpine-induced SE, in mice that undergone i.c.v. pilocarpine *plus* treatment with NMP and in controls. I have found strong statistic correlations between behavioral and electrocorticographic endpoints and different degrees of histopathologic injury in the KA model. I reported hypertrophy of cholinergic perikarya in three regions of the BF in post-SE animals, which are the main source of cholinergic innervation of the amygdala. The basolateral nucleus (BL) of the amygdala was significantly shrunken (by 25%) in post-SE animals, but the density of axon terminals was not altered. I have observed a dose-dependent effect of NMP to prevent the i.c.v. pilocarpine-induced behavioral deficits and increase in cell death, astrocyte and microglial activation (GFAP and Iba-1), which moved toward values of the sham group. A high docking score between NMP and the GABA transporter 1 (GAT-1), implicating this protein as the putative target of NMP, was found. Further, I quantitated the levels of GAT-1 expression by immunofluorescence and western blot. Expression of GAT-1 was greatly increased in the pilocarpine group and returned to values not distinguishable from controls at both NMP doses. I have found a strong correlation between the latency of the first generalized seizure induced by KA with the latency of the first spontaneous convulsive seizure (Racine’s stage  $\geq 3$ ) of the chronic epilepsy. In addition, the total duration of the KA-induced SE correlated strongly with the number of brain structures injured. Overall, these findings show that: 1) There are hypertrophic changes in the BF cholinergic projections to the amygdala. This may be a relevant mechanism in the pathophysiology of MTLE and a potential target of therapeutic intervention; 2) NMP significantly inhibited memory deficits, neuronal death, glial activation and the increase in the expression of GAT-1, which makes NMP worthy to be

further investigated as a potential adjunctive therapy in MTLE; 3) The dynamic evolution of SE exerts strong influence on the timing of appearance and progression of the spontaneous recurrent seizures (SRS) and on the distribution of histologic damage. This may be useful in the devising markers of disease progression and therapeutic response of epilepsies with prognostic purposes.

**Key words:** epilepsy, amygdala, acetylcholine, neuroprotection, NMP

## **Abstract (Italian version)**

L'epilessia del lobo temporale mesiale (MTLE) rappresenta circa tre quarti dei casi di epilessia negli adulti. La MTLE è associata ad un pattern di lesione ben definito, essendo classificata nel gruppo eziologico delle epilessie "strutturali". Circa due terzi dei pazienti con MTLE non raggiungono un controllo soddisfacente delle crisi epilettiche con la terapia farmacologica che, almeno per quanto riguarda la probabilità di sviluppare morte improvvisa (SUDEP), è considerato ottimale con una frequenza inferiore o uguale ad una crisi epilettica generalizzata all'anno. Le persone con epilessia presentano una maggiore incidenza di comorbidità cognitive e psichiatriche. Negli ultimi anni, lo studio delle alterazioni cerebrali di tipo neuroplastico, sia di tipo sistemico sia di tipo molecolare, hanno attirato notevolmente l'attenzione dei ricercatori. In particolare, si ritiene che la conoscenza dei meccanismi dell'epilettogenesi possa spianare la strada verso un approccio prognostico e terapeutico più efficiente della MTLE e delle sue comorbidità. L'obiettivo di questa attività di ricerca è stato quello di: 1) caratterizzare le alterazioni trofiche nelle proiezioni colinergiche del prosencefalo basale dirette all'amigdala dopo lo stato di male epilettico (SE); 2) testare l'effetto di un derivato della prolina, N-metil-(2S,4R)-trans-4-idrossi-L-prolina (NMP) nel prevenire la morte neuronale (effetto neuroprotettivo) indotta dallo SE. In particolare, ho effettuato l'analisi morfometrica dei neuroni e dei terminali assionali in specifiche divisioni del prosencefalo basale e dell'amigdala nei ratti sottoposti a SE e nei rispettivi controlli. Ho analizzato l'effetto di due dosi di NMP nello SE indotto dalla somministrazione intracerebroventricolare (i.c.v.) di pilocarpina. In questo modello ho analizzato dei parametri di comportamento, morte neuronale e attivazione gliale. Oltre a questo, ho caratterizzato la correlazione statistica tra gli endpoint comportamentali ed elettrocorticografici e la distribuzione topografica delle lesioni istopatologiche nel modello di SE indotto con acido kainico. Grazie a questo studio, ho caratterizzato la presenza di ipertrofia dei corpi neuronali colinergici in tre regioni del prosencefalo basale in animali post-SE, ovvero della principale fonte d'innervazione colinergica dell'amigdala. Ho riscontrato che il nucleo basolaterale dell'amigdala subisce un'atrofizzazione di circa il 25% negli animali post-SE, ma la densità dei terminali assionali non è stata alterata. NMP ha prevenuto in modo dose-dipendente i deficit comportamentali e l'aumento di mortalità cellulare, attivazione astrocitaria e microgliale indotti dalla pilocarpina i.c.v. NMP ha, inoltre, presentato un elevato punteggio di docking con il trasportatore del neurotrasmettitore GABA di tipo 1 (GAT-1), il che indica come questa proteina sia il suo bersaglio ipotetico. L'espressione di GAT-1 è notevolmente aumentata nel gruppo trattato con pilocarpina e tale cambiamento è stato impedito dalla somministrazione di NMP. La latenza della prima crisi generalizzata indotta da acido kainico ha presentato forte correlazione con quella della prima crisi convulsiva spontanea (stadio di Racine  $\geq 3$ ) dell'epilessia cronica. Inoltre, ho osservato che la durata totale dello SE indotto da acido kainico è fortemente correlata con il numero di strutture cerebrali danneggiate. Questi risultati suggeriscono che: 1)

c'è ipertrofia nelle proiezioni colinergiche del prosencefalo basale nell'amigdala. Questo può essere un meccanismo fisiopatologico rilevante per la MTLE e le sue comorbidità, che può essere bersaglio d'interventi terapeutici. 2) NMP ha prevenuto i deficit di memoria, la morte neuronale, l'attivazione gliale e l'aumento dell'espressione di GAT-1. Questo rende NMP attrattivo come potenziale terapia aggiuntiva per la MTLE. 3) L'evoluzione dinamica dello SE influenza fortemente i tempi di comparsa e progressione delle crisi ricorrenti spontanee e della distribuzione del danno istologico cerebrale. Questo risultato può essere utile per l'impiego di marcatori di risposta terapeutica e di progressione della malattia a scopo prognostico.

**Parole chiave:** epilessia, amigdala, acetilcolina, neuroprotezione, NMP

## Chapter 2

### *General Introduction*

#### 1. Epilepsy

##### 1.1. Definition of epilepsy

Epilepsy is defined as: I) at least two unprovoked (or reflex) seizures occurring >24 h apart (Hauser, Annegers, and Kurland 1991; Commission on Epidemiology and Prognosis ILAE 1993; Engel 2006); II) one unprovoked (or reflex) seizure and a probability of further seizures similar to the general recurrence risk ( $\geq 60\%$ ) after two unprovoked seizures, over the next 10 years; III) diagnosis of an epilepsy syndrome (Fisher et al. 2014; Scheffer et al. 2017). The second criterion is especially useful when an isolated seizure happens in the chronic period (>60 days) of a remote insult, such as cranioencephalic trauma, cerebrovascular accident, or when it is associated to a documented brain lesion (e.g.: hippocampal sclerosis (HS), cortical dysplasia, glial scar, neurocysticercosis, tumor, etc.) or an epileptic syndrome, all of which bring high probability ( $\geq 60\%$ ) of recurrence (Fisher and Leppik 2008; Fisher et al. 2014; Scheffer et al. 2017). Epilepsy affects between 50 (World Health organization, 2010) and 70 million people worldwide (Sander and Shorvon 1996).

The first international classification of epilepsies (Gastaut et al. 1970) generated intense debates in the expert community. This culminated in the 1985 ILAE Classification of Epilepsies and Epileptic Syndromes, which was reviewed soon in 1989. Even though the 1989 Classification is still valid, the need of revision and expansion has emerged to encompass newly described types of epilepsy and the advances in diagnostic and therapeutic modalities.

The 2017 ILAE Classification of Epilepsies reflects the gain of understanding of the epilepsies and their underpinning mechanisms since 1989. As a critical tool for the clinicians, the Classification is robust and applicable in all geographic regions of the world. Its primary purpose is patient diagnosis, but it can be relevant also for prognostic, clinic communication, as well as for clinical and basic research. The current Classification presents three levels: 1) seizure type, assuming that the patient has seizures as defined in the 2017 Operational Classification of Seizures; 2) epilepsy type, including focal, generalized, combined focal and generalized, and unknown groups; 3) epilepsy syndrome, when a specific syndromic diagnosis can be made. The 2017 Classification also incorporates etiology at each level, emphasizing the need of considering etiology at each step, due to its importance for prognosis and treatment. Etiology is divided into six groups, according to their diagnostic and therapeutic features: structural, genetic, infectious, metabolic, immune, unknown. These etiologic categories are not mutually exclusive. New terminology introduced previously unused terms,

such as “developmental” and “epileptic encephalopathy”. The term “benign” is replaced by “self-limited” or “pharmacoresponsive” when appropriate (Scheffer et al. 2017).

When a person meets the aforementioned epilepsy criteria, the clinician goes through attempting to classify the seizure type and the patient’s epilepsy type. In some cases, an epilepsy syndrome can be further identified. Nevertheless, in some circumstances, the classification of the seizure type may be the maximum level of diagnosis reached, due to the lack of means for further investigation, such as EEG, video or imaging studies (Scheffer et al. 2017).

## **1.2. Classification of epilepsy types**

The 2<sup>nd</sup> level, that is, Epilepsy type, is intended to be based on the aforementioned 2014 ILAE Definition of Epilepsy (Fisher et al., 2014; Scheffer et al. 2017). Apart from the well-established categories “focal” and “generalized”, two more categories were introduced, that are “combined focal and generalized”, and “unknown onset”. The latter must be seen as a provisional category rather than a true class, used when there are no clinical data or tools to make possible a correct classification.

A diagnosis of generalized epilepsy would typically require the presentation of a generalized spike-wave pattern at EEG investigation. People with generalized epilepsies may present a range of motor and non-motor generalized seizures. These patients usually show typical interictal EEG discharges. Care must be taken regarding generalized tonic-clonic seizures (*i.e.*: seizures composed by a tonic phase, that is, bilateral sustained contraction of somatic muscles lasting a few seconds to minutes, then followed by a clonic phase, that is, bilateral brief contractions (<100 ms) of somatic muscles associated to loss of posture and, usually, autonomic phenomena) (Blume et al., 2001) associated with normal interictal EEG. In these cases, supportive evidence such as myoclonic jerks or an important family history of generalized epilepsy would be required before making a diagnosis of the condition (Scheffer et al., 2017).

Epilepsies could be focal, multifocal, and involving one hemisphere. The seizure types that can be seen involve: focal seizures with impaired or preserved awareness; focal motor and non-motor seizures; and focal to bilateral tonic-clonic seizures. The interictal EEG typically shows focal epileptiform discharges. A new group of “combined focal and generalized seizures” was introduced based on the knowledge that people with generalized epilepsies may also present focal seizures. Common examples are the syndromes of Dravet, Lennox-Gastaut and infantile spasms. The diagnosis can be made on a clinical basis supported by interictal EEG. An ictal EEG is not essential for diagnosis. When available, interictal EEG shows typically both focal and generalized spike-wave epileptiform discharges (Scheffer et al., 2017).

The most prevalent epilepsy types are the mesial temporal lobe epilepsy (MTLE), the juvenile myoclonic epilepsy (JME) and the childhood absence epilepsy (CAE) (Behr et al. 2016; Shorvon, Perucca, and Engel Jr 2016). JME accounts for 5% to 10% of all epilepsies and around 18% of idiopathic generalized epilepsies. The age of JME onset spans from 8 to 36 years, peaking between 12 and 18 years (Camfield, Striano, and Camfield 2013). Its hallmark are the myoclonic seizures, that consists of sudden, brief (<100 ms) involuntary single or multiple contractions of muscles or muscular groups of variable topography (axial, proximal limb, distal) (BLUME 2001). Apart from the myoclonus, 80% of these patients may present generalized tonic-clonic seizures, and 1/3 of them may present absence seizures. Interictal EEG shows a normal background with bursts of generalized fast spike-wave or polyspike-wave discharges. Image examination does not show potentially epileptogenic lesions (Camfield, Striano, and Camfield 2013). JME has been tightly correlated to missense mutations in the EFHC1 gene. These mutations were found to be co-segregated with epilepsy or EEG polyspike-waves in affected members of six unrelated families with JME and did not occur in 382 control individuals (Suzuki et al. 2004). The product of the gene EFHC1 is a microtubule-associated protein containing an EF-hand motif, a calcium-binding helix-loop-helix domain. This protein and the calcium channel Cav2.3 are co-immunoprecipitable from and co-distributed over the brain. EFHC1 protein was documented to enhance the R-type Ca<sup>2+</sup> current, which is reversed by epileptogenic EFHC1 mutations (Suzuki et al. 2004).

The CAE, in turn, manifests as non-motor seizures consisting of loss of consciousness with sudden onset and termination and short lasting (until 30 s) without loss of postural tone and reflexes. These seizures begins between 3 and 8 years of age, and have a high daily frequency (Crunelli and Leresche 2002). The electrographic correlate of the absence seizures are the generalized, synchronous, bilateral spike and slow wave discharges (SWD) at a frequency of 3 Hz, approximately. Interictal abnormalities include tracks of generalized SWDs, posterior bilateral delta activity, and focal discharges (Sadleir et al. 2006). Most people remit around the adolescence. Some cases of CAE were related to mutations in the gene CACNA1H, which encodes a T-type Ca<sup>2+</sup> channels (Chen et al. 2003), and in the gene GABRG2, which encodes the  $\gamma$ 2 subunit of the GABA<sub>A</sub> receptor (Crunelli and Leresche 2002). But most of research failed to find one or more genes strongly correlated to CAE, thus evidencing the multifactorial character of the disease (Crunelli and Leresche 2002). The patophysiology of MTLE, in turn, will be approached in depth in the next sections.

### **1.3. Pathology of the mesial temporal lobe epilepsy**

Mesial temporal lobe sclerosis is the brain injury most often found in adults with epilepsy in general. The earliest description of macroscopic alterations in the hippocampi assignable to hippocampal sclerosis (HS) was made by Bouchet and Cazauvieilh (1825), who reported atrophy, stiffening and frailty of that structure,

introducing the term “Ammon’s horn sclerosis”. Sommer in 1880 provided the first report of the corresponding histopathology which consisted of neuronal loss, mostly involving the CA1 region, called “Sommer’s sector” since then. Bratz, in 1899 corroborated the previous findings, assigning them to the loss of pyramidal cells, additionally reporting the preservation of CA2 area and the subiculum. Falconer and colleagues, in 1964, recognized the involvement of temporal lobe structures other than the hippocampus, casting the term “mesial temporal sclerosis” (Blümcke et al. 2013; Hogan 2001; Walker 2015).

Retrospective clinical studies established early childhood initial precipitation injuries (IPI) such as prolonged febrile seizures, hypoxia, infections, or head trauma. In the natural history of the disease, seizures usually emerge after a “latent” or “silent” period over which the pro-epileptic plasticity is thought to take place. In other words, HS is an acquired pathology. Considering the post-traumatic epilepsies, 35-62% of this etiologic type present as MTLE, of which 44-53% show mesial temporal lobe sclerosis (Gupta et al. 2014; Hudak et al. 2004; Ding, Gupta, and Diaz-Arrastia 2016). IPIs, mostly febrile seizures, have been more strongly related with HS type 1 (Blümcke et al. 2007). However, this may be rather due to a sampling bias. On the other hand, the genetic background plays an important role in conditioning the susceptibility to environmental epileptogenic stimuli. This have been supported by several reports of high prevalence of MTLE within some families (Aronica et al. 2017; Cendes et al. 2014).

**Table 1. Classification of hippocampal sclerosis (HS)**

Subtype	Pyramidal cell loss (%)				Description	surgical specimens (%)
	CA1	CA2	CA3	CA4		
no-HS (gliosis only)	<10	<10	<10	<10	Neuronal cell density not different from age-matched necropsy controls. Only reactive gliosis.	20
HS ILAE type 1	>80	30-50	30-90	40-90	Predominant cell loss in CA1, CA3 and CA4. DG 50-60% of loss.	60-80
HS ILAE type 2	~80	<20	<20	<25	Predominant cell loss in CA1. Usual DG dispersion.	5-10
HS ILAE type 3	<20	<25	<30	~50	Predominant cell loss in CA4. DG ~35% of loss.	4-7

(modified from: Blümcke et al. 2013)

An appropriate histologic evaluation requires a resection “*en bloc*”, that is, a resection of a relatively large piece of tissue. Unfortunately, this is not possible for every patient, nor is a routine in most of the epilepsy surgery services. Some services carry out rather the aspiration of the mesial temporal structures, thus precluding an accurate histopathological assessment. In any case, when just a fragmentary specimen is available, the ILAE strongly recommends that at least CA1 and CA4 hippocampal subfields must be histologically evaluated (Blümcke et al. 2013; Cendes et al. 2014). The best postoperative seizure control (*i.e.*: Engel class I) after mesial temporal lobectomy has been most often achieved in the HS stage I (Na et al. 2015;

Jardim et al. 2012). However, the less common stages of HS are associated with a poorer prognosis in the regard of seizure control.

Despite the attention devoted to HS, intracranial EEG studies demonstrate that in MTLE, the ictogenic foci are not always restricted to the hippocampus. They may involve the amygdala, or both amygdala and hippocampus, parahippocampal gyrus, uncus, temporal pole, the entorhinal, insular and perisylvian cortices (Kahane and Bartolomei 2010). Sometimes there is a complex ictogenic network that also involves the insula, orbitofrontal cortex, the frontal and parietal operculum. This is called temporal-plus epilepsy (Barba et al. 2007; Bartolomei et al. 2010).

## 2. Pharmacoresistance

The mainstay of the clinical therapy of the epilepsies is composed of the voltage-operated sodium channel blockers, the enhancers of the GABAergic transmission, and the voltage-operated calcium channel blockers. Over the last two decades, drugs with innovative pharmacodynamics were introduced, such as levetiracetam, which have a broad action spectrum. In this specific case, the action mechanism consists of the inhibition of the protein SV2A, a part of the presynaptic apparatus of vesicle fusion (Shorvon, Perucca, and Engel Jr 2016).

In spite of the advances in the pharmacotherapy of the epilepsies, estimates point that 30-40% of cases become resistant to clinical treatment (antiepileptic drugs, AED), which can reach 60-70% at some point in time (Janmohamed, Brodie, and Kwan 2020; Kwan and Brodie 2000; Panayiotopoulos 2010). People with drug-resistant epilepsy (DRE) deal with considerable socioeconomic and psychological handicaps (Mula and Sander 2016). Epilepsies are associated with increased risk for morbidity and mortality (Sveinsson et al. 2017; 2020). The uncontrolled seizures, mainly those of generalized tonic-clonic type, are the strongest risk factor for sudden unexpected death in epilepsy (SUDEP) (Hesdorffer et al. 2011; Zhang et al. 2016).

At least four patterns of drug resistance are recognized in clinical epilepsy: 1) *de novo* or *ab initio*: the patient never enters in seizure freedom from the onset of the beginning of the symptoms; 2) late or delayed resistance: the patient initially responsive and free of seizures becomes tolerant to treatment. Seizures recur and become uncontrollable; 3) Waxing-and-waning or fluctuating drug resistance: the patient alternates periods of seizure freedom associated to the therapeutic response with periods of uncontrolled seizures; 4) epilepsy initially resistant but becomes progressively sensitive to treatment (Löscher et al. 2020). Follow-up studies suggest that the probability of success of pharmacologic treatments drops to about 10% or even less after failure of 2 trials with AEDs appropriately chosen for a given type of seizure in optimized dosing scheme. The resistance pattern is often identified early in the patient managing. This supports the concept that DRE is an *ab initio* condition in most of DRE cases (Chen et al. 2018).

In 2010 DRE was defined by ILAE as “failure of adequate trials of two tolerated, appropriately chosen, and used AED schedules (whether as monotherapy or in combination) to achieve sustained seizure freedom (all types of seizures) for 12 months, or 3 times the interseizure interval before treatment started” (Kwan et al. 2010). The primary aim of the ILAE definition is operational, that is to guide clinical management of patients. A DRE incidence of 30-40% in general population with epilepsy has been recurrently reported (Alexopoulos 2013; Wheless, Gienapp, and Ryvlin 2018). Yet these studies do not take into account the current definition of DRE. Furthermore, the validity of the definition of DRE given by ILAE was not yet assessed in large population-based cohorts. Thus, accurate epidemiologic estimates of risk factors for DRE and of its prevalence would be invaluable to develop targeted treatment programs and to optimize the allocation of healthcare resources.

A systematic review (Kalilani et al. 2018) evaluated the consistency among the definitions of drug-resistant epilepsy in the literature and the ILAE definition. From 35 studies, they pooled 13,080 cases of epilepsy, from which 3,941 were identified as DRE in original reports. Most epidemiological studies applied inhomogeneous DRE case definitions. From the 35 studies which met the inclusion criteria, just four which were published after Kwan et al. (2010) applied the ILAE definition. Among these, only two studies employed the ILAE definition in a prospective design (Kalillani et al. 2018).

The ability of collect information will determine the ability of correctly classify the patients. This is a particular concern for retrospective studies, as the medical records cannot be detailed enough to make possible an inference on AED adequacy. Thirty-one studies included the criterion of appropriateness of the AED when evaluating for DRE. Among them, five works considered all three aspects of appropriateness (adequacy, compliance, and adverse effects). Among the 11 articles that evaluated adverse effects, five categorized discontinuation associated to adverse effect as treatment failure, four did not consider this as treatment failure, and two did not provide any information of categorization of such cases. As such, these reported estimates may not be representative of the current DRE incidence in accordance with the current guidelines (Kalilani 2018).

The evaluation of AED therapy trial requires the patients to be managed by a clinical epileptologist, rather than by a general neurologist. Consequently, most of the patients recruited into studies are from specialized tertiary health care centers. This makes a selection bias, as those patients are not representative of the general population of people with epilepsy. A relatively long follow-up is required for establish surely that the patient completed two AED trials in optimized dosing scheme. This may be precluded by a significant loss of follow-up. In addition, cycles of remission and relapses have been reported in DRE (Berg et al. 2009) . Indeed, it is estimated that 4% of DRE patients can enter in remission (Laxer et al. 2014) . This could explain why there are more people with DRE among chronic patients than among newly diagnosed ones. Therefore, measures

integrating the time as variable, such as incidence rate, rather than incidence proportion could be more suitable to depict this dynamic feature (Kalilani 2018).

Such factors as early age onset, SE history, symptomatic epilepsy, history of neurological deficits, abnormal imaging findings, psychiatric comorbidities and mental retardation were all associated with an increased risk of DRE. However, sex, family history, febrile seizures or seizure type were found not to be risk factors. These may be actual correlations, but also may reflect a small sample size and variations in methodology across the studies. Therefore, future studies are needed in which consistent DRE definition (according to ILAE guidelines) should be applied and homogeneous well-established classification criteria should be set for risk stratification (Kalilani 2018).

The mechanisms of pharmacoresistance are most likely multifactorial. None of them is able to explain all cases of DRE. Two or more mechanisms may coexist and carry a complex synergistic interplay in the same patient. The pathophysiologic hypotheses of pharmacoresistance can be grossly divided into three categories: disease-related, drug-related, and genetic/epigenetic. Among them, those of molecular target modification, and the efflux carriers are the most explored hypotheses (Tang, Hartz, and Bauer 2017; Löscher et al. 2020).

### **2.1. Hypothesis of the drug molecular target alteration**

This theory states that epilepsy-related (acquired) alterations of the structure or function of molecular targets of AEDs may decrease their sensitivity to the pharmacodynamic mechanism. This hypothesis is based primarily on studies about the response of voltage-gated  $\text{Na}^+$  currents in hippocampal neurons to carbamazepine (Remy, Urban, et al. 2003). They have shown that the use-dependent blockage of the voltage-gated  $\text{Na}^+$  channels in dentate granule cells by carbamazepine is completely lost in patients with carbamazepine-resistant MTLE compared with responsive patients. Also, the fast recovery from inactivation of the fast  $\text{Na}^+$  currents was carbamazepine-insensitive, while it is significantly slower in responsive patients. Similar alterations were reported in the dentate granule cells from rats post-SE induced by pilocarpine (Remy, Gabriel, et al. 2003). In this rat model, the accessory  $\beta 1$  and  $\beta 2$  subunits of those channels were found to be downregulated. This was proposed to be the substrate of the altered channel function.

In the same pilocarpine model of rats, functional alterations in the  $\text{GABA}_A$  receptor have been documented. Expressions of the  $\alpha 1$  and  $\beta 1$  subunits of  $\text{GABA}_A$  receptor were decreased, while its  $\alpha 4$  and  $\delta$  subunits were upregulated. The  $\text{GABA}_A$  receptors of such subunit composition are highly  $\text{Zn}^{+2}$ -sensitive and lack sensitivity to modulation by zolpidem at the benzodiazepine allosteric binding site. Also in the pilocarpine-induced model of MTLE, animals nonresponders to phenobarbital had significant increase in dentate gyrus (DG)

diazepam-insensitive binding at autoradiography compared to responders (Volk et al. 2006). The nonresponders had a decreased expression of  $\alpha 1$ ,  $\beta 1$ ,  $\beta 2$  and  $\gamma 2$  in CA1, CA2, CA3 and DG compared to responders, which in turn had much less spread alterations (Bethmann et al. 2008). In addition, protein kinase-mediated phosphorylation and trafficking of GABA<sub>A</sub> receptors from the post-synaptic membrane to intracellular compartments were documented in this model of MTLE. Those findings together explain at least in part the loss of effect of drugs with GABA<sub>A</sub> receptor-mediated mechanism of action (Goodkin, Yeh, and Kapur 2005; Naylor, Liu, and Wasterlain 2005).

The hyperpolarizing effect of the GABA<sub>A</sub> receptors can be shifted to a depolarizing (prenatal/neonatal) pattern. This may come as result of the upregulation of the NKCC1, an inwardly directed Na<sup>+</sup>, K<sup>+</sup>, 2Cl<sup>-</sup> cotransporter, and downregulation of the KCC2, an outwardly directed K<sup>+</sup>, 2Cl<sup>-</sup> cotransporter. This leads to the depletion of neuronal cytoplasmic Cl<sup>-</sup>, which is normally low. The net effect is the loss of the transmembrane gradient of Cl<sup>-</sup>, thus ceasing its passive (hyperpolarizing) influx, replaced by a HCO<sub>3</sub><sup>-</sup> influx at the GABA<sub>A</sub> receptor opening. This has been shown in patients with MTLE, and in the pilocarpine and amygdaloid kindling models of MTLE (Löscher, Puskarjov, and Kaila 2013). In addition, this effect has been imputed as mechanism of pharmacoresistance of neonatal seizures to benzodiazepines and barbiturates (Puskarjov et al. 2014). Nonetheless, a trial of bumetanide, a NKCC1 inhibitor, as add-on therapy for neonatal seizures does not support this view. Furthermore, the fact that most DRE patients exhibit resistance to multiple drugs with distinct molecular targets restricts the usefulness of this theory and suggests a rather nonspecific mechanism of drug resistance (Tang, Hartz, and Bauer 2017).

## **2.2. Hypothesis of the efflux transporters**

This theory attributes drug resistance to inadequate drug permeation across the blood brain barrier (BBB). The effect has been assigned to an increased expression of nonspecific transporters that take the drug from the brain parenchyma back to the bloodstream. Tishler et al. (1995) firstly proposed the theory based on their finding of significant upregulation of the MDR1, the gene coding the P-glycoprotein (Pgp), in the majority of analyzed surgical specimens of MTLE. The BBB efflux transporters, such as Pgp and breast cancer-related protein (BRP), have a well-known role in limiting the access by passive diffusion of lipophilic xenobiotics to the central nervous system, thus avoiding intoxication (Abbott 2013; König, Müller, and Fromm 2013; Saunders et al. 2016). Indeed, Pgp has been implied in the failure of treatment of infections, tumors, among other disorders in the brain (Mahringer and Fricker 2016). The findings by Tishler et al. (1995) have been corroborated by many others. Furthermore, the expression of Pgp and other multidrug resistance-associated proteins (MDRs) was found to be increased in the endothelium and astrocytes inside the epileptic

foci, but not in those of surrounding healthy tissue. In addition, similar upregulation was found in tissue from necropsy of nonresponders compared to responders. In view of the local and transient disruption of BBB in epileptic foci during seizures (van Vliet, Aronica, and Gorter 2015), the overexpression of MDRs in astrocyte endfeets seems to be a compensatory phenomenon creating a “double cuff” to limit excessive BBB permeability. Besides, the PET-measured uptake of radiolabeled [<sup>11</sup>C]verapamil, a Pgp substrate, was compatible with an increased Pgp activity in epileptogenic brain areas of nonresponder patients versus responders and healthy controls (Feldmann et al. 2013).

In the models of amygdaloid kindling and KA-induced SE in rodents, Pgp is acute and transiently overexpressed in endothelium, astrocytes and neurons in limbic regions. This indicates that ictal activity itself can trigger Pgp overexpression (Löscher and Potschka 2005; Tang, Hartz, and Bauer 2017). The finding fits to the fact that a high seizure frequency before the beginning of the pharmacologic treatment is the most important risk factor for DRE (Dalic and Cook 2016; Hitiris et al. 2007). Notwithstanding, a rather constitutive overexpression of MDRs was found in MCD surgical specimens (Sisodiya, Heffernan, and Squier 1999). Outflow of AEDs was demonstrated by the use of mice knockout for *mdr1a/b* and microdialysis with Pgp inhibitors. Furthermore, the increase in the transcript mRNA of that gene measured by qPCR was associated to a 30% decrease in the phenytoin concentration in hippocampi of animals post-SE induced by KA. Indeed, concentration of phenytoin was decreased in topographical coincidence with Pgp overexpression compared to other brain regions of epileptic rats, and this was counteracted by Pgp inhibitors (van Vliet et al. 2007). In animals nonresponders to phenobarbital, the add-on of tariquidar, a Pgp inhibitor, was able to rescue the responsiveness to the AED. In humans, the add-on therapy with the nonselective Pgp inhibitor verapamil yielded promising seizure control results in DRE (Asadi-Pooya et al. 2013; Borlot et al. 2014; Narayanan et al. 2016).

### **3. In vivo models of epilepsy**

The maximal electroshock used since Merritt and Putnam (1936) and the subcutaneous pentylenetetrazol treatment since the 1950s (Krall et al. 1978; Swinyard 1972) have been the gatekeepers of the classical AED screening. Indeed, the AEDs discovered between 1936 and 1998 were firstly identified in those tests (Löscher 2011; Löscher et al. 2020;).

However, acute seizures induced in otherwise healthy animals lack the modifications present in the epilepsy, which render the ictal threshold of the brain constitutively low. In other words, those acute models are rather models of ictogenesis than true epilepsy. Their pathophysiology does not overlap necessarily that of chronic SRS. The pharmacologic response of the chemoconvulsant-induced acute seizures in large measure

relies on the neurotransmitter system affected by the chemoconvulsant (Löscher 2020). Most importantly, the AEDs developed between 1936 and 1998 in the so-called classical paradigm, failed to modify the prevalence of pharmacoresistance. In other words, they were not more effective than older AEDs, even though they had improved pharmacokinetic and side effect profiles (Löscher 2011). Even so, reports on electrically- or chemically-induced acute seizures evoked in post-SE animals support that this approach provides reliable data on AED response (Bankstahl, Bankstahl, and Löscher 2013; Leclercq and Kaminski 2015; Löscher 2017).

On this background, a chronic model of MTLE *in vivo*, namely the electrical kindling of a limbic structure (mostly the amygdala), was perhaps the most often used animal model to investigate epileptogenesis (i.e. neurodegeneration, neurogenesis, neurite sprouting and pruning, which are among the mechanisms believed to render a brain chronically prone to seizures) (Pitkänen et al. 1998; Tuunanen, Halonen, and Pitkänen 1997; Tuunanen and Pitkänen 2000). However, SRSs are never seen in fully kindled animals. Interestingly, SRS can be obtained in the so-called “extended” kindling, in which two distinct limbic structures are kindled separately (Michael et al., 1998; Brandt, Ebert, Löscher 2004). On the other hand, models in which an electrically- or chemically-induced self-sustained SE is generated, disregarding how the SE is induced, are usually characterized by the development of a chronic epileptic state with limbic SRS and neuropathology recapitulating those of MTLE (Dudek and Staley 2017).

In this regard, tetanic electrical stimulation of limbic structures such as the perforant path or the angular bundle consistently yields a post-SE state with limbic SRS and other MTLE features (Gorter and van Vliet 2017). SE can be also induced by systemic or focally-administered pro-excitatory chemicals such as kainic acid (KA) or pilocarpine to generate a subsequent chronic state with limbic SRS.

Pilocarpine has been extensively used at several routes and doses to induce SE and the consequent model of MTLE in rodents. Major shortcomings of this model are the high mortality, the difficult to titrate the SE stage, that is, an all-or-none character of the acute seizures, and a strong and spread pattern of brain lesion in the surviving animals. The intracerebroventricular (i.c.v.) route used herein allows to bypass the peripheral muscarinic side effects such as bronchial hypersecretion and bradycardia, which are in large measure responsible for the deaths (Medina-Ceja, Pardo-Peña, and Ventura-Mejía 2014). In the pilocarpine model, the severity of the injury and its topographic extension seems to correlate with the duration of the latent period and the severity of the seizures in the chronic period, but only to some extent. If the lesions are severe and widespread, the chronic seizures tend to have a milder behavioral phenotype (Biagini et al. 2008; Lemos and Cavalheiro 1995).

Also KA have been used by a broad number of protocol variants to induce SE and the following MTLE-like condition. It should be kept in mind that the outcomes of SE, including the latent period duration, seizure type and frequency, pattern of histopathological changes, may vary considerably depending on treatment protocol (route of administration, animal strain, method of seizure detection, etc.) (Dudek and Staley 2017; Dudek et al., 2006). For example, Sprague-Dawley rats given a systemic single dose of KA usually show lower mortality rates, moderate neuronal loss, and shorter latent period when compared to Wistar rats. The latter, in turn, present very low survival rates, severe neuronal loss, with CA1 affected more than CA3, and a two-fold longer latent period (Bertoglio et al., 2017). In addition, s.c. KA seems to affect more CA3, while i.p. KA affect more CA1, a histopathological pattern resembling closer that of the ILAE type 1 stage (Aronica et al., 2017). Hilar cells are particularly vulnerable in practically all models. In contrast, the granule cells of the DG are reported to be spared across the animal models of MTLE. Nevertheless, the granule cells have been found to be dispersed in the intrahippocampal KA model, a feature which has been related to a long time evolution of MTLE in humans (Dudek et al., 2006). It is worthy of note that the method of monitoring for SRS and the endpoint chosen are critical to determine the length of the latent period. Indeed, post-SE seizures may show a very low frequency and low behavioral scores during the first weeks or months following the treatment. Furthermore, they can be disposed in clusters alternating with long periods of low seizure frequency. Thus, the low frequency seizures are highly probable to be missed if monitoring is performed in a non-continuous way or if it stopped before a critical endpoint (Dudek and Staley 2017).

Many variants of the KA protocol have been described. They include systemic administration routes (i.p., s.c., intravenous), focal routes (intrahippocampal, intracerebroventricular, intracortical), and several dosing schemes such as the single high dose and the repeated low-dose protocols, both through systemic routes. The repeated low dose protocol was designed to improve the survival rate of the animals when compared to high-dose treatments (Hellier et al., 1998; Meier and Dudek 1996). Of note, this protocol entails varying cumulative doses for individual animals to induce SE, which may add a further bias in the interindividual variability of histopathological findings. However, the mortality rate additionally depends on other experimental conditions. For example, in our laboratory, a single high-dose treatment of rats with KA produced very low mortality (typically <7%).

Regarding the plastic changes involving the acetylcholine systems in the SE model of KA, previous works (Soares et al. 2017) reported that the density of the vesicular acetylcholine transporter-immunoreactive (VAcHT-IR) fiber varicosities was increased in epileptic rats in the inner and outer zones of the molecular layer of the DG, but was decreased in its hilus (polymorphic layer), and unaltered in the middle molecular layer. The same work reports that both, the number of the choline-acetyltransferase-immunoreactive (ChAT-IR) perikarya in the medial septum, and their density were increased in epileptic rats. The VAcHT-IR perikarya in

the medial septum were enlarged significantly in epileptic animals. Another work (Soares et al., 2018) on the neuroplastic changes in the pedunclopontine and laterodorsal cholinergic nuclei of the mesopontine tegmentum reports that the former had enlarged VAcHt-IR perikarya, but the latter did not. The estimated number of neurons in both nuclei was unchanged. In addition, the parafascicular thalamic nucleus has shown an increased density of VAcHt-IR varicosities. It is noteworthy that the parafascicular thalamic nucleus is targeted mainly by the pedunclopontine tegmental nucleus, which showed neuronal hypertrophy under those experimental conditions. It is worthy mention that, except for some works addressing amygdala neurodegeneration in several models of epilepsy, the amygdala pathology has been relatively overlooked in experimental epilepsy, as did the cholinergic projection system.

Regarding the remodeling of the serotonin systems in the model of KA single high dose, the number of serotonin transporter-immunoreactive (SERT-IR) neurons in the interfascicular part of the dorsal raphe nucleus was decreased in 30% epileptic animals. The number of SERT-IR neurons in the median raphe nucleus, in turn, was increased in 100% in epileptic animals. The density of the SERT-IR small-sized varicosities was decreased and the density of the large-sized ones was increased in the hilus of the DG, in the infralimbic cortex and the medial septum, but not in the molecular layer of DG of the epileptic animals (Maia et al., 2019). Those researchers have found reasonable to attribute the findings to neurodegeneration of the interfascicular part of the raphe nucleus with compensatory hypertrophy of the median raphe nucleus. Nevertheless, they were aware of other possibilities, such as the change of the neurochemical phenotype of the neurons. Actually, the raphe nuclei contain neurotransmitters other than serotonin, and local circuitry neurons, and the true fate of the serotonergic neurons was not specifically addressed.

With respect to the noradrenaline systems, destruction of noradrenergic terminals from the *locus coeruleus* by the neurotoxin N-(2-chloroethyl)-N-ethyl-2-bromobenzylamine (DSP-4) made sporadic seizures induced by bicuculline infusion in the area tempestas to evolve as SE followed by limbic SRS and DG mossy fiber sprouting (Giorgi et al., 2003). Also, the bilateral lesion of the *locus coeruleus* by 6-hydroxydopamine (6-OHDA) markedly facilitated the development of amygdala kindling (N'gouemo et al., 1990). A decreased density (and staining intensity) of the dopamine-hydroxylase-immunoreactive varicose fibers was found in the thalamus, hippocampus, central nucleus of the inferior colliculus and in the piriform, orbital and somatosensory cortices, but not in other cortical areas, neither in cerebellum and *locus coeruleus* of the GEPR-9 audiogenic rats (Lauterborn and Ribak 1989). Protection against the pro-excitatory remodeling has been claimed to account for the antiepileptic action of noradrenalin in chronic epilepsy models rather than its ambiguous antiepileptic action mediated by noradrenergic receptors agonism (Giorgi et al., 2003; Akyuz et al., 2021).

Concerning the dopamine system, degeneration of the dopaminergic neurons in the *substantia nigra pars compacta* was shown in the absence epilepsy-prone WAG/Rij rat strain (Birioukova 2016). The number of dopaminergic neurons remaining at the end of ten months of age was positively correlated to the severity of the epilepsy. Those authors support that the decrease in the number of dopaminergic neurons and in the nigrostriatal innervation may have beneficial effects in the seizure control in this model. Absence seizure-prone rats presented higher indices of dopaminergic metabolism than non-epileptic controls, but the severity of the absence seizures correlated with a widespread dopaminergic deficiency expressed by decreased indices of dopamine metabolism. Brain dopaminergic and serotonergic metabolic indices (ratio of the metabolite to the parent transmitter) were tightly correlated in striatum and pons-medulla of absence seizure-prone rats, but not of controls. Instead, audiogenic seizures had no major effects on monoamine metabolism (Midzyanovskaya 2020). Those authors hypothesize that the enhanced metabolism of dopamine and serotonin are at least partial compensatory antiepileptic mechanisms, and a disturbance of this compensation leads to an aggravation of the absence seizures. The lesion of the *substantia nigra pars compacta* by 6-OHDA did not affect the acquisition of the amygdala electrical kindling (N'gouemo et al., 1990). In addition, the mRNA of the dopamine-beta-hydroxylase and of norepinephrine transporter in the *locus coeruleus* were upregulated respectively at the second and the 7<sup>th</sup> days after KA-induced SE, but the mRNA of the vesicular monoamine transporter-2 (VMAT2) was not (Bengzon et al. 1999).

The pharmacologic response of the KA-induced post-SE model has been extensively investigated. In the KA repeated low dose protocol, carbamazepine injected at doses of 30 and 100 mg/kg i.p. strongly suppressed SRS (Grabenstatter, Clark and Dudek 2007). Topiramate (10, 30 and 100 mg/kg i.p.) has shown a dose-dependent effect on SRS. The effect on the seizures was significantly stronger at 30 mg/kg, and not significantly different from that of the highest dose (Grabenstatter et al., 2005). In addition, carisbamate (0.3, 1, 3, 10 and 30 mg/kg i.p.) exhibited a dose-dependent effect on the SRS, apparently more effective than topiramate (Grabenstatter and Dudek 2008). Those researchers established a crossover scheme of short duration AED trials alternated with washouts under full time (24 hours a day, 7 days per week) radiotelemetric video-EEG recordings in order to overcome biasing factors such as the clustering and the natural worsening of the seizures, as well the pharmacokinetics, which is faster in laboratory animals in such a way that most of AEDs, with exception of phenobarbital, have a half-life about five hours or less. Without this methodological refinement it is quite difficult to determine surely the AED responsiveness (or resistance) of SRS in post-SE models.

The model of intrahippocampal KA in mice and rats, designed to produce a focal damage, has drawn much attention in the last years. Indeed, similarly to other SE models, it replicates many pathological features of human TLE (Barker-Haliski and White 2017; Henshall 2017; Klee et al., 2017). In mice, this model has been

deemed for AED testing, even at high throughput fluxes. However, despite all the advantages intrinsic to this model, a relatively small percentage of animals (<50%) show SRS following the treatment (Rusina, Bernard, and Williamson 2021).

#### 4. Drug development

Compounds from natural and synthetic sources are extensively used in drug development. The knowledge of herbal medicines, phytochemistry and pharmacology, when properly articulated, may assist the prospection biologically active plant-derived compounds. These compounds, even when not suitable for clinical use due to pharmacokinetic or toxic properties, may be molecular prototypes to model synthetic compounds with improved properties, in other words, more “druggable” compounds (Bohni et al. 2013; Brillatz et al. 2020). In this regard, the plant *Sideroxylon obtusifolium* has been used in the folk medicine of the northeastern Brazil due to its claimed anti-inflammatory, wound healing and anticonvulsant properties. Previous studies evidenced its anti-inflammatory property, as well as N-methyl-(2S,4R)-trans-4-hydroxy-l-proline as the major constituent of the extracts of this vegetable (Aquino et al. 2016). This is why the standardized extract of *Sideroxylon obtusifolium* was thought to be worth to investigate for possible anticonvulsant activity.

In the context of the modern drug discovery, the molecular docking is an *in silico* technique able to produce insights into the action mechanism in early stages of drug development. Starting from the tridimensional structure of the protein and the small molecule ligand, a software runs functions involving entropy and van der Waal forces (such as dipoles, hydrogen bonds and hydrophobic forces) to compare many potential binding sites in the protein and many poses of the ligand, in order to find those of lowest Gibbs free energy. The docking technique varies with respect to the use of a rigid or flexible structure of the protein and the ligand, and the method of ligand conformational search, which can be systematic or stochastic (Pagadala, Syed, and Tuszynski 2017).

Given that the present work started from the small molecule ligand, its protein target had to be predicted. To do so, the Swiss Target Prediction could be used. This tool, on the basis of large datasets of protein-small molecule interactions, measures the bi- and tridimensional similarity between known ligands and that one fed by the user, which could be useful for N-methyl-(2S,4R)-trans-4-hydroxy-l-proline in this case (Gfeller, Michielin, and Zoete 2013; Gfeller et al. 2014).

#### 5. The basolateral nuclear complex of the amygdala and its cholinergic innervation

Unlike the pathology of hippocampus, that of amygdala has been relatively overlooked in the context of epilepsy. As other limbic areas, amygdala has been longly recognized as an area of very low ictal threshold. It has reciprocal connections with most parts of paleocortex and neocortex, as well as some thalamic and brainstem structures (Table 2). This makes amygdala not only an important relay station for information exchange and modulation, but also a way by which ictal activity initiated focally in any part of a wide brain territory can easily recruit many far distant structures.

**Table 2. Extra-amygdalar input output relationships of the basolateral nuclear complex of the amygdala (BL)**

<b>REGION</b>	<b>Afferents</b>	<b>Efferents</b>
<b>Cortex</b>	AIP, Cg1, DI (gustatory visceroreceptor), EC (medial lateral), IL, M1, M2, Pir, PL, SM, VI	AID, AIP, DI (gustatory), EC, IL, M1, M2, PaRH, PL, PRCv, PRh, SM
<b>Basal forebrain</b>	Acc, BNST, Cl, CPu, OT, VDB, VP/SI	Acc, CPu (dorsal and ventral), HDB, IPAC, OT, VP
<b>Thalamus</b>	IAM, MD, MG, PP, Re, SPFPC	MD, PaV
<b>Hypothalamus</b>	DM, LPO, PH, PM, VM	LH, LPO
<b>Hippocampal formation</b>	CA1, CA3, ParaS, S	CA1, S
<b>Brainstem</b>	RRF (A8)	-

(Modified from: Pitkänen et al. 2000, Paxinos 2015)

Acc - Accumbens, AID - Anterior agranular insular cortex, AIP - Posterior agranular insular cortex, BNST - Bed nucleus of stria terminalis, CA1 - Cornu ammonis 1, CA3 - cornu ammonis 3, Cg1 - Cingulate cortex area 1, Cl - Claustrum, CPu - Caudate-putamen or striatum, DI - Dysgranular insular cortex, DM - Dorsomedial nucleus of the hypothalamus, EC - Entorhinal cortex, HDB - horizontal limb of the diagonal band (of Broca), IAM - Interanteromedial nucleus of the thalamus, IL - Infralimbic cortex, IPAC - Interstitial nucleus of the posterior limb of the anterior commissure, LH - lateral hypothalamic area, LPO - Lateral preoptic area, M1 - primary motor cortex, M2 - secondary motor cortex, MD - Mediodorsal nucleus of the thalamus, MG - Medial geniculate nucleus, OT - Olfactory tubercle, ParaS - Parasubiculum, PaRh - Parietal rhinal cortex, PaV - Paraventricular nucleus of the thalamus, PH - Posterior nucleus of the hypothalamus, Pir - Piriform cortex, PL - Prelimbic cortex, PM - Premamillary nucleus of the hypothalamus, PP - Peripeduncular nucleus of the thalamus, PRCv - Perirhinal cortex ventral portion, PRh - Perirhinal cortex, PT - Paratenial nucleus, Re - Nucleus reuniens of the thalamus, RRF - Retrorubral field, S - Subiculum, SI - Substantia innominata, SM - nucleus of the stria medullaris of the thalamus, SPFPC - Suprafascicular nucleus parvicellular division, VDB - ventral limb of the diagonal band (of Broca), VI - Primary visual cortex, VM - Ventromedial nucleus of the hypothalamus, VP - Ventral pallidum.

Cholinergic innervation of the amygdala in epilepsy is worthy to investigate by many reasons. Amygdala, namely its basolateral complex, BL, contains the densest cholinergic axonal plexus in the brain. Although the normal cholinergic innervation of the amygdala has been studied in depth (Carlsen and Heimer 1986; Muller, Mascagni, and McDonald 2011; Muller et al. 2013; 2016; Nitecka and Frotscher 1989), the state of such innervation in experimental epilepsy has drawn little attention. Apart from the cholinergic apparatus of synaptic and nonsynaptic transmission, amygdala contains an important monoaminergic innervation, such as

the noradrenergic plexus of its centromedial nuclear complex. Many of these monoaminergic terminals were documented to express cholinergic receptors, and vice versa. Therefore, amygdala is an important place of crosstalk between cholinergic and monoaminergic systems (Li et al. 2001; Muller, Mascagni, and McDonald 2011). Oscillatory rhythm synchronization of distant areas promoted by amygdala makes easier synaptic interaction among them. This is crucial for memory acquisition processes (Paré, Collins, and Pelletier 2002; Muller, Mascagni, and McDonald 2011). Impairment of such mechanisms, at least in part, underpin the memory and learning disturbances often seen in people and animals with limbic epilepsy. Indeed, post-training infusion of cholinergic muscarinic antagonists in BL or lesion of the BF parts which provide cholinergic inputs to BL impairs significantly the acquisition of several memory modalities. Also, degeneration of BF cholinergic neurons has been assigned a role in the pathophysiology of some demential syndromes, such as the Alzheimer's disease, the so-called "cholinergic failure hypothesis" (Muller et al. 2013; 2016; McDonald and Mascagni 2010; 2011; Giorgi et al. 2020).

Synaptic contacts have been described between cholinergic terminals and post-synaptic elements of pyramidal and interneuronal origin. The GABAergic interneurons, after the pyramidal cells, make the second main target of cholinergic innervation in amygdala. Among the GABAergic interneurons, those reactive for parvalbumin (PV) are the most prevalent accounting for 40% of all interneurons in BL. They are reactive also for calbindin and comprise the basket cells and the chandelier or axoaxonic cells. Many of them possess a fast-spiking nonaccommodating firing pattern (Rainnie et al. 2006; Woodruff and Sah 2007). Both muscarinic and nicotinic receptors were documented to increase the excitability of fast-spiking interneurons in BL. An indirect effect of muscarinic excitation of BL fast-spiking interneurons is the rapid-onset early hyperpolarization of pyramidal cells followed by prolonged depolarization, which in turn is the direct effect of muscarinic agonism on pyramidal neurons (Muller, Mascagni, and McDonald 2011).

Several neuronal populations in the amygdala present a differential susceptibility to neurodegeneration induced by epileptogenic stimuli. PV-immunoreactive cells are the most degeneration-prone neurons in models such as amygdala electrical kindling and systemic KA. At least in part, this may reflect their larger prevalence. On the other hand, if the epileptogenic insult is quite strong, such as the SE induced by electrical tetanic stimulation or systemic pilocarpine, neurodegeneration is less selective, affecting interneurons disregarding their neurochemical identity, and even pyramidal neurons (Narkilahti et al. 2003; Nissinen et al. 2000; Tuunanen and Pitkänen 2000; Pitkänen et al. 2002; Tuunanen, Halonen, and Pitkänen 1996).

As in the hippocampus, the loss of parvalbumin GABAergic cells, and consequently of GABAergic inhibitory inputs on the pyramidal cells were classically assigned a major role in the hyperexcitability of the latter. In other words, the loss of GABAergic inputs on the principal neurons makes them disinhibited (Morimoto,

Fahnestock, and Racine 2004; McDonald, Muller, and Mascagni 2011). Nevertheless, the phenomena underlying an overall outcome of disinhibition may not be so straightforward to interpret. A reorganization of the synaptic inputs due to the massive loss of postsynaptic elements in amygdala is probable to affect the remaining components in a complex way. Very few studies, if any, have addressed the synaptology of specific elements of the amygdala in epileptic animals.

Pyramidal cells are 85% of the neurons in amygdala. Synaptic modulation of BL by cholinergic afferents from BF seems to be mediated mainly by the inputs to the distal dendritic compartment of pyramidal cells. This is consistent with electrophysiological studies which have shown that cholinergic projections from BF increase excitability of BL by means of both muscarinic and nicotinic cholinergic receptors (McDonald, Muller, and Mascagni 2011). Cholinergic activation of pyramidal perikarya and dendrites in BL have a fast kinetics typical of nicotinic receptors and is pharmacologically selective to  $\alpha 7$  subunit-containing receptors (McDonald, Muller, and Mascagni 2011). In turn, the main effect of muscarinic agonism in BL is to enhance the excitability of pyramidal neurons as result of the suppression of many potassium currents, which include: the muscarine sensitive M-current ( $I_M$ ), a voltage insensitive leak current ( $I_{leak}$ ), a hyperpolarization-activated inward rectifier current ( $I_Q$ ), and a calcium-activated slow afterhyperpolarization current ( $sl_{AHP}$ ). Electrophysiological studies evidenced that most  $sl_{AHP}$  channels are located in pyramidal distal dendrites, in topographical coincidence with the large majority of cholinergic synaptic inputs to pyramidal neurons (McDonald, Muller, and Mascagni 2011; Muller, Mascagni, and McDonald 2011).

Dendritic spines, most present in pyramidal neurons, are structures specialized in glutamatergic excitatory transmission. Dendritic spines account for 50% of elements post-synaptic to cholinergic terminals. Of them, 86% were M1-immunoreactive. In this case, the overall local effect of M1 agonism may be more difficult to predict, as the M1 effect in the spines is mostly depolarizing, while the M1 effect in the presynaptic terminal is mainly inhibitory of glutamate release. M1 and NMDA glutamate receptors were documented to colocalize in hippocampal dendritic spines, where M1 potentiates NMDA-mediated LTP and synaptic plasticity. The presence of M1 immunoreactivity just in a subset of spines suggests specificity for some excitatory inputs, of possible thalamic, cortical, hippocampal or intra-amygdalar sources (McDonald and Mascagni 2010; Muller et al. 2013).

Washburn and Moises (1992) have found that muscarinic agonists reduced the amplitude of synaptically-evoked excitatory post-synaptic potentials (EPSP) and inhibitory post-synaptic potentials (IPSP) in pyramidal cells by means of a presynaptic mechanism, even if the subtype of muscarinic receptor was not ascertained. Yajeya and colleagues (Yajeya et al. 2000), using pirenzepine to block M1 muscarinic receptors, documented 20% of reduction of synaptically-evoked EPSPs in pyramidal cells. Liu and colleagues (2012) have found that

acetylcholine suppresses both cortical and thalamic inputs to BL pyramidal neurons via M1 receptors (Muller et al. 2013).

In ultrastructural investigation of BL, VAcHT+ terminals are often seen in close proximity to noncholinergic unlabelled terminals forming symmetrical synapses and to terminals unlabelled or immunoreactive for calcium-calmodulin dependent kinase II (CaMKII) forming asymmetrical synapses. Most of symmetrical synapses on pyramidal cells in BL are originated from the several types of GABAergic interneurons. Nonetheless, some symmetrical synapses in BL are formed by presynaptic elements of monoaminergic or cholinergic types. Cholinergic terminals also form synaptic contacts of asymmetrical type, even if less frequently (Muller et al. 2013, 2016).

The close proximity enables cholinergic synapses to modulate other neurotransmitter's inputs (and vice versa) to BL neurons, as well as the post-synaptic response of the latter. In addition, during bursts of high activity of the cholinergic afferents, the spillover from cholinergic synapses is probable to modulate the release of neurotransmitters, such as GABA and glutamate, from noncholinergic terminals, if they express cholinergic receptors. In general, presynaptic muscarinic receptors inhibit, while nicotinic receptors stimulate the neurotransmitter release from glutamatergic and GABAergic terminals. In the lateral nucleus of the BL complex, muscarinic suppression of the GABA and glutamate release has been proven to be subtype specific, mediated by M1 and M3 muscarinic receptors (Sugita et al. 1991). Also, M2 receptor was documented to differentially reduce the inhibitory transmission in distinct subpopulations of GABAergic interneurons in hippocampus (Szabó et al. 2010).

Nicotinic enhancement of GABA and glutamate release also was proven to be subtype specific. Terminals forming asymmetrical synapses in BL have been proven to be terminals from glutamatergic projection neurons in the cortex, midline/intralaminar thalamic nuclei, and inter/intranuclear amygdalar connections. Cortical afferent glutamatergic and GABAergic terminals express nicotinic receptors respectively with  $\alpha 7$ ,  $\alpha 4/\beta 2$  subunits, and  $\alpha 3/\beta 4$  subunits (Muller, Mascagni, and McDonald 2011). The presence of specific subtypes of muscarinic and nicotinic receptors in elements of GABAergic and glutamatergic synapses in amygdala most probably represents a specialization to promote the selective enhancement of specific bi- or trisynaptic pathways depending on the pattern of cholinergic firing (Muller, Mascagni, and McDonald 2011; Muller et al. 2016).

Muscarinic receptors in presynaptic terminals usually inhibit neurotransmitter release. They are present also in BL GABAergic terminals from projection neurons located in BF (which accounts for 10-15% of the BL terminals from BF source), where they cause a fast attenuation of vesicle fusion and exocytosis. This should contribute to a short-lasting rapid disinhibition of pyramidal neurons. This complex interplay between

acetylcholine and GABA from BF neurons is postulated to play a key role in the synchronization of oscillatory activity in the networks of amygdala, hippocampus and other limbic areas (Muller, Mascagni, and McDonald 2011).

The main function associated with cholinergic neurotransmission in the amygdala is the consolidation of several types of memory. It is thought that BL makes possible memory consolidation by enhancing interactions between hippocampus and neocortical areas of memory storage (Paré, Collins, and Pelletier 2002). These interactions seem to depend on the synchronization of theta rhythm across the networks of the aforementioned areas. This creates recurring time windows which make easier synaptic interactions and, therefore, synaptic plasticity. Many anatomical and physiological research data support the critical role of the BF cholinergic input on BL pyramidal and PV-immunoreactive neurons in generating these synchronized oscillations.

Apart from the extensive projections to far distant areas such as cortex and hippocampus, BL pyramidal cells also send massive local inputs to other surrounding pyramidal cells. This could promote synchronous firing of BL neurons (Paré and Gaudreau 1996; Smith, Paré, and Paré 2000). PV+ basket cells in hippocampus are interconnected by dendritic gap junctions in addition to GABAergic chemical synapses. This also has been proven to promote synchronized firing of basket cells, which is important for the generation and maintenance of synchronous oscillations in hippocampus (Freund and Gulyás 1997; Szabó et al. 2010). Interactions like these were recently proven to occur also in BL, where they can promote the firing of a large number of neighboring pyramidal cells via important inhibitory perisomatic inputs (Rainnie et al. 2006; Woodruff and Sah 2007).

## Chapter 3

### Aims and thesis overview

This thesis contains research on the pathophysiology of MTLE. This disease has a relatively high prevalence in adult population, being often complicated by comorbidities and poor response to the clinical treatment. This PhD research aimed to deepen the understanding of some aspects of pathologic plasticity in MTLE, which may be useful as framework for disease modifying treatments as well as response predictors. The results obtained may help to better understand pathological plasticity of cholinergic elements in some brain nuclei. In addition, an investigational molecule was evidenced as a prototype for AED development.

In the chapter 4, we quantified and discussed the neuroplastic changes in the BF of rats submitted to the KA model of MTLE at a cell and circuitry level. In order to do this, we employed morphometric analysis on slices immunostained for the vesicular acetylcholine transporter (VAcHT). Plastic alterations in the limbic system have been exhaustively investigated in MTLE models. In contrast, such alterations in BF areas have been rather overlooked, in spite of the important connections between both systems. We found hypertrophy of cholinergic neuronal bodies in three different areas of BF that projects mainly to the amygdala, but also to the cortex and thalamus. One of the four BF areas analyzed had no change in the cholinergic cell volumes. This area projects almost exclusively to the olfactory (piriform) cortex and tubercle, which are extensively damaged in post-SE animals. The volume of the basolateral amygdaloid nucleus, which is the main target of cholinergic projection in amygdala, was reduced about 25%. The density of cholinergic axon nerve thickenings (varicosities) in the basolateral nucleus was not changed. This apparent discrepancy may be related to neurodegeneration, mostly of parvalbumin interneurons in the basolateral nucleus, and consequent reorganization of synaptic terminals and its post-synaptic targets.

In the Chapter 5, we studied the antiepileptic and neuroprotective effects of a proline derivative, (NMP), the major constituent of a plant extract, in the model of MTLE induced by i.c.v. pilocarpine. The NMP-enriched extract counteracted in a dose-dependent fashion the loss of neurons in CA1 and CA2 subfields of the hippocampus in the mice post-SE. At the same time, the counting of viable cells in DG was not altered. The immunoreactivity for Iba-1 and GFAP, respectively markers of activated microglia and astrocytes, was significantly decreased by the two higher doses. The performance in the memory tests of novel object recognition and T-maze was significantly impaired by i.c.v. pilocarpine. It returned to control levels in both higher NMP doses. *In silico* docking experiments showed that the most probable target of NMP is the GABA uptake GAT-1, the same of the antiepileptic tiagabin.

In the Chapter 6, we report moderate to strong correlations between the dynamics of the acute symptomatic SE induced by systemic KA in rats and the latency and staging of the spontaneous recurrent seizures of the chronic period, as well as with the resulting lesions in the acute and chronic time points.

In the chapter 7, the thesis is discussed and summarized under the perspective of the future efforts to identify pathophysiological processes, which may offer a window for therapeutic intervention.

## Chapter 4

### Neuroplasticity in cholinergic projections from the basal forebrain to the basolateral nucleus of the amygdala in the kainic acid model of temporal lobe epilepsy<sup>1</sup>

Ítalo Rosal Lustosa,<sup>1</sup> Joana I. Soares,<sup>2,3,4,5</sup> Giuseppe Biagini,<sup>6,7,\*</sup> and Nikolai V. Lukoyanov<sup>2,3,4,\*</sup>

<sup>1</sup>Clinical and Experimental Medicine PhD Program, University of Modena and Reggio Emilia, Modena, Italy;

<sup>2</sup>Instituto de Investigação e Inovação em Saúde, Universidade do Porto, Porto, Portugal; <sup>3</sup>Instituto de Biologia

Molecular e Celular da Universidade do Porto, Porto, Portugal; <sup>4</sup>Departamento de Biomedicina, Faculdade de

Medicina da Universidade do Porto, Porto, Portugal; <sup>5</sup>Programa Doutoral em Neurociências, Universidade do

Porto, Porto, Portugal; <sup>6</sup>Department of Biomedical, Metabolic and Neural Sciences, University of Modena and

Reggio Emilia, Modena, Italy; <sup>7</sup>Center for Neuroscience and Neurotechnology, University of Modena and

Reggio Emilia, Modena, Italy

#### ABSTRACT

The amygdala is a cerebral region whose function is compromised in temporal lobe epilepsy (TLE). Patients with TLE present cognitive and emotional dysfunctions, of which impairments in recognizing facial expressions have been clearly attributed to amygdala damage. However, damage to the amygdala has been scarcely addressed, with the majority of studies focusing on the hippocampus. The aim of this study was to evaluate epilepsy-related plasticity of cholinergic projections to the basolateral nucleus (BL) of the amygdala. Adult rats received kainic acid (KA) injections and developed status epilepticus. Weeks later, they showed spontaneous recurrent seizures documented by behavioral observations. Changes in cholinergic innervation of the BL were investigated by using an antibody against the vesicular acetylcholine transporter (VAcHT). In KA-treated rats, it was found that (i) the BL shrunk to 25% of its original size ( $p < 0.01$  vs. controls, Student's  $t$ -test), (ii) the density of vesicular acetylcholine transporter-immunoreactive (VAcHT-IR) varicosities was unchanged, (iii) the volumes of VAcHT-IR cell bodies projecting to the BL from the horizontal limb of the diagonal band of Broca, ventral pallidum, and subcommissural part of the substantia innominata were significantly increased ( $p < 0.05$ , Bonferroni correction). These results illustrate significant changes in the basal forebrain cholinergic cells projecting to the BL in the presence of spontaneous recurrent seizures.

**Keywords:** acetylcholine, basolateral nucleus of amygdala, basal forebrain, kainic acid, neuronal plasticity, temporal lobe epilepsy

#### INTRODUCTION

---

I *Published in International Journal of Molecular Sciences, 2019*

Epilepsy is a neurological disease (Fisher et al. 2014) affecting 65 million people around the world (Moshé et al. 2015). Associated with inherent comorbidities, this condition brings about decreased life expectancy, impaired life quality, loss of working years, and heavy healthcare costs (Beghi 2016; Cameron et al. 2012; Kwan et al. 2010; Mula et al. 2016; Thurman et al. 2017). The enduring tendency of generating spontaneous recurrent seizures, which characterizes epilepsy, is believed to be due to neuroplastic alterations at molecular, cellular, and circuitry levels, such as aberrant neurogenesis subsequent to the death of susceptible cell populations, rewiring, neuronal hyperexcitability and/or hypoexcitability, and other pathophysiological changes, including neuroinflammation and alterations in the extracellular matrix and blood-brain barrier (Clossen and Reddy 2017; Klement et al. 2018; Łukawski et al. 2018; Ravizza and Vezzani 2018; van Vliet et al. 2018). Temporal lobe epilepsy (TLE) accounts for approximately 75% of epilepsy cases in adults, and is the most prevalent type of focal epilepsy in that population (Behr et al. 2016; Singh and Trevick 2016; Thom and Bertram 2012).

The administration of kainic acid (KA) to rodents (Ben-Ari et al. 1980; Ben-Ari 1985; Cronin and Dudek 1988; Dudek et al. 2006; Hellier et al. 1998) followed by status epilepticus (SE) represents one of the best characterized models of TLE, which, compared to other animal models, most closely mimics the behavioral, histopathologic, electrographic, and drug-response features of human TLE (Du et al. 1995; Gill, Mirsattari, and Leung 2017; Lothman and Collins 1981; Nadler 1981; Parrish et al. 2013; Schwob et al. 1980; Suzuki et al. 1997). Previous works from our group have found that the KA model of TLE is characterized by neuroplastic alterations in cholinergic neurons of the medial septum and vertical limb of the diagonal band of Broca (MS/VDB) projecting to the hippocampal formation (Soares et al. 2017), as well as in the brainstem pedunculopontine and laterodorsal nuclei (Soares et al. 2018). Since the amygdaloid complex, or more precisely its basolateral (basal) nucleus (BL), receives the densest cholinergic terminal projection in the central nervous system of both rodents and primates (Ben-Ari et al. 1977; Carlsen, Záborszky and Heimer 1985; Li et al. 2001), and because various subdivisions of the BL undergo remarkable structural changes in epilepsy, we found it of interest to evaluate the effects of KA-induced epilepsy on the BL cholinergic afferents.

## **RESULTS**

### **Monitoring for Spontaneous Seizures**

Two rats died acutely within 24 h following treatment with KA. During the first four weeks following KA injection, spontaneously recurrent stage 1–3 seizures on the Racine scale (Lothman and Collins 1981; Racine 1972), that is, uncontrolled mouth and facial clonic movements and moderate forelimb clonus, were observed in only three rats from the KA group. However, in the remaining period of observation, all rats in

the KA group displayed spontaneous stage 1–3 seizures. At least two spontaneous generalized behavioral seizures of stage 4–5 on the Racine scale were documented in all remaining KA-treated rats. Thus, the final group size for the KA-treated rats was  $n = 6$ . No behavioral seizures were observed in the control group ( $n = 6$ ).

### **Basolateral nucleus volume**

[Figure 1](#) shows representative images of level-matched sections cut through the BL and stained for vesicular acetylcholine transporter (VAcHT) of a control rat and a KA-treated epileptic rat. As can be seen in these images, the epileptic state was associated with a decrease in volume of the BL. Volumes of the BL, estimated with an average coefficient of errors equal to 0.019, are shown in [Figure 2](#) for both groups. Statistical comparisons of these estimates confirm significant shrinkage of the BL, approximately 25%, in KA rats, when compared to control rats ( $p < 0.01$ , Student's  $t$ -test).

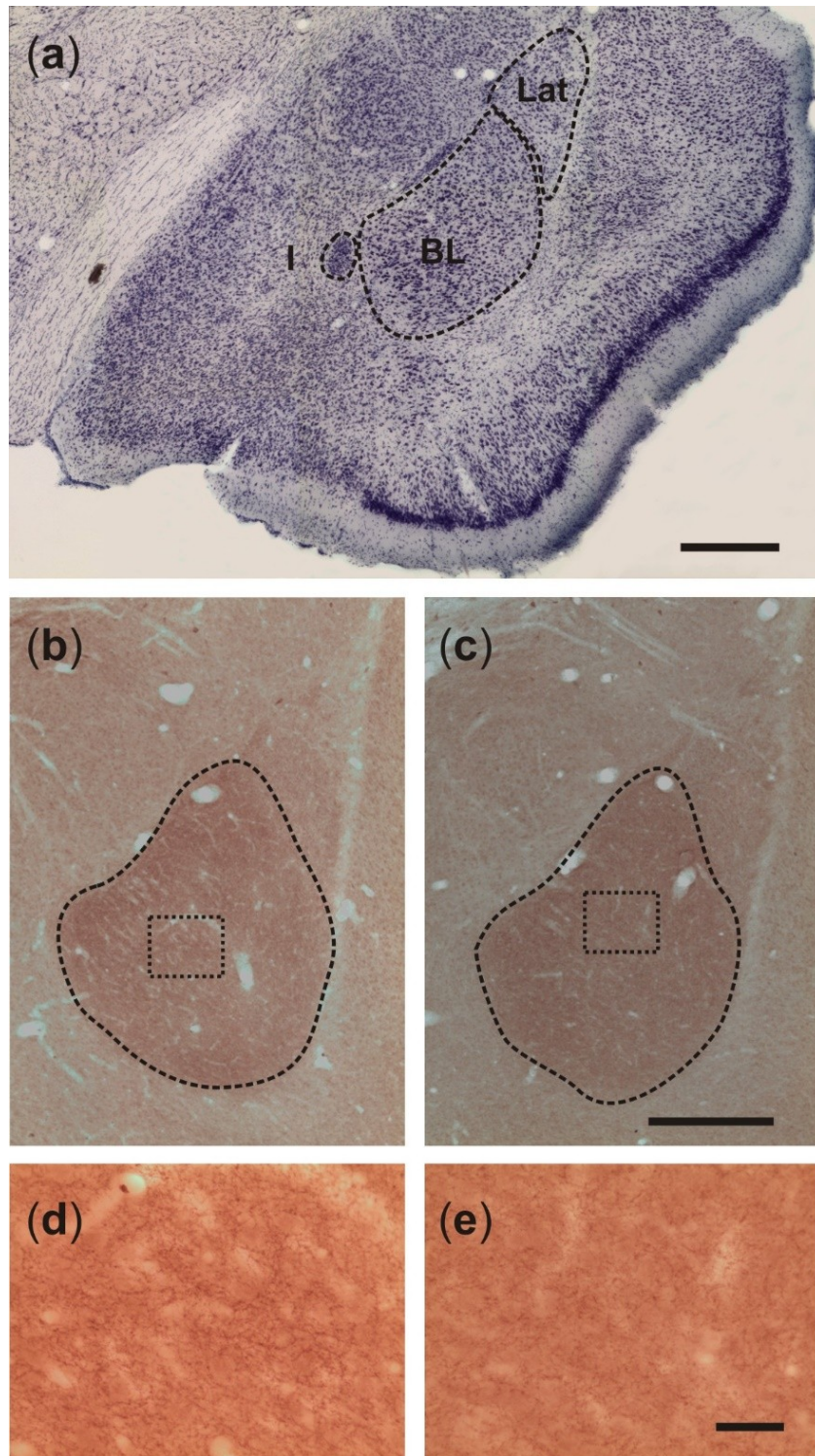


**Figure 1** (a) Photograph of a representative Nissl-stained coronal section cut through the anterior part of the temporal lobe and showing the location of the basolateral nucleus (BL) relative to the neighboring lateral (Lat) and intercalated (I) nuclei. Scale bar, 200  $\mu\text{m}$ . (b,c) Photomicrographs of representative vesicular acetylcholine transporter (VACHT)-stained sections obtained from control and post-SE rats, respectively. Note that the BL is more densely stained when compared to the lateral nucleus and other surrounding amygdaloid nuclei. The images are suggestive of moderate shrinkage of the BL in the post-SE rat. Scale bar, 200  $\mu\text{m}$ . (d,e) Higher-power photomicrographs taken from the areas shown in insets (b,c),

respectively. Note that the density of VAcHT-stained fibers and fiber varicosities do not differ between the rats. Scale bar, 30  $\mu\text{m}$ .

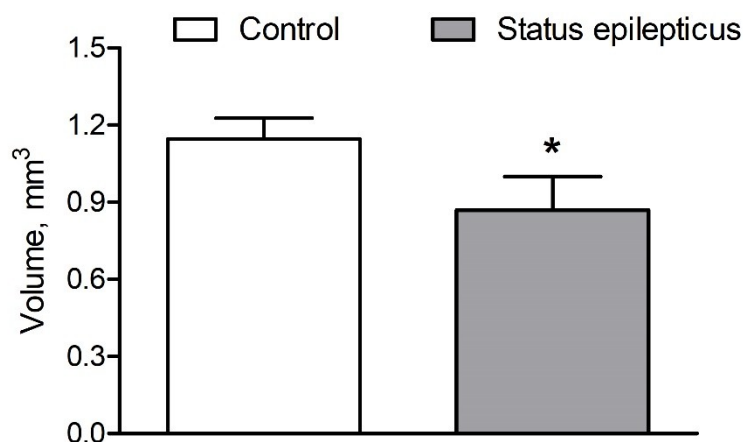


**Figure 2. Effect of KA-induced status epilepticus (SE) on the total volume of the BL (mean  $\pm$  standard deviation).** Note that kainate treatment resulted in a 25% shrinkage of the BL as delineated in immunostained material (Figure 1). \*  $p < 0.01$ , Student's  $t$ -test.

#### Density of VAcHT-Immunoreactive Fiber Varicosities

Representative photomicrographs shown in [Figure 1b-e](#) illustrate VAcHT-immunoreactive fibers organized in a dense network of terminals, which bear many varicosities of different shapes and sizes in the rat BL. However, the densities of the fibers and varicosities do not appear to differ considerably between control rats and post-SE rats. [Figure 3](#) shows quantitative estimates of the areal density of VAcHT-IR varicosities in the BL of control rats and post-SE rats. Both visual inspection of this plot and statistical analysis of the estimates (Student's  $t$ -test) confirmed no differences between the two groups ( $p > 0.05$ ).

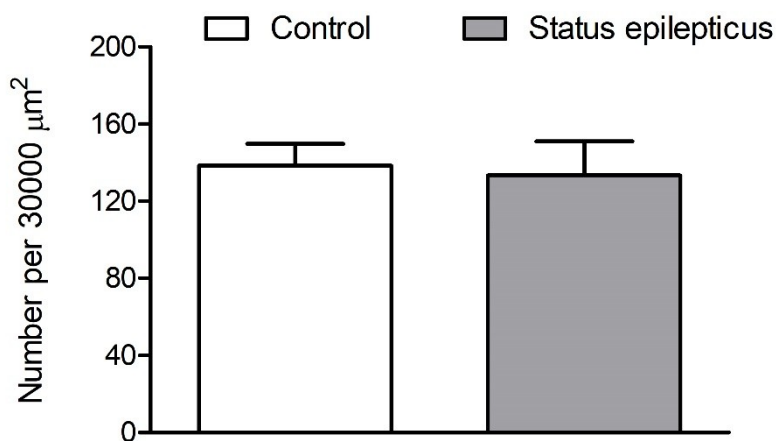


**Figure 3. Graphic representation of the quantitative estimates obtained for the areal densities of vesicular acetylcholine transporter (VAcHT)-stained varicosities in the BL of control and epileptic rats (see Figure 6).** Values represent mean  $\pm$  standard deviation. No differences between the groups were found.

### **Somatic Volume of VAcHT-Immunoreactive Cells**

[Figure 4](#) shows representative microphotographs of VAcHT-immunostained sections cut through the basal forebrain of a control rat ([a,b](#)) and a KA-treated epileptic rat ([g,h](#)). As can be inferred from the higher-power images in [Figure 4c-f, i-l](#), respectively, the VAcHT-IR cells of epileptic rats possess larger perikarya compared to respective cells of control rats. The mean somatic volumes of the VAcHT-stained cells measured in four distinct areas of the basal forebrain are graphically represented in [Figure 5](#). Multivariate analysis of variance (MANOVA) of these data yielded a significant main effect of treatment (Rao's  $R_{4,5} = 6.65$ ,  $p < 0.05$ ). Bonferroni correction for multiple comparisons revealed that the perikarya of cholinergic cells were significantly enlarged in post-SE rats in the horizontal limb of the diagonal band of Broca (HDB; 44%,  $p < 0.05$ ), ventral pallidum (VP; 75%,  $p < 0.005$ ), and substantia innominata (SI; 66%,  $p < 0.005$ ), but not in the magnocellular preoptic nucleus (MCPO; 9%,  $p > 0.05$ ).

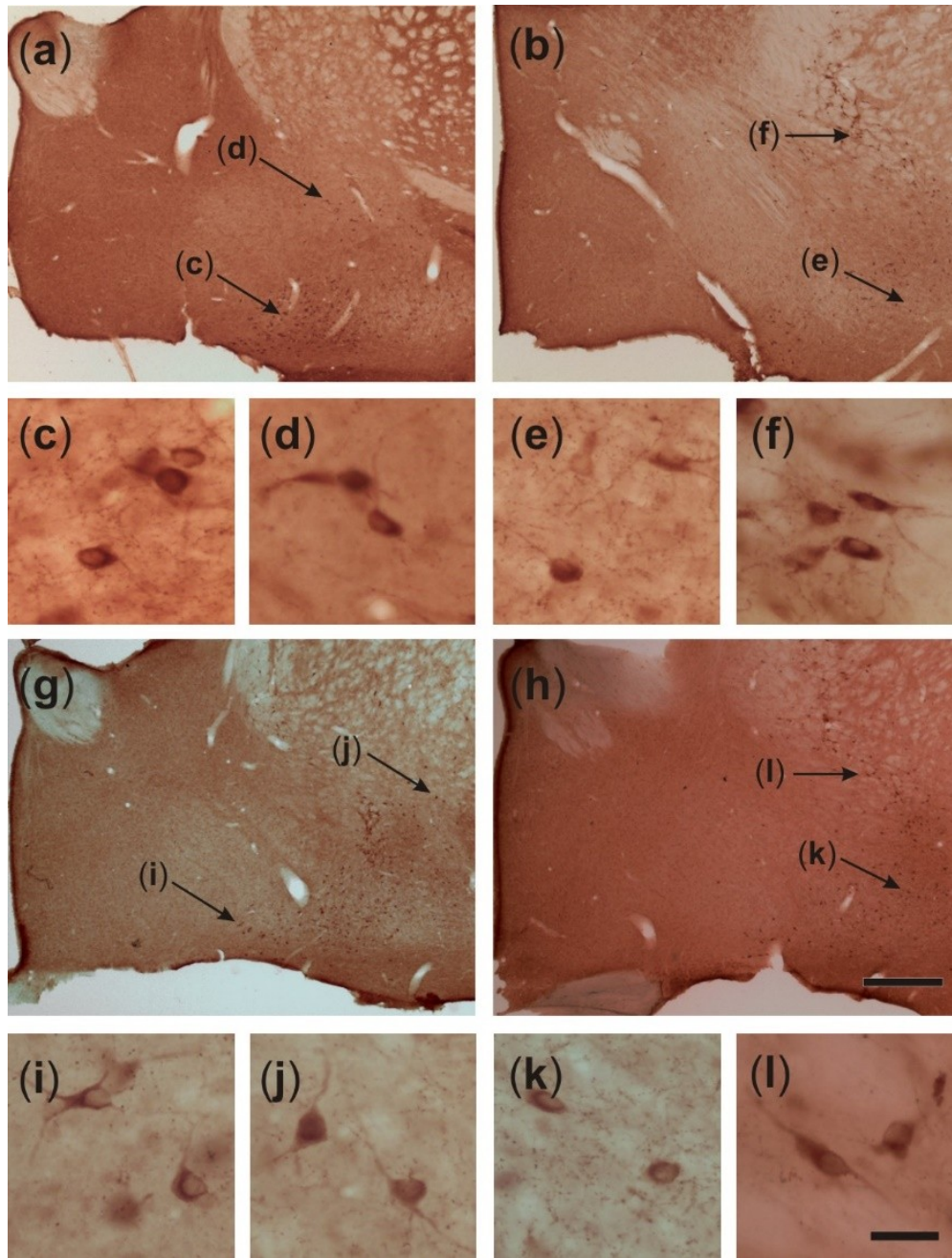


**Figure 4.** (a,b) Photomicrographs of representative vesicular acetylcholine transporter (VAcHT)-stained coronal sections obtained from the brain of a control rat and showing four subdivisions of the basal forebrain projecting to the BL, horizontal limb of the diagonal band of Broca (HDB) (c), subcommissural part of substantia innominata (SI) (d), magnocellular preoptic nucleus (MCPO) (e), and ventral pallidum (VP) (f). The sections shown in (a,b) were cut approximately at levels of  $-0.72$  and  $-1.20$  mm, posterior to bregma, respectively (c-f). Higher-power photomicrographs of neurons indicated in (a,b) by arrows and belonging to the four basal forebrain subdivisions. (g,h) Photomicrographs of the respective VAcHT-stained sections obtained from an epileptic rat. The sections (a-g,b-h) were cut at approximately the same levels relative to the bregma. (i-l) Higher-power photomicrographs of neurons found in the HDB, SI, MCPO, and VP of the epileptic rat. Precise locations of these neurons in the basal forebrain subdivisions are shown by arrows in (g,h). Note that neurons located in the HDB, SI, and VP of the epileptic rat possess larger perikarya than respective neurons of the control rat. Scale bars, 400 (a,b,g,h) and 30  $\mu\text{m}$  (c-f,i-l).

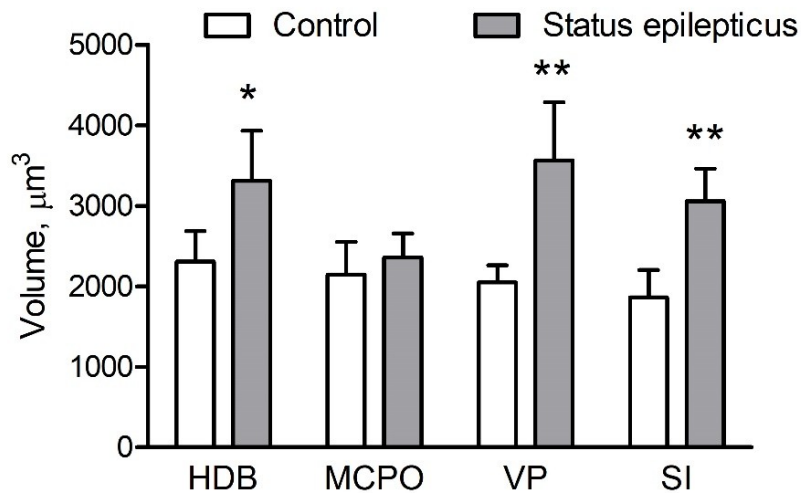


**Figure 5. Graphic representation of stereological estimates for the mean somatic volume (mean  $\pm$  standard deviation) of vesicular acetylcholine transporter-immunoreactive (VACHT-IR) cells in four distinct subdivisions of the basal forebrain.** Note that post-SE rats have enlarged cholinergic neurons located in the HDB, VP, and SI, but not in MCPO. \*  $p < 0.05$  and \*\*  $p < 0.005$  vs the respective control region, Bonferroni correction.

## DISCUSSION

The basolateral region of the amygdala is densely innervated by cholinergic afferents originating in different subdivisions of the basal forebrain, which suggests an important role of acetylcholine in modulating amygdala functions, including the processing of memory and emotion (Emre et al. 1993; Pitkänen, Jolkkonen and Kempainen 2000; Ménard, Hodes and Russo 2015). The main results of the present study are that, in epilepsy, this projection system undergoes severe modifications, which include significant decreases of that part of the amygdala that receives the densest cholinergic innervation, and abnormal increases of the perikarya of cells projecting to that part. Thus, it is likely that the changes in the amygdalopetal cholinergic connections to the basal forebrain described here may contribute to epilepsy-related hyperexcitability of amygdaloid neurons and comorbid deficits in amygdala-dependent behaviors.

Compared to the large body of data regarding the hippocampal pathology in TLE and respective animal models, the pathology of the amygdala in epilepsy has been relatively overlooked, having been addressed in just a few studies (Narkilahti et al. 2003; Pirttila et al. 2001; Pitkänen et al. 1998; Salmenperä et al. 2002; Tuunanen, Halonen and Pitkänen 1996; Tuunanen, Halonen and Pitkänen 1997; Tuunanen et al. 1999; Tuunanen and Pitkänen 2000). However, the amygdala is equally acknowledged as a brain area of very low ictal threshold, and kindling of the amygdala is one of the best known and characterized models of epilepsy (Goddard, McIntyre, and Leech 1969; McIntyre 2006). Furthermore, in models where focal seizures are elicited in extra-amygdaloid areas, the amygdala plays a pivotal role in seizure spreading. For instance, in the

audiogenic model of seizures, the ictal activity initiated in a primary brainstem focus (inferior colliculus of the mesencephalon) subsequently recruits the amygdala via the medial geniculate body prior to spreading to other forebrain structures (Dutra Moraes, Galvis-Alonso and Garcia-Cairasco 2000; Galvis-Alonso, Cortes De Oliveira and Garcia-Cairasco 2004; Faingold 2012). Moreover, in human TLE, the amygdala can contain the main epilepsy focus in 5% of patients (Wieser 2000). In the present study, we found that chronic epilepsy in rats is associated with dramatic shrinkage of the BL, which is consistent with the results of prior studies (Cendes, Andermann, Dubeau et al. 1993; Cendes, Andermann, Gloor et al. 1993; Cendes, Leproux, Melanson et al. 1993; Kälviäinen and Salmenperä 2002; Pitkänen et al. 1998; Salmenperä et al. 2002). Similarly, magnetic resonance volumetric measurements of the amygdala in TLE have shown an average 20% volume reduction in 19% of the general population with TLE (Bronen et al. 1995; Kälviäinen et al. 1997), and a 10%–30% volume reduction in patients with drug-refractory TLE (Cendes, Andermann, Dubeau, et al. 1993; Cendes, Andermann, Gloor, et al. 1993). Shrinkage of the amygdala in epilepsy is likely to result from neurodegenerative changes in this brain region, similar to those described in hippocampal sclerosis. Indeed, significant neuronal loss or reactive gliosis were reported in the basal (Margerison and Corsellis 1966; Pitkänen et al. 1998) and lateral (Hudson et al. 1993; Miller et al. 1994; Pitkänen et al. 1998) nuclei of the amygdala in TLE patients. In animal models, some amygdala components, including the anterior cortical and medial nuclei, the medial division of the lateral nucleus, the parvicellular division of the basal nucleus, and the accessory basal nucleus were reported to be more susceptible to neuron loss with respect to other cerebral regions (Tuunanen, Halonen and Pitkänen 1996; Tuunanen et al. 1999; Pitkänen et al., 1998). In addition, there is evidence that GABAergic interneurons are particularly vulnerable to seizure-induced damage (Tuunanen, Halonen, and Pitkänen 1996, 1997; Tuunanen et al. 1999; Tuunanen and Pitkänen 2000; Pitkänen et al. 1998; Callahan et al. 1991) which leads to impaired feed-forward inhibition of principal amygdaloid neurons (Rainnie, Asproдини and Shinnick-Gallagher 1992).

Cholinergic afferents play an important role in modulating the excitability of intrinsic neuronal circuits of the amygdala. The vast majority of cholinergic terminals form symmetric (putatively inhibitory) synapses on the dendritic shafts and spines of principal pyramidal neurons and on the perikarya of interneurons (Carlsen and Heimer 1986; Muller et al. 2016). However, parts of the synapses possess characteristics of excitatory synapses (Muller et al. 2016) and principal cells of the amygdala are rich in both M1 (depolarizing) (McDonald and Mascagni 2010) and M2 (hyperpolarizing) (McDonald, Muller and Mascagni 2011) muscarinic receptors. Thus, it is plausible that cholinergic afferents have rather modulatory than inhibitory effects in the amygdala. Complementing previous experiments that illustrated an approximate 20% reduction in choline acetyltransferase activity (Schliebs et al. 1989), accompanied by a remarkable decrease in muscarinic receptor binding, we found that the areal density of cholinergic terminals was unchanged in the epileptic BL

despite the considerable reduction of the total BL volume innervated by cholinergic fibers. Considered together with prior data showing preferential loss of GABAergic neurons in the amygdala of epileptic animals (Callahan et al. 1991; Tuunanen, Halonen, and Pitkänen 1996, 1997; Tuunanen et al. 1999), our results suggest that induction of the chronic epilepsy state, at least in this model, alters the main pattern of cholinergic innervation in the BL. More specifically, it can be hypothesized that the cholinergic terminals, due to GABAergic cell loss, were relocated toward new targets, which could be dendritic and somatic membranes of pyramidal cells. This mechanism may be either compensatory, that is, aimed to provide additional inhibitory drive upon hyperexcitable BL principal neurons, or, in contrast, it may contribute to their hyperexcitability. Although further studies are necessary to address this issue in detail, the present findings clearly show that reorganization of the BL cholinergic network is likely to be one of the fundamental mechanisms underlying amygdala dysfunction in epilepsy.

These findings are consistent with our previous reports showing that KA-induced SE triggers marked reorganization of cholinergic afferents in the hippocampal formation, namely relocation of VAcHT-containing terminals from the hilus of the DG to its molecular layer (Soares et al. 2017; Lukoyanov et al. 2004). This reorganization was found to be associated with a general activation of the septohippocampal cholinergic projection system, as indicated by the fact that cholinergic cells located in the MS/VDB regions projecting to the DG of epileptic rats had approximately 40% larger cell bodies compared to control rats (Soares et al. 2017). In this study, we estimated the somatic volumes of cholinergic cells in four distinct subdivisions of the basal forebrain, all of which project to the BL, although to different extents. In the HDB the cholinergic cells were enlarged by 44%, which is similar to what was previously found in the MS/VDB. Yet, even more profound hypertrophic changes were found in VAcHT-IR cells located in the VP (75%) and SI (66%), suggesting that these regions are particularly implicated in epilepsy-related cholinergic plasticity. These data are compatible with the results of neuroanatomical studies showing that VP and SI neurons make a major contribution to cholinergic innervation of the amygdala (Carlsen, Zaborszky and Heimer 1985; Soares et al. 2019; Woolf, Eckenstein and Butcher 1984). Interestingly, neurons located in the MCPO, which send only a small number of cholinergic afferents to the amygdala, were not significantly enlarged. Although the importance of cholinergic plasticity in epilepsy is not yet clarified, the results of one study (Soares et al. 2019) indicate that site-specific inhibition of neuronal hypertrophy in the medial septum reduces seizure susceptibility and partially prevents epileptogenesis in a subset of KA-treated rats. Considered together with the present findings, these data suggest that a more widespread blockage of seizure-driven cholinergic hypertrophy, including in the medial septum and the regions examined in this study, might provide better protection against seizures and epileptogenesis.

In conclusion, the present study provides the first evidence of hypertrophic changes in the basal forebrain cholinergic cells projecting to the amygdala. These findings support the idea that epilepsy-related neuroplasticity of the forebrain cholinergic neurons can contribute to epileptogenesis as well as to epilepsy-related comorbid diseases. Thus, unraveling the biochemical pathways and physiological mechanisms that prompt hypertrophic changes in cholinergic neurons may offer new molecular targets for the development of novel therapeutic approaches to drug-resistant types of epilepsy.

## **MATERIALS AND METHODS**

### **Ethical statement**

The handling and care of animals was conducted according to the “Principles of laboratory animal care” (NIH publication No. 86-23, revised in 1985) (Committee for the Update of the Guide for the Care and Use of Laboratory Animals 2011) and Directive 2010/63/EU of the European Parliament. All experiments have been previously carefully evaluated and received approval by the Ethics Committee (Faculty of Medicine of Porto) and the General Veterinary Direction (3 April 2012) for the FCT application grant PTDC/SAU-NSC/115506/2009. Animals used were only those strictly required for the experiments and suffering was limited as much as possible.

### **Animals and treatments**

Ten-week-old male Wistar rats were randomly assigned to two groups, respectively, and given intraperitoneal (i.p.) injections of either kainic acid, 9.5 mg/kg, (KA group,  $n = 9$ ) or the corresponding volume of saline (Ctrl group,  $n = 6$ ). The animals were placed in individual boxes for behavioral observation and quantification for 6 h. Motor seizures were scored according to the modified Racine scale for generalized motor seizures of focal limbic initiation (Lothman and Collins 1981; Racine 1972). The onset of SE was defined as seizures scored as Racine’s stage 3–5, lasting for at least 20 min with no recovery of “baseline” behavior, such as grooming, sniffing, and exploratory activity (Soares et al. 2019). One animal from the KA group exhibited numerous wet dog shake seizures, but did not reach Racine’s stage 3 or higher; this rat was excluded from the experiment. No seizure-like behavior was observed in rats given saline. Post-SE care consisted of evaluating the general state of animals twice a day, and giving subcutaneous saline injections, as well as moisturized chow from a plastic syringe. Starting from the second week after KA or vehicle treatments, the rats were daily monitored (except weekends) for the appearance of spontaneous motor seizures during at least two 2 h intervals (9:00–11:00 and 14:00–16:00) by an investigator blind to treatment groups.

### **Immunohistochemistry and histology**

Four months after the induction of SE, i.p. pentobarbital (90 mg/kg) was administered to animals to induce a deep anesthesia; then, animals were transcardially perfused with phosphate buffered saline (PBS), pH 7.4, 150 mL for vascular rinse, followed by paraformaldehyde 4% diluted in PBS, 250 mL for fixation. After removal, brains were immersed in fixative for 2 h and then immersed in 10% sucrose solution for 36 h at 4 °C. Afterwards, brains were vibratome-cut in 40 µm sections and stored in cryoprotectant (sucrose 30%, ethylene glycol 30%, polyvinylpyrrolidone 0.25%, in PBS) at -20 °C until use.

Every sixth section, including basal forebrain and BL, was systematically sampled and immunostained for VAcHT. Preceding primary antibodies, sections were rinsed in PBS (3 times) and endogenous peroxidases were blocked by immersing the sections in 1% H<sub>2</sub>O<sub>2</sub> PBS solution for 15 min. Then, sections were washed in PBS (6 times, 5 min each) and blocked for nonspecific staining by immersion in 10% normal goat serum (NGS) + 0.5% Triton X-100 in PBS. Subsequently, sections were incubated in the presence of a VAcHT guinea-pig primary antibody (Merck Millipore AB1588; 1:1250 dilution in PBS) for 72 h at 4 °C. After washing in PBS containing 2% NGS (3 times, 10 min each), sections were incubated with a biotinylated anti-guinea-pig antibody (BA7000, Vector Laboratories, Burlingame, CA 94010, USA, diluted 1:200 in 0.02 M PBS). Finally, sections were washed 3 times (10 min each) and incubated with avidin-biotin-peroxidase complex (Vector laboratories, Vectastain Elite ABC Kit) to perform the peroxidase reaction with 3,3'-diaminobenzidine (1 mg/mL) and H<sub>2</sub>O<sub>2</sub> (0.08% in PBS). Further washing (2 times) with PBS preceded section mounting on gelatin-coated slides and overnight drying. For glass coverslipping, sections were dehydrated and covered with Histomount (National Diagnosis, Atlanta, GA, USA).

Nissl staining was performed using another set of regularly sampled sections (1:6), which were mounted on gelatin-coated slides and air-dried to be stained with Giemsa, dehydrated, and coverslipped with Histomount.

### **Density of VAcHT-immunoreactive varicosities**

Three to four consecutive VAcHT-stained sections containing the BL were sampled from each brain. Sections were level-matched in all animals included in our analysis, by means of the rat brain atlas (Paxinos and Watson 2005). An Axio Scope.A1 microscope (Zeiss, Germany) equipped with a Leica EC3 color digital camera was used to visualize sections. BL boundaries were defined with a 10× objective lens on the basis of the rat brain atlas. For the purposes of the present study, we did not distinguish between the subdivisions of the BL nucleus (Pitkänen, Jolkkonen and Kempainen 2000; Paxinos and Watson 2005). In each section, four photomicrographs of the central area of the BL were taken, bilaterally, with a 100× objective lens, totaling 24–32 images per animal. Using the Fiji image-processing software (<http://rsb.info.nih.gov/ij/>) and a frame

of 1421  $\mu\text{m}^2$  superimposed onto each image, we measured all varicosities and their respective cross-sectional areas as found within the frame. Only fiber varicosities within cross-sectional areas ranging between 0.11 and 0.21  $\mu\text{m}^2$  were then included for further analysis. Varicosities' densities were normalized using an arbitrary area of 30,000  $\mu\text{m}^2$  and averaged for all sections/animal.

### **Estimation of BL volume**

An Olympus BX-53 microscope equipped with a computer-controlled motorized stage system (MBF Bioscience, Williston, ND, USA) was used to visualize all sections containing the BL. The boundaries of the BL were consistently defined at all levels along the rostrocaudal axis using the rat brain atlas and the distinct pattern of BL VAcHT staining, which is characteristic of this part of the amygdaloid complex. Estimations were carried out using the Cavalieri estimator probe of the Stereo Investigator software (MBF Bioscience). The regions of interest were delineated with a 4 × objective lens and a grid size of 20 × 20  $\mu\text{m}^2$  was applied.

### **Estimation of somatic volume of VAcHT-immunoreactive neurons**

VAcHT-stained cells were sampled using an optical fractionator probe (Stereo Investigator software, MBF Bioscience, Williston, VT 05495, USA) to measure each somatic volume. The nucleator probe for isotropic systematically random sampled sections was used for measurements (Gundersen 1988), and each cellular nucleolus was set as a central point. The estimates included the HDB, MCPO, VP, and the subcommissural part of SI. The ROIs were carefully outlined using a 10× objective lens, according to Paxinos and Watson (2005) for the HDB and MCPO, and Geeraedts, Nieuwenhuys and Veening (1990) for the VP and SI. The coefficient of error for each individual estimate was inferior to 0.04 in all measurements for each animal.

### **Statistics**

The volumes of cell bodies were analyzed using MANOVA followed by the Bonferroni post-hoc test for multiple comparisons (Bonferroni correction). The estimates of the BL volume and the density of VAcHT-IR varicosities were analyzed by the two-tailed Student's *t*-test. Results were presented as mean ± SD.

### **AUTHOR CONTRIBUTIONS**

Conceptualization, Í.R.L., J.I.S., G.B. and N.V.L.; investigations, Í.R.L. and J.I.S.; methodology, J.I.S. and N.V.L.; data curation, Í.R.L. and J.I.S.; writing—original draft preparation, Í.R.L., G.B. and N.V.L.; writing—review and editing, Í.R.L., G.B. and N.V.L. supervision, G.B. and N.V.L.; funding acquisition, G.B. and N.V.L. All authors agreed on the results and commented on the manuscript.

**FUNDING**

This work was supported by FEDER Funds through the Programa Operacional Factores de Competitividade COMPETE and National Funds through FCT Fundação para a Ciência e a Tecnologia within the scope of the Project PTDC/SAU-NSC/115506/2009 FCOMP-01-0124-FEDER-015919. The work was supported by the University of Modena and Reggio Emilia (FAR 2018 to GB) for Ítalo Rosal Lustosa.

**CONFLICTS OF INTEREST**

The authors declare no conflict of interest.

## Chapter 5

**A proline derivative-enriched fraction from *Sideroxylon obtusifolium* protects the hippocampus from intracerebroventricular pilocarpine-induced injury associated with *status epilepticus* in mice<sup>II</sup>**

**Pedro Everson Alexandre de Aquino<sup>1</sup>, Jéssica Rabelo Bezerra<sup>1</sup>, Tyciane de Souza Nascimento<sup>1</sup>, Juliete Tavares<sup>1</sup>, Ítalo Rosal Lustosa<sup>2</sup>, Adriano José Maia Chaves Filho<sup>1</sup>, Melina Mottin<sup>3</sup>, Danielle Macêdo Gaspar<sup>1</sup>, Geanne Matos de Andrade<sup>1</sup>, Kelly Rose Tavares Neves<sup>1</sup>, Giuseppe Biagini<sup>4,5,\*</sup>, Edilberto Rocha Silveira<sup>6</sup> and Glauce Socorro de Barros Viana<sup>1,\*</sup>**

<sup>1</sup>Department of Physiology and Pharmacology, Federal University of Ceará, Fortaleza, Brazil; <sup>2</sup>PhD Program in Clinical and Experimental Medicine, University of Modena and Reggio Emilia, Modena, Italy; <sup>3</sup>Laboratory of Molecular Modeling and Drug Design, LabMol, Faculty of Pharmacy, Federal University of Goiás, Goiás, Brazil; <sup>4</sup>Laboratory of Experimental Epileptology, Department of Biomedical Metabolic and Neural Sciences, University of Modena and Reggio Emilia, Modena, Italy; <sup>5</sup>Center for Neuroscience and Neurotechnology, University of Modena and Reggio Emilia, Modena, Italy; <sup>6</sup>Department of Organic and Inorganic Chemistry, Federal University of Ceará, Fortaleza, Brazil

### ABSTRACT

The *N*-methyl-(2*S*,4*R*)-*trans*-4-hydroxy-*L*-proline-enriched fraction (NMP) from *Sideroxylon obtusifolium* was evaluated as a neuroprotective agent in the intracerebroventricular (icv) pilocarpine (Pilo) model. To this aim, male mice were subdivided into sham (SO, vehicle), Pilo (300 µg/1 µL icv, followed by the vehicle *per os*, *po*) and NMP-treated groups (Pilo 300 µg/1 µL icv, followed by 100 or 200 mg/kg *po*). The treatments started one day after the Pilo injection and continued for 15 days. The effects of NMP were assessed by characterizing the preservation of cognitive function in both the Y-maze and object recognition tests. The hippocampal cell viability was evaluated by Nissl staining. Additional markers of damage were studied—the glial fibrillary acidic protein (GFAP) and the ionized calcium-binding adaptor molecule 1 (Iba-1) expression using, respectively, immunofluorescence and western blot analyses. We also performed molecular docking experiments revealing that NMP binds to the  $\gamma$ -aminobutyric acid (GABA) transporter 1 (GAT1). GAT1 expression in the hippocampus was also characterized. Pilo induced cognitive deficits, cell damage, increased GFAP, Iba-1, and GAT1 expression in the hippocampus. These alterations were prevented, especially by the higher NMP dose. These data highlight NMP as a promising candidate for the protection of the hippocampus, as shown by the icv Pilo model.

**Keywords:** mesial temporal lobe epilepsy; pilocarpine; GABA transporter 1; glial fibrillary acidic protein; ionized calcium-binding adaptor molecule 1; *N*-methyl-(2*S*,4*R*)-*trans*-4-hydroxy-*L*-proline; neuroprotection

## INTRODUCTION

Epilepsy affects approximately 65 million people around the world (Moshé et al. 2015), and apart from cerebrovascular diseases, is the third common neurological disorder after dementias and headache (Feigin et al. 2017). Different types of epilepsy exist, with a broad phenotypic spectrum ranging from mild to disabling and life-threatening states. They share recurrent unprovoked or reflex seizures as the hallmark (Fisher et al. 2014). Mesial temporal lobe epilepsy (MTLE) is the most prevalent type of adult epilepsy (Téllez-Zenteno and Hernández-Ronquillo 2012) and is characterized by hippocampal sclerosis (Blümcke et al. 2013), a lesion that has been related to a triggering event such as febrile seizures in childhood, facilitated by a genetic susceptibility background (Shorvon 2011). Hippocampal sclerosis has been hypothesized to contribute to refractoriness to antiepileptic drugs (AEDs), a condition that characterizes most patients with MTLE (Kwan et al. 2010) even when biasing factors such as poor adherence to treatment have been accounted for. Indeed, the poor responsiveness to AEDs requires a major effort for the health care system in assisting patients and undoubtedly represents a social burden for difficulties encountered by patients to achieve life satisfaction (Beghi 2016). For these challenging reasons, more effective therapeutic options are required to address MTLE.

Drug development must be guided by the underlying pathophysiology of the considered disease. In this regard, seizures have been related to the imbalance of neuronal excitation and inhibition determined, respectively, by glutamate and  $\gamma$ -aminobutyric acid (GABA). Accordingly, GABA enhancers, i.e., agents which either bind directly to and positively modulate the type A GABA ( $GABA_A$ ) receptor (such as benzodiazepines and allopregnanolone), or delay the GABA clearance (tiagabine and vigabatrin) exhibit antiepileptic activity in MTLE (Greenfield 2013). An interesting target is the GABA transporter 1 (GAT1), which is the main GABA sink mechanism. This protein is expressed by neurons and astrocytes throughout the whole brain. By taking up GABA from synaptic clefts, GAT1 contributes to limit the synaptic-mediated phasic inhibition but also accounts for the homeostasis of the interstitial GABA concentration, contributing to the control of extrasynaptic  $GABA_A$  receptor-mediated tonic inhibition. In this way, GAT1 modulates neuronal network excitability in states of basal, as well as enhanced synaptic activity. GAT1 was the first GABA transporter of a four-member family of neurotransmitter- $Na^+$  symporters to be cloned and crystallized (Scimemi 2014). Tiagabine, a drug used for the treatment of MTLE, acts by binding and inhibiting the GAT1-mediated GABA uptake mechanism. This ultimately leads to increased concentrations of the endogenous ligand, enhancing GABA-mediated hyperpolarization, so producing beneficial effects.

Neuroinflammation has also been involved in the pathophysiology of MTLE. Both types of glial cells, microglia, and astrocytes participate in neuroinflammation, which is mainly contributed by leukocytes at least in the acute phase (Vinet et al. 2016). Microglia are the brain resident immune cells. They can be

activated by many stimuli, ultimately implying brain tissue function. Activated microglia release various mediators of inflammation after trauma and seizures, including metalloproteinase-12, leading to neuron degeneration, as well as astrogliosis (Vinet et al. 2018). Thus, microglia take an active part in the process of neural tissue remodeling, known as epileptogenesis, which has been thought to turn the healthy brain tissue hyperexcitable.

Astrocytes have also been recognized to play a role in epileptogenesis and ictogenesis. Apart from the widely known functions such as neurotransmitter clearance, ionic balance and buffering, glycogen storing, and selective permeability from capillaries, they also express cytokine receptors and secrete trophic factors. Astrocytes may secrete molecules able to enhance or suppress ongoing inflammatory processes during neurologic diseases, including epilepsy (Setkowicz, Kosonowska and Janeczko 2017). Early studies (Steward et al. 1992; Steward, Kelley, and Schauwecker 1997) have shown that a single electroconvulsive seizure is able to elicit a remarkable increase in glial fibrillary acidic protein (GFAP) expression. This represents an initial step in the astrocyte's reaction leading to their hypertrophy, whose precise contribution to epileptogenesis has to be enlightened.

A well-known consequence of damage to the hippocampus and related structures, as found in MTLE, is that patients have a prevalence of neuropsychiatric comorbidities significantly higher than age- and sex-matched healthy people (Mula et al. 2016). Among the comorbidities that strongly impact patient's life quality in MTLE are (i) cognitive impairments, i.e., impairment of learning and memory related to injury in the hippocampus, DG, and entorhinal cortex (Helmstaedter and Kockelmann 2006), and (ii) mood or affective disturbances, i.e., anxiety and depression related to amygdala pathology (Marco Mula et al. 2016; Josephson et al. 2017). Further, during seizures, the mesial temporal lobe structures give origin to amnesic or dyscognitive auras, as well as vegetative and fear-related symptoms, due to ictal activation of, respectively, perirhinal cortex and amygdala (van Elst et al. 2000). Behavioral and cognitive deficits have also been consistently reported in animal models of MTLE (Epps et al. 2013; Klein et al. 2015).

Innovative drugs for patients with MTLE should be able to address both the acute and chronic mechanisms responsible for the seizures, neurodegeneration, and comorbidities, as previously outlined. Molecules obtained from biological sources have yielded important prototypes for drug development (Brillatz et al. 2018; Bohni et al. 2013). On this background, the shrub *Sideroxylon obtusifolium*, which grows spontaneously in semi-arid regions from Northeastern Brazil, is widely used in local folk medicine due to its wound healing, antinociceptive, anti-inflammatory, and claimed anti-seizure properties (Aquino et al. 2016; Araujo-Neto et al. 2010). As we recently characterized the anti-inflammatory properties of *N*-methyl-(2*S*,4*R*)-trans-4-hydroxy-*L*-proline (NMP) from *Sideroxylon obtusifolium*, the objectives of the present work were to study the effects of NMP on the behavioral and brain changes occurring after intracerebroventricular (icv) pilocarpine

(Pilo)-induced *status epilepticus* (SE) and brain damage, by considering the expression of GAT1, neuroinflammation, and gliosis, as evaluated by Nissl staining, immunohistochemistry assays, and western blotting. Specifically, we considered four groups of mice subdivided into the (i) sham group, surgically operated but not exposed to seizures, and given vehicle (hereafter referred as SO), (ii) Pilo-damaged and vehicle-treated group, and finally, (iii) two groups of Pilo-damaged mice treated with the NMP (Pilo + NMP) fraction from the medicinal plant *Sideroxylon obtusifolium* at two different doses. In addition, molecular docking experiments for GAT1 were also carried out.

## RESULTS

### Behavioral tests

Three out of 27 mice died after Pilo treatment (11% mortality), whereas all SO mice survived. In the novel object recognition test (ORT) for short-term memory, control mice of the Pilo group exhibited significantly impaired performance compared to the SO group (Figure 6). On the other hand, treatment with *per os* (po) NMP at both doses of 100 mg/kg and 200 mg/kg was able to prevent the short term memory impairment related to pilocarpine-induced injury ( $p < 0.0001$ , one-way analysis of variance—ANOVA—followed by Dunnett's test), since the performance of these NMP-treated animals was not different from the SO group.

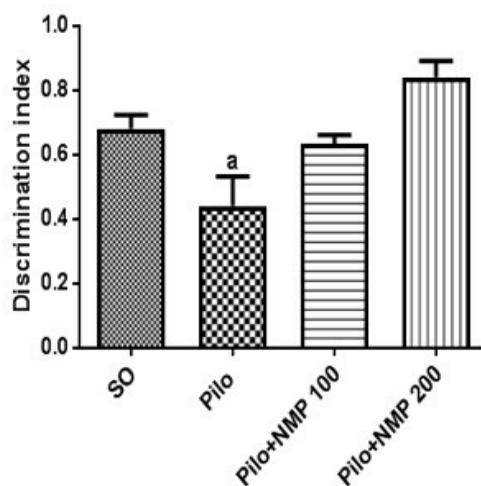


**Figure 6.** The N-methyl-(2S,4R)-trans-4-hydroxy-L-proline-rich fraction (NMP) prevented the behavioral changes in the recognition memory induced by the intracerebroventricular (icv) injection of pilocarpine (Pilo), evaluated by the novel object recognition test in mice. The animals received Pilo (300  $\mu$ g/1  $\mu$ L, icv) and, 24 h after, were treated for 15 days with NMP (100 or 200 mg/kg, *per os*, po; Pilo + NMP groups) or with distilled water (vehicle po; sham-operated, SO group). Groups were composed of eight animals/group, average). The behavioral tests were performed 1 h after the last drug administration. a. vs. SO,  $p < 0.0001$  (one-way analysis of variance followed by Dunnett's multiple comparisons test).

We also investigated the behavioral performance in the Y maze test, which was used to evaluate both short-term and operative memory. In this test, the Pilo group exhibited a significantly reduced percentage of spontaneous side alternation compared to the SO group ( $p = 0.0063$ , one-way ANOVA followed by Dunnett's test, Figure 7). Treatment with NMP prevented the cognitive impairment significantly at both doses (Figure 7), thus preserving mouse memory functioning.

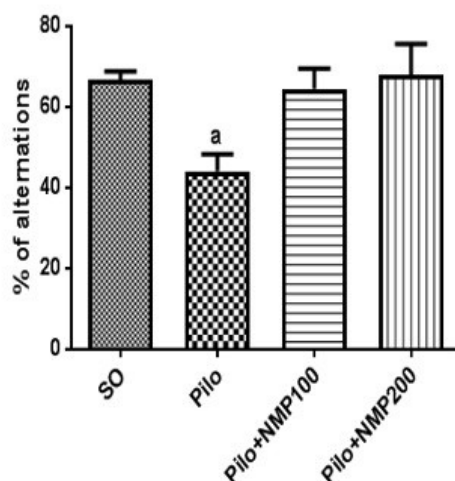


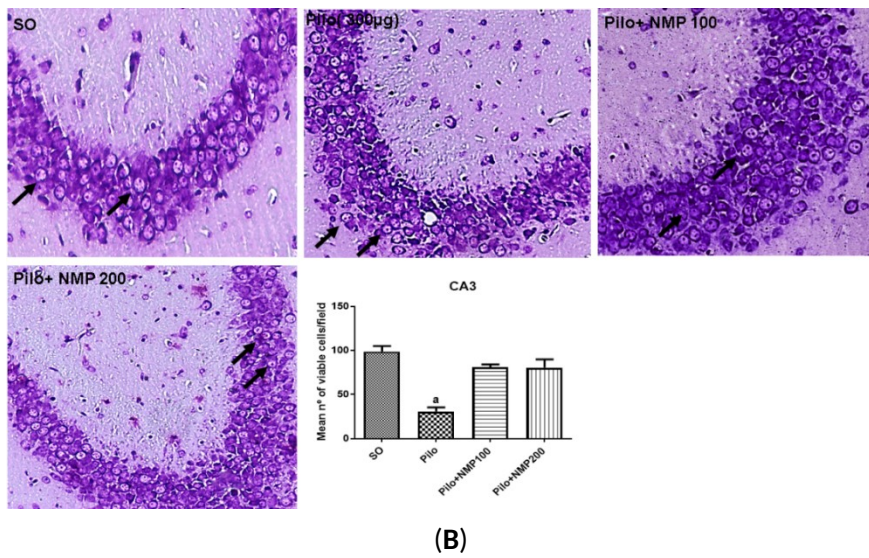
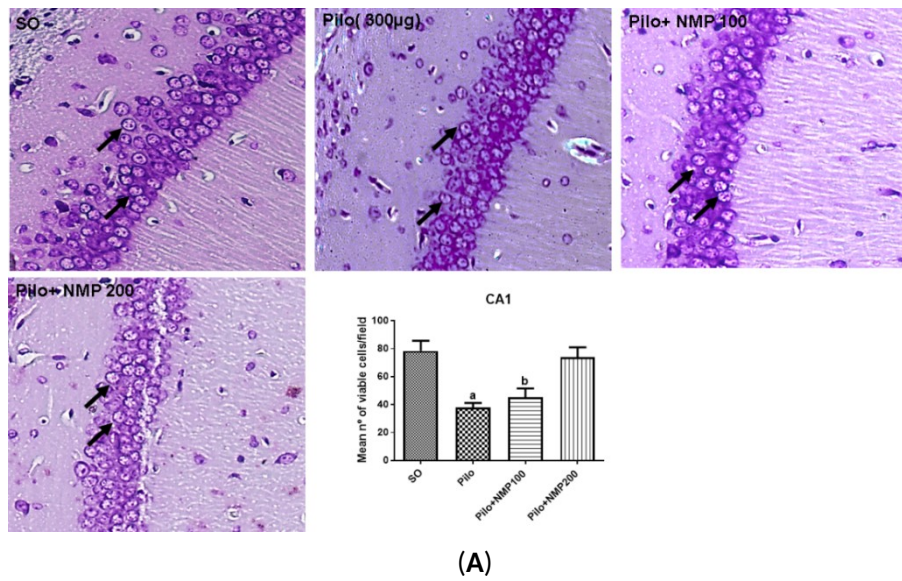
**Figure 7. The N-methyl-(2S,4R)-trans-4-hydroxy-L-proline-rich fraction (NMP) prevented the behavioral changes in the operational memory, induced by the intracerebroventricular (icv) injection of pilocarpine (Pilo), evaluated by the Y-maze test in mice.** The animals received Pilo (300  $\mu\text{g}/1 \mu\text{L}$ , icv) and, 24 h after, were treated for 15 days with NMP (100 or 200 mg/kg, *per os*, *po*; Pilo + NMP groups) or with distilled water (vehicle *po*; sham-operated, SO). Groups were composed of eight animals/group on average. The behavioral tests were performed 1 h after the last drug administration. a. vs. SO,  $p = 0.0063$  (one-way analysis of variance followed by Dunnett's multiple comparisons test).

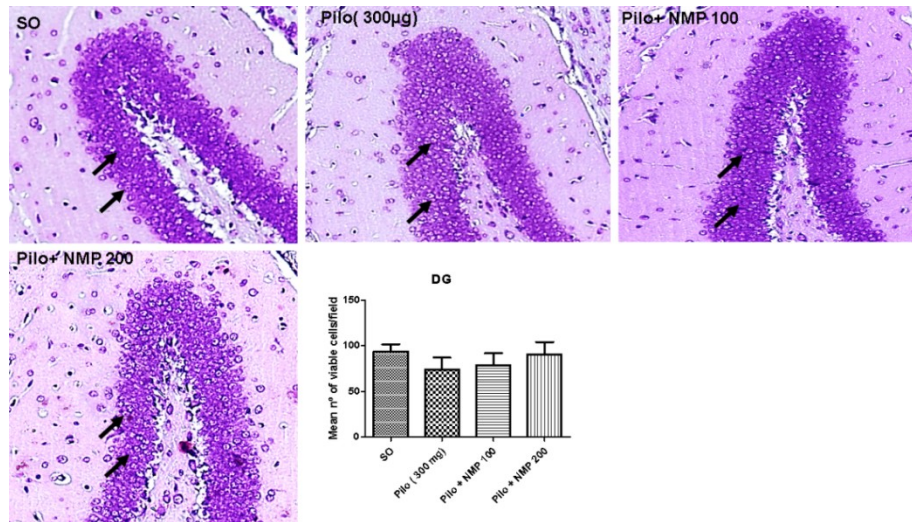
Even though we did not monitor the animals in the long-term, in order to record the occurrence of spontaneous recurrent seizures, which mainly appear from the 2nd week after Pilo injection onwards, it is worth to mention that we noticed an overt behavior consisting of remarkable aggressiveness and hyperreactivity in response to noises and handling. This behavior is often reported in animals with spontaneously recurrent seizures documented by electrocorticographic video recording in the Pilo MTL model (Curia et al. 2008).

#### **Nissl staining and neuronal viability**

The Pilo treatment induced a remarkable reduction in Nissl stained neurons of the *cornu Ammonis* (CA) region CA1 (52% decrease), compared to the SO group ( $p < 0.0004$ ). The treatment with NMP at the dose of 100 mg/kg resulted in values similar to those of the Pilo group (43% decrease) and, thus, did not significantly prevent the reduction in CA1 pyramidal neurons when compared to the SO group. In contrast, no statistical

difference was noticed between the Pilo + NMP group treated with the dose of 200 mg/kg, and the SO group (Figure 8A).





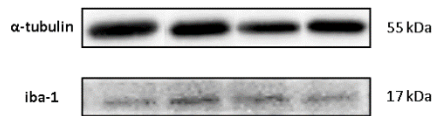
(C)

**Figure 8. Representative photomicrographs (100 $\times$  magnification) of the hippocampal cornu Ammonis (CA) subfields CA1 (A), CA3 (B), and (C) dentate gyrus (DG), showing that the N-methyl-(2S,4R)-trans-4-hydroxy-L-proline-rich fraction (NMP) increased the number of hippocampal viable cells in mice subjected to the intracerebroventricular (icv) injection of pilocarpine (Pilo). The animals received Pilo (300  $\mu$ g/1  $\mu$ L, icv) and, 24 h after, were treated with NMP (100 or 200 mg/kg *per os*, *po*), for 15 days. The sham-operated (SO) group received the vehicle, distilled water *po*. After the behavioral tests, animals were euthanized for histological analysis with cresyl violet ( $n = 4$  animals/group, three slices/animal). Bar charts show the mean value of viable cells/field (seven fields/group). CA1: a. vs. SO,  $p < 0.0004$ ; b. vs. SO,  $p < 0.001$ . CA3: a. vs. SO,  $p < 0.0001$  (one-way analysis of variance, followed by the Dunnett's test for multiple comparisons). Black arrows point to viable neurons. The cells were considered viable neurons when they presented violet staining in the cytoplasm, as well as normal morphological aspects (round or oval cells with centralized nuclei).**

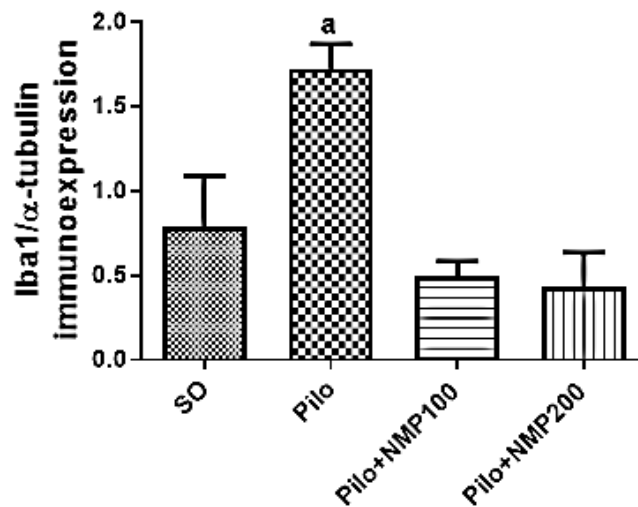
In the CA3 region, a 69% reduction in viable cells (indicated by black arrows in Figure 8) was observed in the Pilo group, compared to the SO group. The treatment with NMP, at both doses, limited to 18% the decrease in the percentage of viable cells, in contrast to Pilo, which instead presented a significant lesion when compared to the SO group ( $p < 0.0001$ , one-way ANOVA followed by Dunnett's test, Figure 8B). In the dentate gyrus (DG) area, there was no significant reduction of neurons in the granular layer, showing a greater resistance of these cells in this region (Figure 8C) as repeatedly reported in the literature on animal models of SE (Curia et al., 2008).

#### **Ionized calcium-binding adaptor molecule 1 (Iba-1) western blot**

The western blot for Iba-1 in hippocampi, standardized for  $\alpha$ -tubulin, showed a 2.2-fold significant increase of this marker of inflammatory cells in the Pilo group compared to the SO group ( $p < 0.0033$ , one-way ANOVA followed by Dunnett's test) (Figure 9). Remarkably, in both the Pilo-NMP100 and Pilo-NMP200 groups, the values were below the basal level of the SO group, even though not significantly.



(A)

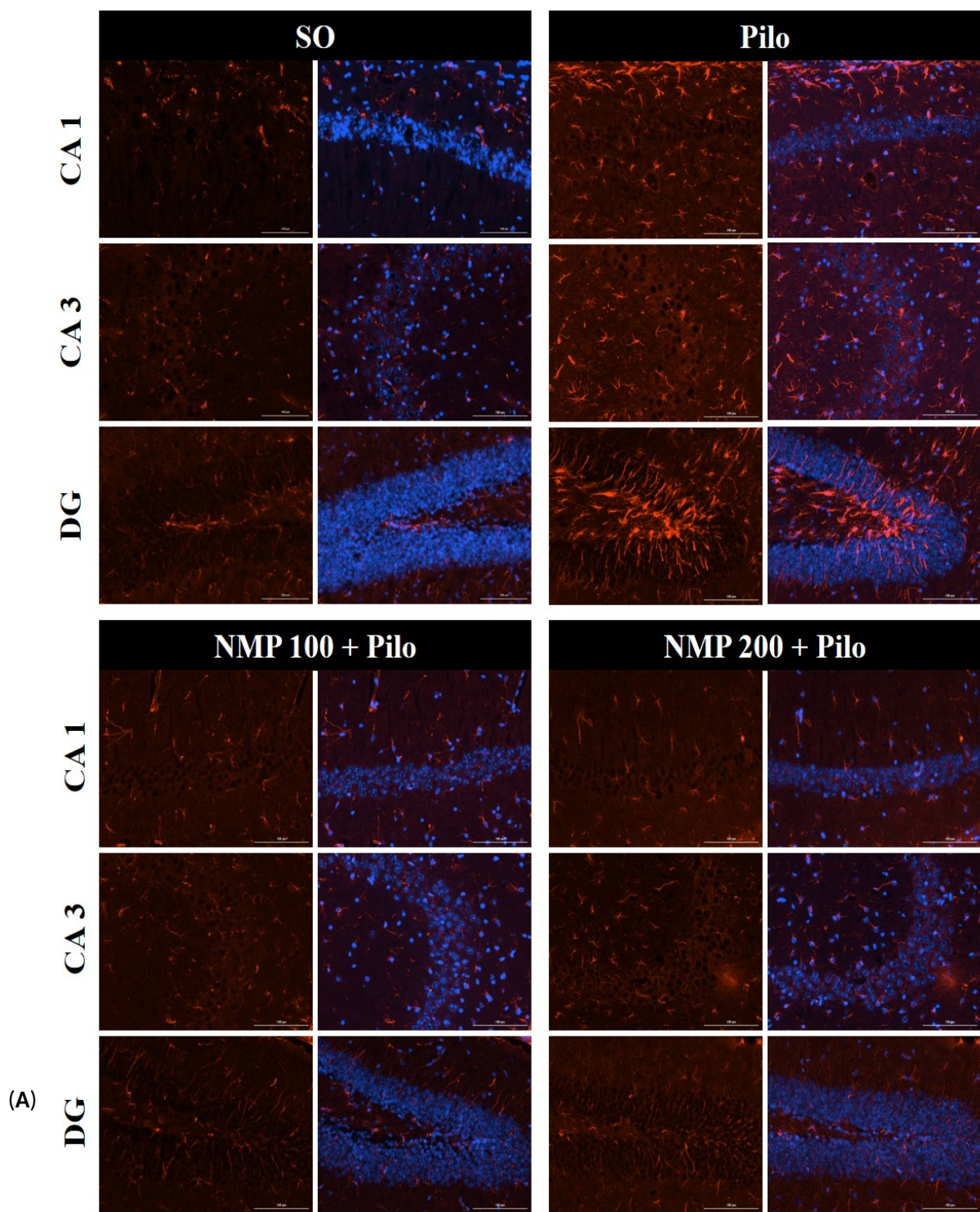


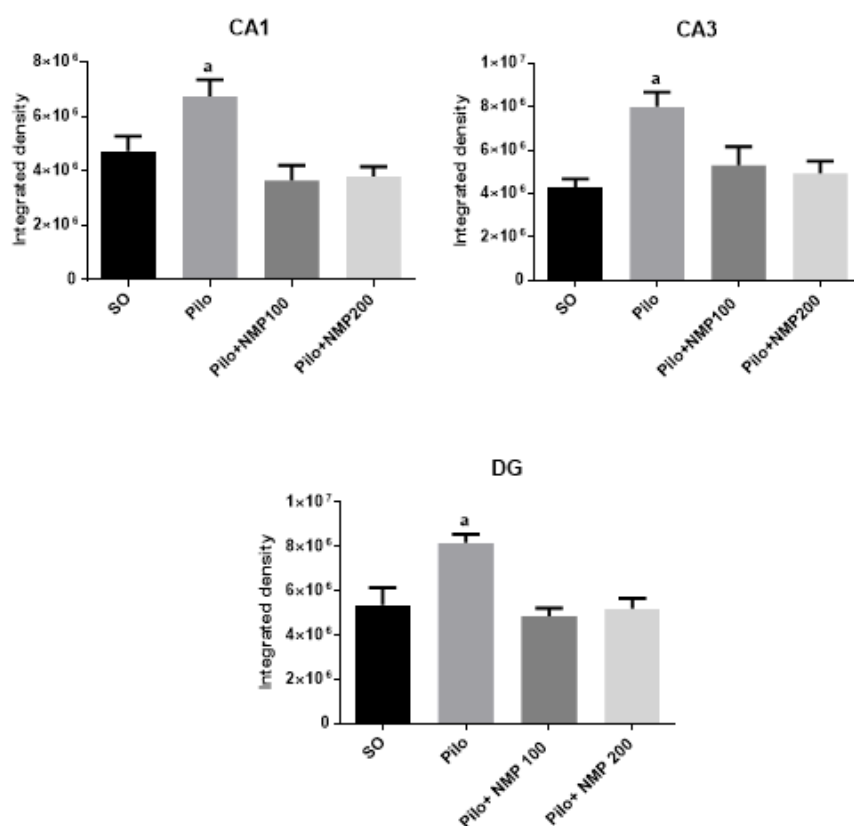
(B)

Figure 9. The N-methyl-(2S,4R)-trans-4-hydroxy-L-proline-rich fraction (NMP) partly reversed the increased microglia activation, in mice subjected to the intracerebroventricular (icv) injection of pilocarpine (Pilo), compared with the SO group as evaluated by western blot for the ionized calcium-binding adaptor molecule 1 (Iba-1). Representative blots (A) show the higher intensity band which corresponds to standard  $\alpha$ -tubulin (55 kDa), and the 15 kDa band which corresponds to the Iba-1 band (four mice per group). Below, the densitometric quantification of the bands (B), performed by the Image J software (NHI, USA), is shown. a. vs. SO,  $p < 0.0033$  (one-way analysis of variance and Dunnett's multiple comparisons test).

### GFAP immunofluorescence

The immunofluorescence analysis for GFAP (Figure 10A) showed in the CA1 a 1.5-fold significant increase of labeling in the Pilo group compared to SO ( $p < 0.0002$ , one-way ANOVA followed by Dunnett's test). The immunolabelling intensity in both NMP100 and NMP200 groups was lower than the values found in the SO group (Figure 10B). Similar data were also seen in the CA3 and DG, in which a respective two-fold ( $p < 0.0001$ ) and 1.8-fold ( $p < 0.0001$ ) increase was present. Values were similar to those of the SO group in both NMP groups, with no significant difference among the three mentioned groups.





(B)

**Figure 10.** The N-methyl-(2S,4R)-trans-4-hydroxy-L-proline-rich fraction (NMP) completely prevented the increase in hippocampal glial fibrillary acidic protein (GFAP) immunorepression in mice subjected to the intracerebroventricular (icv) injection of pilocarpine (Pilo). The animals received Pilo (300  $\mu$ g/1  $\mu$ L, icv) and, 24 h after, were treated with NMP (100 or 200 mg/kg, *per os*, *po*), for 15 days. The sham-operated (SO) group received the vehicle, distilled water, *po*. After the behavioral tests, the animals were euthanized for immunofluorescence assays, performed with four animals per group. On the left, photomicrographs are presented for each group, in hippocampal fields showing cells stained for GFAP only (in red) and nuclei counterstained with 4',6-diamidino-2-phenylindole (DAPI) (in blue) (A). Quantification (bars on the right) is referred to the fluorescence integrated density in the various hippocampal subfields (B). CA1: a. vs. SO,  $p < 0.0002$ ; CA3: a. vs. SO,  $p < 0.0001$ ; DG: a. vs. SO,  $p < 0.0001$ ; (one-way analysis of variance and Dunnett's test for multiple comparisons).

### Target prediction results for NMP

To estimate the most probable human targets for NMP protective effects, we submitted the chemical structure of NMP (in SMILES format) to the SwissTargetPrediction server. The server algorithm predicted the most probable human proteins, based on the similarity of NMP with chemical structures of the drug database, and ranked proteins from the most to the less probable ones (Table 3). Based on this prediction, GAT1 was recognized as the most probable target for NMP, considering the quantitative

probability rate and the number of known actives with similar chemical properties. According to these results, then we investigated the NMP interaction with GAT1, as well as its expression in our animals.

**Table 3. Predicted targets for NMP based on its chemical similarity with SwissTargetPrediction drug database.**

Target	Uniprot ID	Target Class	Probability	Known Actives (3D/2D)
GABA transporter 1	P30531	Electrochemical transporter	0.03	5/4
GABA A receptor lpha-3/beta-2/gamma-2	P34903 P47870 P18507	Ligand-gated ion channel	0.03	3/0
GABA A receptor alpha-2/beta-2/gamma-2	P47869 P47870 P18507	Ligand-gated ion channel	0.03	4/0
Renin	P00797	Protease	0.03	0/13
Egl nine homolog 1	Q9GZT9	Oxidoreductase	0.02	1/0
Adenosine A3 receptor	P0DMS8	Family A G protein-coupled receptor	0.02	2/3
GABA-B receptor	O75899 Q9UBS5	Family C G protein-coupled receptor	0	8/0
Thrombin	P00734	Protease	0	0/8
Leukotriene A4 hydrolase	P09960	Protease	0	0/4
GABA receptor rho-1 subunit	P24046	Ligand-gated ion channel	0	4/0
Phospholipase A2 group IIA	P14555	Enzyme	0	0/6
Phospholipase A2 group V	P39877	Enzyme	0	0/3
Integrin alpha-IIb/beta-3	P08514 P05106	Membrane receptor	0	0/11
Leucine aminopeptidase	P28838	Protease	0	0/5
Bile acid receptor FXR	Q96RI1	Nuclear receptor	0	0/1
Neprilysin	P08473	Protease	0	0/23
Voltage-gated calcium channel alpha2/delta subunit 1 (by homology)	P54289	Calcium channel auxiliary subunit alpha2delta family	0	10/0
Metastin receptor	Q969F8	Family A G protein-coupled receptor	0	0/2
11-beta-hydroxysteroid dehydrogenase 1	P28845	Enzyme	0	0/9
Nitric-oxide synthase, brain	P29475	Enzyme	0	0/9

## Molecular docking for the NMP

Firstly, we built the human GAT1 structure through a homology modeling approach, using the SwissModel server. The model was based on dopamine receptor from *Drosophila melanogaster* (Protein Data Bank identifier 4XP4), which had 45.88% of sequence identity and 0.89% of coverage with the human GAT1. The model was analyzed at the MolProbity server and showed a MolProbity score of 1.35. The MolProbity score provides a log-weighted combination of the clashscore, the Ramachandran score not favored, and the percentage of bad side-chain rotamers, reflecting the crystallographic resolution at which those values would be expected. The analysis of the Ramachandran plot of the GAT1 model showed that 99.06% of the residues lie in the most favorable regions, which was more than satisfactory since ideally, 98% of the residues should lie in the favorable regions. After modeling, molecular docking calculations were performed in order to investigate the binding affinity of NMP against GAT1, as well as to study the possible binding mode and the interactions among them. NMP docked into GAT1 and presented a docking score of  $-4.38 \text{ kcal}\cdot\text{mol}^{-1}$ . We also performed docking calculations of tiagabine, a GAT1 blocker that acts as a GABA reuptake inhibitor. Tiagabine docked into GAT1 and presented a docking score of  $-5.13 \text{ kcal}\cdot\text{mol}^{-1}$ . Our data point out that the binding affinity and docking score of NMP against GAT1 was similar to that of tiagabine. However, tiagabine showed fewer hydrogen bonds with GAT1 residues and more hydrophobic interactions compared with NMP, which justify its slightly different docking score. Furthermore, the action mechanism of NMP is at least partly the result of its GAT1 blocking properties (Figure 11).

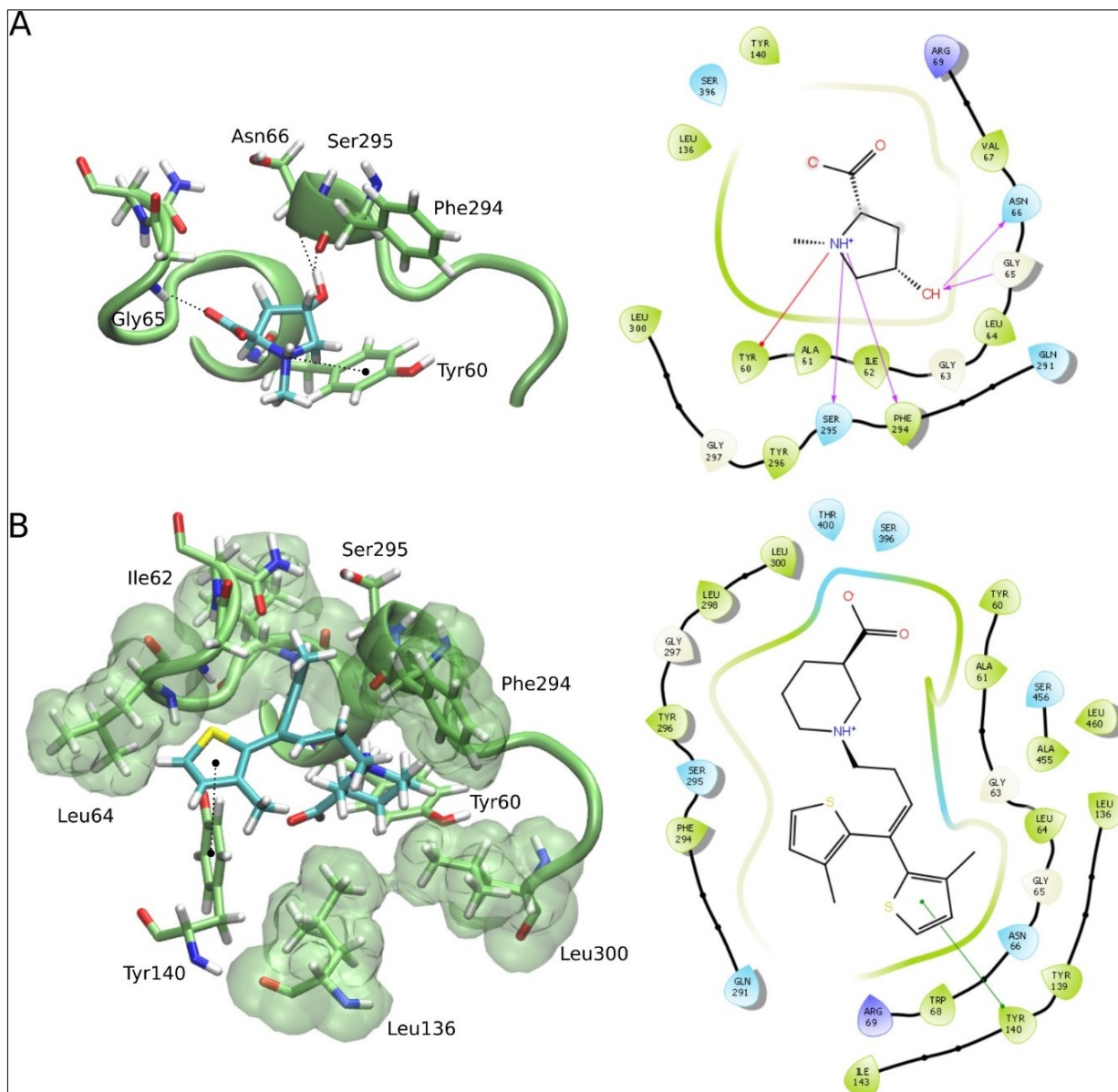


**Figure 11. Predicted binding mode for the *N*-methyl-(2*S*,4*R*)-trans-4-hydroxy-L-proline-rich fraction (NMP) and the tiagabine molecule, into the GAT1 binding site. (A) Intermolecular 3D and 2D interactions of NMP with the main GAT1 model obtained by docking in the 3D representation; H-bonds are presented as black dashed lines and the hydrophobic interactions as green surfaces. In the 2D interaction diagram, hydrogen bonds are presented as magenta arrows and cation-Pi interaction as red arrows. (B) Intermolecular 3D and 2D interactions of tiagabine with GAT1: in the 3D representation, the Pi-Pi interaction is presented as black dashed lines and the hydrophobic interactions as a green surface. In the 2D interaction diagram, the Pi-Pi interaction is represented as green arrows.**

### GAT1 immunohistochemistry

Immunohistochemistry findings for GAT1 were analyzed in the hippocampus. In the CA1 hippocampal subfield, GAT1 in the Pilo group was increased almost 12-fold ( $p < 0.0002$ , Kruskal-Wallis test followed by Dunn's test) compared to the SO group. This change was much lower (respectively, 4.6-fold and 5.3-fold) in

the Pilo + NMP groups at the doses of 100 and 200 mg/kg, and did not differ significantly from the levels of the SO group. In other words, NMP at both doses partly prevented the icv Pilo-induced GAT1 increase in CA1 (Figure 12A). A similar effect was seen in CA3, where GAT1 labeling was increased 17-fold ( $p < 0.0002$ ), compared with the SO group. Although not significantly different from the SO group, fewer consistent (three-fold and four-fold) increases were seen after NMP treatment, respectively, at the doses 100 and 200 mg/kg (Figure 12B). Moreover, DG exhibited a remarkable 24-fold increase in GAT1 labeling in the Pilo group compared to the SO group ( $p < 0.0002$ ). Although not significant, an increase (around three-fold) compared with the Pilo group was seen at both NMP doses (Figure 12C).

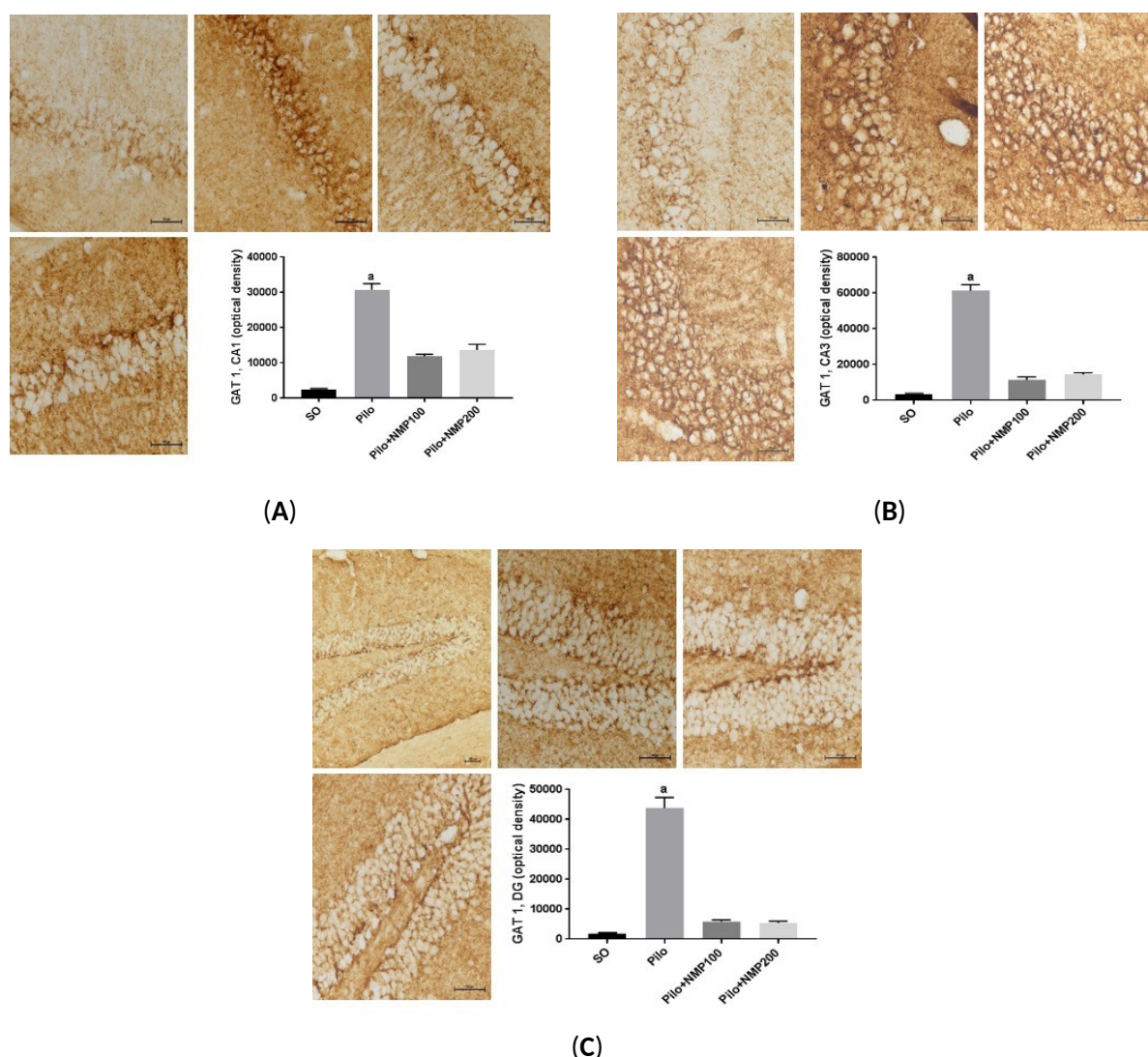


**Figure 12.** The N-methyl-(2S,4R)-trans-4-hydroxy-L-proline-rich fraction (NMP) prevented the hippocampal immunoexpression increases of the GABA transporter (GAT1), in the various hippocampal regions (A, cornu Ammonis 1 - CA1; B, CA3; C, dentate gyrus - DG) of mice subjected to the intracerebroventricular (icv) injection of pilocarpine (Pilo), compared with the SO group. The animals received Pilo (300  $\mu\text{g}/1 \mu\text{L}$ , icv) and, 24 h after, were treated with NMP (100 or 200 mg/kg, *per os*, *po*) for 15 days (Pilo + NMP100 and Pilo + NMP200 groups). The sham-operated (SO) group received

distilled water (vehicle, *po*). After the behavioral tests, the animals were euthanized for the immunohistochemistry assays, performed in four animals per group. CA1: a. vs. SO,  $p < 0.0002$ . CA3: a. vs. SO,  $p < 0.0002$ . DG: a. vs. SO,  $p < 0.0002$  (Kruskal–Wallis test and Dunn’s multiple comparisons test).

### GAT1 western blot

The results of the immunohistochemical analysis for GAT-1 were confirmed by western blot experiments in whole hippocampi. The Pilo group exhibited a 1.9-fold significant increase in GAT1 immunoeexpression compared to the SO group ( $p < 0.0014$ , Kruskal–Wallis test followed by Dunn’s test). The group Pilo + NMP100 exhibited a GAT1 expression 53% lower compared to the Pilo group ( $p < 0.0293$ ). There was no significant difference between the SO and Pilo + NMP200 groups (Figure 13).

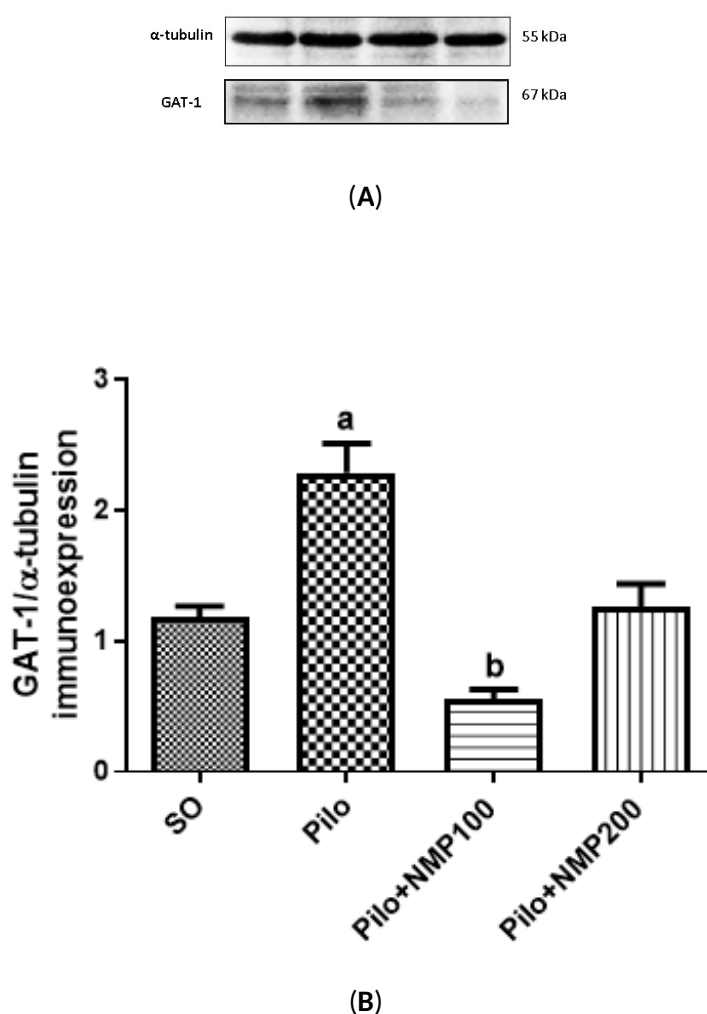


**Figure 13.** The N-methyl-(2S,4R)-trans-4-hydroxy-L-proline-rich fraction (NMP) partly prevented the increased  $\gamma$ -aminobutyric acid (GABA) transporter (GAT-1) expression in mice subjected to the intracerebroventricular (icv) injection of pilocarpine (Pilo), compared with the SO group as evaluated by western blot analysis. Representative blots (A) show the higher intensity band, which corresponds to standard  $\alpha$ -tubulin (55 kDa), and the 67 kDa band corresponding to the GAT-1 band (four mice per group). Below, the densitometric quantification

of the bands is shown (B), as performed by the ImageJ software (National Institute of Health - NHI, USA). **a.** vs. SO,  $p < 0.0014$ ; **b.** vs. SO,  $p < 0.0293$  (Kruskal-Wallis test and Dunn's multiple comparisons test).

## DISCUSSION

We showed that the NMP fraction from *Sideroxylon obtusifolium* leaves exerts anti-inflammatory and neuroprotective activities in the icv Pilo model of MTLE. The antiepileptic activity was demonstrated previously by our group, in the systemic Pilo model (Aquino et al. 2018), but also in the model of icv Pilo, which was the subject of the present study. Most importantly, this effect was presented not only by NMP but also by l-proline and trans-hydroxyproline, suggesting that the NMP activity in the Pilo model of the mesial temporal lobe injury is due to its L-proline content. In the present study, by using the icv injection of Pilo, we showed that NMP exerts a protectant, presumably antiepileptic activity that has a relationship with its anti-inflammatory action, as we have demonstrated previously (Aquino et al 2016). The icv injection of Pilo is an MTLE model, useful as a tool for investigating the mechanisms underlying the generation and maintenance of seizures (Medina-Ceja, Pardo-Peña and Ventura-Mejía 2014).

Comorbid behavioral disorders are part of the epilepsy-interictal spectrum (Curia et al. 2008). Epilepsy-related behavioral disorders include depression, psychosis, and severe cognitive deficits, which significantly impair a patient's life functionality (Cornaggia et al. 2006). We showed that icv Pilo-treated mice presented a marked deficit in the short-term memory, which was prevented by both the NMP doses evaluated here. The ORT is a behavioral test often used for the investigation of several aspects of learning and memory in mice (Lueptow 2017). Pilo also significantly reduced the number of correct spontaneous alternations, compared with the SO group, as evaluated by the Y-maze test used to assess the working memory in mice (Kraeuter, Guest, and Sarnyai 2019). Therefore, NMP, as other proline derivatives (Sarhan and Seiler 1989), can represent not only a useful tool for the control of the pro-seizure activity but also to counteract the epilepsy-associated cognitive deficits that represent a great burden for these patients.

According to Furtado and colleagues (Furtado et al. 2002; Furtado et al. 2011), icv Pilo in mice provokes remarkable neurodegeneration in CA1 and CA3 hippocampal subfields, as confirmed in the present study. Comparatively, kainic acid (after icv, as well as after intrahippocampal injections in Sprague-Dawley rats), which is a more widely used model of MTLE, induces neurodegeneration in the CA3, leaving the CA1 and DG almost intact (Lancaster and Wheal 1982; Nadler and Cuthbertson 1980). Both NMP doses were able to protect the CA3 subfield, whereas only the highest dose was effective in the CA1 subfield. This observation suggests that the results obtained in the described behavioral tests could be more dependent on protection in the hippocampal CA3 subfield.

Epilepsy is a neurologic disease of sporadic and progressive disruption of neuronal activity or of a heterogeneous neuronal-glia network (Binder and Carson 2013). Evidence shows that brain activity and

connectivity are drastically altered during epileptic seizures. Brain networks are known to shift from a balanced resting state to a hyperactive and hypersynchronous state (Diaz Verdugo et al. 2019; Yang et al. 2010). Pilo-induced SE was shown to induce a prominent activation of astrocytes and microglia in the DG, from three up to 20 days after the initial seizures in rats (Schartz et al. 2016). The time interval of our study was within the mentioned period of glial activation and demonstrated that NMP is able to maintain both astrocytes and microglia in the resting state.

Microglia are known to play a critical role in brain homeostasis. Microglia are the brain resident immune cells that play important roles in the development and maintenance of neural circuits, and activated microglia exert different effects on brain function (Hiragi et al. 2018). Recently (Zhao et al. 2018), elevated mTOR signaling in mouse microglia was demonstrated to lead to phenotypic changes, without significant induction of pro-inflammatory cytokines, disrupting the brain homeostasis, and leading to reduced synaptic density, marked neuronal degeneration and massive proliferation of astrocytes. According to our findings, NMP at both tested doses has the potential to prevent all these detrimental effects.

In the present work, we showed that astrocytes were activated in the hippocampi of mice subjected to the icv injection of Pilo. These effects were substantially decreased after treatments of mice with NMP, at both doses, suggesting that NMP exerts a neuroprotective effect on epileptic mice. Astrocyte and microglial activation occur following seizures and, for this reason, could play an important role in epileptogenesis (Shapiro, Wang, and Ribak 2008). Importantly, these hippocampal changes manifested as increased Iba-1 and GFAP expressions occur rapidly after Pilo-induced seizures in rats, and last for several weeks (Schartz et al 2016). An increase in Iba-1 positive cells was also demonstrated in the hippocampus after Pilo-induced SE, suggesting that SE triggers time-dependent alterations in the microglia morphology (Wyatt-Johnson, Herr and Brewster 2017). Although we did not investigate the morphological changes of microglia, the findings on Iba-1 expression in the presence of NMP administration suggest a possible effective modulation of the tested active compound.

The extensions of astrocytes with presynaptic terminals and postsynaptic spines generate a complex, so-called tripartite synapse (Xu et al. 2019). The phenomenon named reactive astrogliosis is characterized by hypertrophy of primary processes and a dramatic increase in the expression of GFAP (Steward, Kelley, and Schauwecker 1997; Steward et al. 1991). A number of studies have provided compelling evidence of dramatic alterations in the morphology and function of astrocytes in epilepsy, leading to reactive astrogliosis (Arisi et al. 2011; Binder and Steinhäuser 2017; Coulter and Steinhäuser 2015; Robel et al. 2015). All these findings suggest that astrocytes are crucial players in epilepsy, thus representing an important target for the NMP effects.

In the last decades, computational methods have been widely used in drug development studies for providing several advantages compared to traditional methods. For example, computational tools brought to drug development pipelines higher successful rates, shorter time, and less costs. Also, these methods represent an ethical gain since they reduce the number of animals and biological resources used in experimental research (Challal et al. 2012). Here, we firstly applied a target prediction algorithm to obtain the most probable biological targets for NMP interaction, which could guide our research efforts. Interestingly, we found for NMP several targets involved in the GABAergic transmission, being GAT1 the most predicted. Based on this, we conducted a molecular docking approach to better clarify the binding mode and affinity of NMP to this transporter. Our experiments showed docking score values of NMP that were quite similar to those of tiagabine, a GABA reuptake inhibitor. Tiagabine, an antiepileptic drug, has a specific and unique mechanism of action involving the inhibition of GABA reuptake into neurons and glia (Schachter 2001). Despite facilitating the induction of GABA-mediated depolarization, tiagabine also increases the effectiveness of synaptic inhibition during the synchronous high-frequency activation of inhibitory interneurons (Jackson, Esplin and Čapek 1999). By elevating GABA levels and availability in the synaptic cleft, GAT-1 inhibition represents an established approach for the treatment of epilepsy and is the potential target for the NMP mechanism of action.

However, other possible mechanisms might contribute to NMP effects. Indeed, midazolam, which is known to modulate the GABA<sub>A</sub> receptor by interacting with the benzodiazepine binding site, was reported to modify potassium currents (So et al. 2014; Vonderlin et al. 2015). Moreover, vigabatrin has been shown to reduce astroglial the weak inward rectifier K<sup>+</sup> (TWIK)-related acid-sensitive K<sup>+</sup> channel 1 (TASK1) in the hippocampus of seizure-sensitive gerbils (Kim et al. 2007). Recently, vigabatrin was also found to influence the activity of intermediate-conductance calcium-activated K<sup>+</sup> channels in human glioma cells (Hung et al. 2020). Another possible target of NMP could be the A<sub>3</sub> purinoceptor, as revealed by our prediction analysis. This is a G<sub>i/o</sub> protein-coupled receptor activated just at very high adenosine concentrations (i.e., during seizures or ischemia). The role of A<sub>3</sub> in epilepsy and ictogenesis is poorly understood and does not appear to exert an univocal proconvulsant effect. Its activation has been demonstrated to elicit desensitization of GABA<sub>A</sub> and A<sub>1</sub> (anticonvulsant) adenosine receptors, as well as to modulate the presynaptic glutamate release and post-synaptic K<sup>+</sup> currents, which are believed to be the A<sub>3</sub> downstream effector mechanisms (Tescarollo et al. 2020). Thus, NMP effects could not be simply attributable to inhibition of GAT1 and the reduction in GABA clearance, because it might also be associated with potential modulatory effects on different types of ionic currents present in central neurons, astrocytes, or microglial cells, which would be intriguingly investigated in the near future.

## **MATERIALS AND METHODS**

### **Plant material extraction and purification**

*Sideroxylon obtusifolium* leaves were collected from specimens in the rural district from the Mauriti municipality, Ceará State, in August 2014. A voucher specimen (#10,648) was deposited in the Herbarium "Dárdano de Andrade Lima", from the Regional University of Cariri (URCA), Crato-Ceará, Brazil, Dr. Maria Arlene Pessoa da Silva being the person responsible. The bioactive, NMP-enriched fraction was obtained by the procedure previously described (Aquino 2016), and dissolved in fresh distilled water (vehicle) before *po* administration. The quantitative <sup>1</sup>H nuclear magnetic resonance (qHNMR) method was used to determine the *N*-methyl-trans-4-hydroxy-L-proline concentration in the methanol fraction (NMP) used in the present study. The quantification was based on the internal standard method, which is widely accepted as the primary approach to qNMR. The NMP content observed in the methanol fraction was 121.7 ± 5.1% mg/g, corresponding to 12% of NMP present in the leaves from *Sideroxylon obtusifolium*. Consistently, the <sup>1</sup>H NMR spectra of NMP was the same as that of the isolated pure compound *N*-methyl-(2*S*,4*R*)-trans-4-hydroxy-L-proline.

### **Animals**

Male Swiss mice (25–33 g; 8–9 per group before Pilo treatment, eight per group after SE) were kept at 25 ± 2 °C, under a 12/12 h light/dark cycle beginning at 7:00 a.m. Food and water were provided *ad libitum*. The experiments were carried out in strict observance of the USA National Research Council guidelines for the care and use of laboratory animals (Committee for the Update of the Guide for the Care and Use of Laboratory Animals 2011). This study was submitted to and approved (2017, project code 59/17) by the Animal Research Ethical Committee of the Federal University of Ceará (CEUA/UFC).

### **Drugs and chemicals**

Pilo (Sigma-Aldrich, São Paulo, Brazil) was dissolved in artificial cerebrospinal fluid (aCSF) (composition in mM: NaCl 125, KCl 2.5, NaH<sub>2</sub>PO<sub>4</sub> 5, CaCl<sub>2</sub> 1.2, MgCl<sub>2</sub> 1) (Murphy and Maidment 2002), pH adjusted to 7.4. Ketamine and xylazine were from König (Argentina). Drug solutions were prepared freshly before use. All other drugs and reagents were of analytical grade. The solutions were administered in a volume of 0.1 mL/10 g of body weight.

### **Stereotaxic-guided injection of Pilo or ACSF in the left lateral ventricle of the brain, and treatments**

Mice were given intraperitoneal (ip) methyl scopolamine 3 mg/kg as prophylaxis for the peripheral effects of muscarinic activation by Pilo. Five min later, they were anesthetized with ketamine *plus* xylazine, respectively,

90 and 10 mg/kg ip. By using an electric razor, the fur was removed from the head. Then, the animals were placed and centered in a 10  $\mu$ m precision motorized stereotaxic apparatus (51730M, Stoelting, Wood Dale, IL, USA), taking care to avoid ear bar misplacement. The eyes were kept wet by 0.9% saline to prevent keratitis. The skin disinfection was carried out by applying iodine-polyvinylpyrrolidone (Povidone, Vick Pharma, São Paulo, Brazil). Then, a midline incision between ears and eyes, about 1.5 cm long, was made with a scalpel. Validation of the flat skull position of reference was carried out by measuring and noticing bregma and lambda dorsoventral coordinates. From this point, the level of the tooth bar was lowered or lifted, so tilting the cranium downwards or upwards to measure the dorsoventral coordinates of bregma and lambda in a cycle repeated as many times as necessary until the dorsoventral coordinates of both craniometric points differ from each other not more than 10  $\mu$ m. After that, taking as reference the mediolateral and craniocaudal coordinates of bregma, a point 0.5 mm caudal and 1.1 mm left-sided lateral to bregma was pinpointed on the skull cap corresponding to the projection of the left lateral ventricle of the brain (Paxinos and Franklin 2003). A hole was drilled by a 1016 spherical FG dental bur mounted on a low rotation handpiece from Beltec, LB100, by a high speed friction grip adapter mandrel, taking care not to injure the dura and the underlying cortex. Eventual bleeding was plugged at this point. Then, the tip of the needle of the Hamilton syringe was placed at the center of the trepanation. Starting from the dorsoventral level of the skull surface at that point, the tip of the needle was dorsoventrally lowered 2.8 mm. Either Pilo 300  $\mu$ g/1  $\mu$ L diluted in aCSF, or aCSF (1  $\mu$ L) were injected slowly (over 1 min). The needle was kept in place for 5 min to prevent reflux through the needle track. After that, the syringe was removed, and the wound edges were fitted together by nylon 4-0 thread in separate stitches (Ferry, Gervasoni, and Vogt 2014). Animals were left to recover from anesthesia on a thermal pad to avoid hypothermia, with the cranial part of the body slightly lifted to avoiding airway obstruction. They were injected twice a day for two days, in alternate times, with Ringer lactate solution and glucose 5% subcutaneously, approximately 0.5 mL/25 g of body weight. Animals were given distilled water, NMP 100, or 200 mg/kg (groups: SO, Pilo, Pilo + NMP100, and Pilo + NMP200 respectively) daily, over 15 days beginning from the first postoperative day. In this so-called “silent period”, between the primary injury and the clinical manifestation of disease, the epileptogenic process which renders the animals epileptic is thought to take place (Cavalheiro, Santos and Priel 1996).

### **Behavioral tests performed on the 15th postoperative day**

#### **Novel ORT**

The novel ORT is used to evaluate recognition memory, that is, short term memory. This task is based on the innate tendency of rodents to explore unfamiliar objects within their environment. This test assesses the

mouse's ability to discriminate between familiar and novel objects. Firstly, mice were individually habituated to an open field plexiglass box (30 × 30 × 40 cm) for 5 min. After 15 min, mice were allowed to explore a set of two identical objects for 5 min (acquisition phase). These objects were suitably heavy and long to guarantee that mice could neither move them nor climb over them. After a 5 min interval, mice were presented to a similar set of objects in the same environment, with the replacement of one familiar object by a novel/unknown object (testing phase). The animals were allowed to freely explore the objects again for a 5 min period. A discrimination index was calculated as follows: (time exploring new object-time exploring familiar object)/(time exploring new object + time exploring familiar object) (Dix and Aggleton 1999).

### **Y-maze test**

The working memory and learning were assessed by the rate of spontaneous alternations in the Y-maze three arms (40 × 5 × 16 cm), positioned at equal angles, as previously described (Sarter, Bodewitz and Stephens 1988). Before running the test, the arms were numbered, and the animal was placed in one arm and spontaneously alternated the entries in the other arms for 8 min. The sequence of the arms into which the animal entered was then noted, and the information analyzed, in order to determine the number of arm entries without repetition.

### **Euthanasia and tissue harvesting**

Immediately after behavioral tests, the animals were randomly assigned to groups for either immunohistochemistry or western blot assays. For immunohistochemistry, mice were deeply anesthetized with ketamine (90 mg/kg) and xylazine (15 mg/kg) ip. After they lost the withdrawal reflex to the hind paw pinch, the rib cage was cut longitudinally exposing the mediastinum. A cannula was inserted in the heart left ventricle. Then, the animals were transcardially perfused with 0.9% saline (about 60 mL) for vascular rinsing, and afterwards, with 60 mL of a 4% paraformaldehyde (PFA) solution in phosphate buffered saline (PBS) (pH 7.4). Skull was opened on an aluminum foil-covered ice bar, and brains were carefully collected, post-fixed for 2 h in the same PFA 4% solution at 4 °C, and then cryoprotected in 30% sucrose diluted in PBS (pH 7.4) for 72 h. Brains were sliced in a cryostat (Leica, Wetzlar, Germany) into 10 µm coronal sections, which were stored in cryoprotectant at -20 °C for further use. Diversely, for western blot assays, mice were euthanized by decapitation, brains were quickly dissected on an aluminum foil-covered ice bar, whole hippocampi were freshly harvested and stored in vials at -80 °C until use.

### **Nissl staining**

In this study, cell viability was analyzed by the cresyl violet staining. The cresyl violet staining is used to highlight the Nissl corpuscles present in the cytoplasm of viable neurons (Scorza et al. 2005). The slides with

the brain slices of cortex and hippocampus were dipped in distilled water for 1 min and immersed in a 0.5% cresyl violet solution prepared in acetate buffer (20% sodium acetate [2.7%] + 80% glacial acetic acid [1.2%]) for 3 min. The staining was desaturated with two washes in acetate buffer. Then, the sections were dehydrated in alcohol (50%, 70%, and 100%). Finally, they were dipped in xylol and assembled with Entellan (Merck, Whitehouse Station, NJ, USA). For the quantification of Nissl stained neurons, the slides were visualized with a microscope (Nikon Elipse E200, Nikon, Shinjuku, Japan) under a 100 $\times$  magnification objective lens. Three slices of each animal were randomly selected, and the quantification of stained neurons was performed using the ImageJ software (NIH, Bethesda, MD, USA) with a grid of 1000 pixels in the hippocampus subfields CA1, CA3, and DG. The value of each animal was taken as the average of the three slices, and the results expressed as the number of viable cells. The cells were considered viable neurons when they presented violet staining in the cytoplasm, as well as normal morphological aspects (round or oval cells with centralized nuclei).

## **Drug discovery computational tools**

### **Target prediction**

The prediction of biological targets of the NMP was performed through the SwissTargetPrediction Server (Bateman et al. 2017). This server estimates the most probable macromolecular targets of a small molecule, assumed as bioactive. The prediction is based on a combination of 2D and 3D similarity with a library of 370,000 known actives on more than 3000 proteins. The results are presented in probability rates that can guide the subsequent experiments.

### **Homology modeling and molecular docking calculations: comparing the interaction of NMP and tiagabine with GAT-1**

The structure of sodium chloride dependent GAT1 was built by homology modeling, through the SwissModel server. The primary sequence of GAT1 was searched at the Uniprot server (Bateman et al. 1996). The model that presented higher sequence identity and coverage with the template was selected to the refinement step, at the GalaxyRefine server. The MolProbity server was used to add hydrogen atoms and to analyze the quality of the statistics of the modeled protein. The NMP, as well as the GAT-1 blocker tiagabine, were docked into GAT-1 using the Glide software in extra precision (XP) mode. We prepared the protein structures through a Protein Preparation Wizard tool, adding the hydrogen atoms and minimizing the energy, using the OPLS-2005 force field. The ligands were prepared through the LigPrep tool, correcting protonation, according to Epik, and performing energy minimization. The protein grid coordinates were built, based on the coordinates of the ligand cocaine, co-crystallized in the structure used as templates of the model (from PDB ID 4XP4). The

Visual Molecular Dynamics program (VMD) (Humphrey, Dalke, and Schulten 1996; Pagadala, Syed, and Tuszynski 2017) was used for the visual inspection of 3D docking poses and to render the 3D molecular images.

### **Immunohistochemistry for GAT-1**

Sections operationally defined as -2.46 mm to -2.92 mm (caudal) to bregma containing hippocampi (Kim et al., 2007) were chosen and fixed in methanol. After cooling, they were washed four times with PBS, and the endogenous peroxidase blockade with a 3% H<sub>2</sub>O<sub>2</sub> in PBS (15 min) was carried out. The sections were incubated overnight (4 °C) with the primary antibodies (anti-GAT-1 1:200, Abcam ab426, Cambridge, UK) in PBS, according to the manufacturer's instructions. On the following day, the sections were washed in PBS four times, incubated (30 min) with the secondary biotinylated rabbit antibody (anti-IgG) in PBS (1:200), washed four times in PBS, and incubated (30 min) with the conjugated streptavidin-peroxidase complex (Burlingame, CA, USA). After rinsing, the sections were developed with 3,3-diaminobenzidine mounted on glass slides, dehydrated, and coverslipped for the analysis. The data were semi-quantified with the ImageJ software, NIH, USA (Hsu, Raine, and Fanger 1981).

### **Western blotting assays for GAT1 and Iba-1**

Hippocampi for immunoblotting were washed with ice-cold PBS and put in radioimmunoprecipitation assay buffer (RIPA) lysis buffer (25 mM Tris—HCl, pH 7.6; 150 mM NaCl; 5 mM EDTA; 1% NP40; 1% Triton X-100; 1% sodium deoxycholate; 0.1% sodium dodecyl sulphate) with protease inhibitor (1 µL inhibitor: 100 µL RIPA). The lysed samples were transferred into microcentrifuge tubes, sonicated two times for 5 s, and then cleared by centrifugation (12,000 rpm, 15 min) at 4 °C. Total protein concentration in lysates was determined by the bicinchoninic acid (BCA) method according to the manufacturer's protocol (Pierce BCA Protein Assay Kit, Thermo Fisher Scientific, Waltham, MA, USA). SDS polyacrylamide gel electrophoresis (10%) was performed using 20 µg of protein (previously prepared with Laemmli sample buffer and heated to 95 °C for 5 min). The proteins were transferred to PVDF membrane, blocked with 5% BSA for 1 h, and incubated overnight with rabbit polyclonal for Iba-1 (1:1000, Santa Cruz Biotechnology, Dallas, TX, USA) or rabbit polyclonal antibody for GAT-1 (1:600) or mouse antibody for α-tubulin IgG primary antibody (1:4000; Sigma-Aldrich). After washing, the blots were incubated with horseradish peroxidase-conjugated goat anti-rabbit IgG secondary antibody (1:1000, Thermo Fisher Scientific, Waltham, MA, USA) or goat anti-mouse IgG secondary antibody (1:1000, Thermo Scientific) for 90 min at room temperature. The signal was detected using the ECL system (Bio-RAD, Hercules, CA, USA) according to the manufacturer's instructions, and then the bands were

captured with a CCD camera using the ChemiDoc system (Bio-Rad, Hercules, CA, USA). Densitometric quantification of bands was performed with NIH ImageJ software (n = 4/group).

### **Immunofluorescence for GFAP**

Slices containing hippocampi, identical to those aforementioned, were rinsed four times in PBS. They underwent an antigen recovery process and were incubated overnight at 4 °C with the mouse monoclonal anti-GFAP (1:200, Santa Cruz Biotechnology). After, slices were rinsed four times with PBS and then incubated for 2 h at room temperature with AlexaFluor-594 conjugated goat anti-mouse IgG antibody (1:400; Invitrogen, Carlsbad, CA, USA). Finally, they were stained with 1 µg/mL 4',6-diamidino-2-phenylindole (DAPI) (Invitrogen, Carlsbad, CA, USA). Subsequently, slides were rinsed in PBS and coverslipped using ProlongGoldAntifadeMountant (ThermoFisher Scientific, Waltham, MA, USA). Slides were imaged using a Zeiss LSM 700 confocal microscope (Carl Zeiss, White Plains, NY, USA) through a magnification of 20X objective lens, at constant exposure, gain, and offset. The hippocampal subfields CA1, CA3, and DG were identified according to Paxinos, and Franklin's Mouse Brain Atlas (Paxinos and Franklin 2003) and four to five photomicrographs of each area for each group were analyzed. The experimenter who took the images was blinded to treatments. The fluorescence intensity was semi-quantitative, using the ImageJ software package.

### **Statistical analysis**

Data were tested for goodness of fit to a normal distribution and are presented as mean ± SEM. The analysis was performed by one-way ANOVA, followed by the Dunnett's for multiple comparisons test or the nonparametric rank-based Kruskal-Wallis test followed by the Dunn's multiple comparisons test. Values of  $p < 0.05$  were considered as significant.

### **AUTHOR CONTRIBUTIONS**

Conceptualization—P.E.A.d.A., Í.R.L., G.B., E.R.S., G.S.d.B.V.; investigations—P.E.A.d.A., J.R.B., T.d.S.N., J.T., A.J.M.C.F., M.M., K.R.T.N.; methodology—P.E.A.d.A., D.M.G., G.M.d.A., E.R.S., G.S.d.B.V.; data curation—P.E.A.d.A., Í.R.L., G.B., G.S.d.B.V.; writing: original draft preparation—P.E.A.d.A., Í.R.L., G.S.d.B.V.; writing: review and editing—P.E.A.d.A., Í.R.L., G.B., G.S.d.B.V.; supervision—D.M.G., G.M.d.A., G.B., E.R.S., G.S.d.B.V.; funding acquisition—D.M.G., G.M.d.A., G.B., E.R.S., G.S.d.B.V. All authors agreed on the results and commented on the manuscript.

### **FUNDING**

Brazilian National Research Council (CNPq) and Ceará State Foundation for Scientific and Technological Development Support (FUNCAP). This work was supported by the University of Modena and Reggio Emilia for Í.R.L. (FAR 2018 to GB).

#### **ACKNOWLEDGMENTS**

The authors thank Maria Arlene Pessoa da Silva for identifying the exsiccates, and Maria Janice Pereira Lopes from the Faculty of Medicine of Juazeiro do Norte (Estácio/FMJ) for the technical support.

#### **CONFLICTS OF INTEREST**

The authors declare no conflict of interest.

## Chapter 6

### Status epilepticus dynamics predicts latency to spontaneous seizures in the kainic acid model <sup>III</sup>

Anna Maria Costa, Chiara Lucchi, Cecilia Simonini, Ítalo Rosal Lustosa, Giuseppe Biagini

Department of Biomedical, Metabolic and Neural Sciences, University of Modena and Reggio Emilia, Modena, Italy

#### ABSTRACT

**Background/Aims:** Status epilepticus (SE) might be followed by temporal lobe epilepsy (TLE), a common neurologic disorder characterized by spontaneous recurrent seizures (SRSs). However, the relationship between SE and TLE is still incompletely characterized. For this reason, in a model of TLE we evaluated the lesion extent and the onset of SRSs to determine if they were influenced by the SE dynamics. **Methods:** Sixty-two adult male Sprague-Dawley rats were implanted for video-electrocorticographic (v-ECOG) monitoring and intraperitoneally treated with saline or kainic acid (KA, 15 mg/kg) at 8 weeks of age. v-ECOG recordings were obtained during SE, in the following 9 weeks, and assessed by amplitude or power band spectrum. Rats were euthanized 3 or 64 days after SE to evaluate the lesion. **Results:** SE lasted about 10 h during which the mean duration of convulsive seizures (CSs) increased from 39 s, at 30 min, to 603 s at 4 h. The gamma power peaked 30 min after the SE onset and its peak was correlated ( $r^2=0.13$ ,  $p=0.042$ ) with the overall SE duration. Subsequently, the gamma power was reduced under the baseline until the end of SE. The theta power increased at approximately 150% of basal levels 3 h after KA injection, but it went back to basal levels with the full development of CSs. Interestingly, the timing of the first SRS in chronic epilepsy was correlated with the latency to develop the first CS with loss of posture during SE ( $r^2=0.60$ ,  $p<0.001$ ). Additionally, the overall duration of CSs observed during SE was related to the number of damaged brain regions ( $r^2=0.60$ ,  $p=0.005$ ), but it did not influence the timing of the first SRS in chronic epilepsy. **Conclusion:** Overall, our results show that the onset of chronic epilepsy is modulated by SE dynamics, whereas brain damage is related to prolonged convulsions in SE.

**Key Words:** Epileptogenesis, Gamma power, Kainic acid, Status epilepticus, Temporal lobe epilepsy, Theta power

#### INTRODUCTION

Temporal lobe epilepsy (TLE) is a major neurologic disorder characterized by spontaneous recurrent seizures (SRSs) which often follow a presumably causative lesion, also known as the “initial precipitating injury” (Mathern et al. 1993). The SRSs begin after a period named “epileptogenesis” during which degeneration and

repair, inflammation and aberrant structural phenomena occur in consequence of the initial precipitating injury (Pitkänen et al. 2015). It is currently undetermined which one of the various, possible mechanisms able to contribute to epileptogenesis could be critical for the appearance of SRSs in TLE, and all of them have been addressed in a variety of *in vivo* models reproducing seizures or epilepsy, following a wide-spectrum approach (Morimoto, Fahnestock, and Racine 2004).

Among other hypotheses, it has been proposed that epileptogenesis could be related to the extension of lesions caused by the initial precipitating injury, especially in the hippocampus (Biagini et al. 2008; Klitgaard et al. 2002; Esper and Cavalheiro 1995). This hypothesis was tested in status epilepticus (SE) models by controlling the initial precipitating injury with drugs able to limit the duration of SE to progressively shorter time intervals, so as to obtain a different lesion extent. The prediction made in these experiments was of a possible change in the latency to first SRS in response to the reduction in SE duration. However, the results paradoxically showed both delay and anticipation of SRSs in presence of reduced hippocampal damage (Biagini et al. 2008; Lemos and Cavalheiro 1995). Conversely, in a different study authors did not find differences in the period of time required to the onset of SRSs in rats exposed to a short (30 min) or prolonged (120 min) period of SE (Bortel et al. 2010). In all of these experiments pilocarpine was the proconvulsant used to trigger the SE (Biagini et al. 2008; Bortel et al., 2012; Lemos and Cavalheiro 1995).

Using kainic acid (KA) to model SE (Meinrad Drexel, Preidt and Sperk 2012; Dudek et al. 2006; Lévesque, Avoli and Bernard 2016; Henshall 2017), authors differently approached the relationship between SE and epileptogenesis. Specifically, the onset of convulsive seizures (CSs) in the course of SE (hereafter defined as convulsive SE, CSE) (Trinka et al., 2015) was considered as the possible determinant of SRS onset, independently of the lesion extent (Drexel, Preidt and Sperk 2012). Anyway, also in this case no correlation between the latency to CSE and time required to develop the SRSs was found in animals surviving to KA. A possible explanation to these approaches failing in the tentative to establish a relationship between SE and epileptogenesis could be that all the animals were treated with drugs able to limit the SE duration and inducing neuroprotection. In such a way, drug treatment could have modified the course of subsequent epileptogenesis by interfering with the initial precipitating injury.

To get further insights into the relationship between SE, damage and epileptogenesis in the KA model, we designed experiments without any drug administration to fully characterize the dynamics of SE and the onset of SRSs by video-electrocorticographic (v-ECoG) recordings. Additionally, we also localized the lesions and measured their extension to establish a relationship with the SE dynamics. Finally, we investigated the relationship between epileptogenesis and lesion extent or SE dynamics. Here, we show that some characteristics of SE could be useful in predicting the brain damage and timing of epileptogenesis.

## **MATERIALS AND METHODS**

### **Animals**

A total of 62 male Sprague-Dawley rats (Charles River, Calco, Italy) with initial weight of 175-200 g were used in this study. Animals were housed in a specific pathogen-free facility with controlled environment conditions and ad libitum access to water and food. All experiments were authorized (323/2015-PR) and performed according to the European Directive 2010/63/EU. The local Animal Welfare Body approved the study protocol. All efforts were done to refine procedures, improve the welfare and reduce the number of animals.

### **Experimental design**

Animals were randomly divided into two groups to investigate the lesions (n=34) or epileptogenesis (n=28). The first group consisted of 17 rats that received an injection of KA (15 mg/kg, i.p.; Sigma-Aldrich, Milan, Italy) compared with 17 controls receiving an i.p. injection of saline (1 ml/kg). These rats were euthanized after 3 days from the injection at 8 weeks of age (11 KA-treated rats and 11 controls) to evaluate early brain injuries, or 64 days after injections at 17 weeks of age (6 KA-treated rats and 6 controls) to evaluate the presence of chronic brain injuries. The second group included KA-treated rats used to evaluate the relation between SE and epileptogenesis, and monitored until 17 weeks of age. All rats were treated with KA or saline one week after electrode implantation. At the end of SE, rats were given a subcutaneous (s.c.) injection of Ringer's lactate solution (3-5 ml) and softened rat chow to minimize animal discomfort.

### **v-ECoG recordings**

As described previously (Lucchi et al. 2017), rats were implanted with epidural electrodes in frontal and occipital cortices, in order to continuously record ECoG data of both hemispheres. One electrode was implanted below the lambda on the midline in all animals and used as a reference. For electrode implantation, deep anesthesia was induced with volatile isoflurane and assessed by deep breath, loss of tail and eye reflexes. At the end of the surgery, gel containing 2.5 g lidocaine chloride, 0.5 g neomycin sulfate and 0.025 g fluocinolone acetonide (Neufan® gel; Molteni Farmaceutici, Scandicci, FI, Italy) was applied to reduce acute pain and risk of infection. All animals were monitored until complete recovery from anesthesia and housed in single cages with no grids or environmental enrichments to reduce risk of headset loss. Following guidelines (Kadam et al. 2017), the ECoG was recorded via cable connection between headset and preamplifiers. Electrical brain activity was digitally filtered (0.3 Hz high-pass, 500 Hz low-pass), acquired at 1 kHz per channel, and stored on a personal computer after the mathematical subtraction of traces of recording electrodes from trace of reference electrode, using a PowerLab8/30 amplifier connected to 4 BioAmp preamplifiers (ADInstruments; Dunedin, Otago, New Zealand). Videos were digitally captured

through a camera connected to the computer and synchronized to the ECoG traces through LabChart 8 PRO internal trigger. Baseline ECoG was recorded at least 24-48 h prior to the treatment. Both control and KA-treated rats were recorded in the same manner and data analyses were performed with blind procedures.

### **Behavioral and ECoG analysis**

ECoG traces were digitally filtered offline (band-pass: high 50 Hz, low 1 Hz) and manually analyzed using LabChart 8 PRO software (AD Instruments) by blind to treatment expert raters. Based on the definitions provided in the literature (D'Ambrosio and Miller 2010; Meinrad Drexel, Preidt, and Sperk 2012; Pitsch et al. 2017), all seizures were defined as ECoG segments with minimum duration of 10 s, continuous synchronous high-frequency activity, and amplitude at least twice as the previous baseline. These ECoG segments were also screened for the appearance of a post-ictal depression (below baseline ECoG activity). Seizures and their durations were determined in the ECoG traces, and then investigated for a behavioral correlate (Racine 1972) by using the synchronized video recordings. Particularly, seizures were scored as stage 0 (or subclinical) if a clear epileptiform ECoG signal was present without corresponding evident behavior in the video; stage 1-2 in presence of absence-like immobility, "wet-dog shakes", facial automatisms, and head nodding; stage 3, when presenting with forelimb clonus and lordosis; stage 4, corresponding to generalized seizures with rearing; and stage 5, when seizures consisted of rearing with loss of posture and/or wild running, followed by generalized convulsions. SE was defined as the period of time in which rats either did not recover normal behavior between one seizure and the other, or in which they displayed continuous shaking for more than 5 min (Lowenstein 1999). The end of SE was characterized by a progressive reduction in frequency of the continuous electrographic spikes, preceding a silent period. Moreover, the termination of SE was accompanied by recovery of normal behavior. According to the definition of "early seizure" provided in literature (Dudek and Staley 2017), we considered the ictal events as "early", i.e. additional KA-induced seizures when occurring in the next few days after KA administration. In agreement with Williams and colleagues (Williams et al. 2009), initiation of the first SRS was defined by a single, large ECoG spike, followed by large high-frequency activity. The progression was characterized by individual spike-like events followed by regular, large, high-frequency events. At the end of this activity, large-amplitude waves with multiple superimposed spike-like events were followed by a silent period. Artifacts were carefully removed from the v-ECoG analysis of SRSs. They were identified as (i) high frequency signals associated with masticatory movements in the video recording, (ii) interference appearing as a thickening caused by superposition of 50 Hz mains in the ECoG; (iii) electrode or cable-related technical artifacts. The amplitude spectrum maps, in which amplitude gives a spectrum where the height at a particular frequency is the amplitude at that frequency, were respectively reported as the first nonconvulsive and the first convulsive SRS. Then, ECoG traces were further analyzed using EDFbrowser (1st order butterworth high-pass filter: 1Hz; powerline

interference removal: 50 Hz) (Kemp et al. 2010) to understand whether significant changes in the cortical power band spectrum occurred during the SE. A relative indication of the distribution of power over the frequency regions ranging from 1 to 100 Hz, expressed in percentage (%) and recorded from the frontal electrodes, were determined. Frontal electrodes were preferred because gamma oscillations were shown to be present in the frontal and parietal areas (Bouyer, Montaron and Rougeul 1981), while theta oscillations were particularly pronounced in the frontal midline (Canolty et al. 2020; Guderian et al. 2009; Jensen and Tesche 2002; Kahana et al. 1999; Klimesch et al. 1997) and in the subcortical areas (DeCoteau et al. 2007; Magill et al. 2006; Nerad and McNaughton 2006; Paré, Collins and Pelletier 2002). Thus, the power band spectrum analysis was expressed in percentage and included delta ( $\delta$ , 0–4 Hz), theta ( $\theta$ , 4–8 Hz), alpha ( $\alpha$ , 8–12 Hz), beta ( $\beta$ , 12–24 Hz), and gamma ( $\gamma$ , 24–100 Hz) frequencies in 10-s epochs on a continuous ECoG during 12 h after KA treatment.

### **Immunohistochemistry**

Control rats and rats treated with KA were used for tissue analysis. Rats deeply anesthetized with isoflurane were transcardially perfused with phosphate buffered saline (PBS, pH 7.4) followed by Zamboni's fixative (pH 6.9), 3 or 64 days after treatment. Brains were post-fixed at 4°C in the same fixative for 24 h, cryoprotected in 15% and 30% sucrose solutions (Vinet et al. 2018) and stored at –80°C until use. Horizontal sections of 50  $\mu$ m were cut using a freezing sliding microtome (Leica SM2000R; Leica, Nussloch, Germany). As described previously (Giordano et al. 2016; Vinet et al. 2018) sections were washed three times in PBS, treated with 3% H<sub>2</sub>O<sub>2</sub> in PBS (20 min), and blocked 1 h with 5% normal goat serum (NGS) in PBS containing 0.1% Triton X-100 (PBS-T). Sections were incubated overnight at 4°C in PBS-T containing 1% NGS, respectively with the following antibodies: mouse anti-neuron-specific nuclear protein (NeuN, Millipore, #MAB377 clone A60, 1:200) and mouse anti- glial fibrillary acidic protein (GFAP, Sigma Aldrich, #G3893, 1:500). The next day, sections were incubated 1 h with secondary antibody (biotinylated horse anti-mouse; Vectastain, 1:200). All sections were then processed by the avidin-biotin-peroxidase complex (Elite ABC Kit; Vector Laboratories). Immunostaining was performed in 0.05% 3, 3-diaminobenzidine tetrahydrochloride (DAB, Sigma-Aldrich) for 5 min and developed by adding 0.03% H<sub>2</sub>O<sub>2</sub>. Finally, the sections were washed in PBS, mounted on gelatin-coated slides and coverslipped with Eukitt® (O. Kindler GmbH & Co).

### **Fluoro-Jade B**

As described previously (Vinet et al. 2018), sections were mounted on gelatin-coated slides and dried at room temperature. Slides were immersed for 5 min into a solution containing 1% sodium hydroxide in 80% ethanol, washed for 2 min in 70% ethanol followed by 2 min in distilled water, before being oxidized in 0.06% potassium permanganate for 15 min. Brain sections were then stained for 15 min in 0.004% solution of

Fluoro-Jade B (FJB, Millipore, # AG310-30MG) diluted in 0.1% acetic acid. Slides were rinsed in deionized water for 3 min, dried on a pre-warmed hotplate at 50°C, then cleared in xylene and coverslipped with Eukitt®. Images were acquired using a Leica SP2 AOBS confocal microscope.

### **Image analysis**

Immunostained sections from -8.04 mm to -5.04 mm Bregma level were evaluated with a Nikon Eclipse CiL (Nikon Instruments) at 10X and for each area of interest (Cornu Ammonis 3 stratum pyramidale - CA3 Py, subregion B; hilus of the dentate gyrus - DH; subiculum - Sub; layer III of the medial entorhinal cortex - MEnt L.III; nucleus reuniens - Re; anterior olfactory nucleus - AOP) images were digitally captured by a Nikon DS-Fi3 digital camera. The number of NeuN immunoreactive cells and the FJB-positive cells per mm<sup>2</sup> were quantified and analyzed using the ImageJ software. Particularly, FJB-positive cells were evaluated only in regions in which we localized pannecrosis, as identified by loss of astrocyte GFAP immunostaining. The area selected for each region of interest (ROI) was consistent in all analyzed sections. The image analysis software NIS-Elements was used to manually trace the unstained area upon GFAP detection in the CA3 lacunosum-moleculare (CA3 LMol), as well as in Sub, Re and AOP. To estimate the extent of hippocampal atrophy in epileptic rats, we used the same software, by measuring the ratio between the hippocampal area (from CA3 to CA1, DG, Sub and, excluding the fimbria) and the total brain area (excluding the cerebellum).

### **Statistics**

v-ECoG analysis and the relative distribution of power over the frequency expressed in percentage were both investigated using a one-way repeated measures analysis of variance (ANOVA). Multiple comparisons versus the control group (Dunnett's test) were performed to establish differences between time intervals considered after the induction of SE and a reference starting point, respectively set at 0.5 h in the v-ECoG analysis and 0 h in the power band spectrum analysis expressed in percentage. For immunohistochemical analysis, the statistical comparison between groups was performed using the Student's t-test or one-way ANOVA followed by the Holm-Sidak test. Linear regression was used to model the relationship between two normally distributed variables. Statistical analyses were performed with SigmaPlot 13 (Systat Software). Data are represented as means with standard error of the mean (SEM). appropriate

## **RESULTS**

### **General outcomes of the KA model**

Stage 0-2 nonconvulsive seizures (NCSs) were observed after approximately 14 min from KA administration. The first stage 3 seizure appeared after another additional 23 min, whereas the first CS (stage 4 or 5) required a time interval of approximately 1 h. When considering stage 5 seizures only, the first occurred at 80 min

from treatment. According to our definition, SE was attained at approximately 45 min from KA injection and lasted on average for 10 h. Importantly, almost all rats (93%) developed the SE, and mortality was 4%. After the SE, “early seizures” were generally NCSs observed with 24 h after SE termination in 20% of rats. After 10 days, 97% of rats developed SRSs. The first stage 4 or 5 convulsion was observed 18 days after KA treatment. When considering stage 5 only, the first seizure appeared after 3 weeks at average (Table 4).

### Characterization of the duration and progression of CSs during SE

Significant differences in the duration of stage 4 seizures were found by comparing the 0.5 h time interval with, respectively, 2 h, 2.5 h, and 3 h intervals ( $p < 0.05$  for all of them, Dunnett’s test). Accordingly, significant differences were also found for the duration of stage 5 seizures, which were longer in the 3.5 h and 4 h time intervals than in the 0.5 h interval ( $p < 0.05$ ). By summing up the duration of stage 4 and 5 seizures, significantly higher values were found for 2.5 h, 3 h, 3.5 h, and 4 h compared to the 0.5 h time interval ( $p < 0.05$ ) (Fig. 14A).

### The development and evolution of SE

The percentage of gamma power significantly increased 30 min after the administration of KA (time 0 h vs 0.5 h,  $p < 0.05$ ; Dunnett’s test), but then declined from 1 h to 3 h and 4 h, and also from 5 h to 11 h ( $p < 0.05$  for all time intervals vs 0 h) before to return to baseline at later time intervals. Conversely, the percentage of theta power progressively increased from 0.5 h to 3 h, being significant at 2.5 h and 3 h ( $p < 0.05$ ) in the case of stage 4 seizures (Fig. 19B). Interestingly, the gamma power measured 30 min after the KA injection significantly correlated with total duration of SE ( $r^2 = 0.13$ ,  $p = 0.042$ ) (Fig. 14C), but not with the latency to develop SRSs ( $r^2 = 0.07$ ,  $p = 0.199$ ) (data not shown). Electrographic traces, recorded from frontal and occipital traces (Fig. 1D), were reported in Fig. 14E (I-IV) to illustrate the SE.

**Table 4. Timing of seizure onset during status epilepticus (SE) and chronic epilepsy after kainic acid (KA) treatment.**

Response to KA injection	Latency, duration and percentage of response
First st. 0-2 ECoG seizure	14.37 ± 2.10 min
First st. 3 ECoG seizure	37.27 ± 4.21 min
First convulsive st. 4 or st. 5 ECoG seizure	58.55 ± 4.22 min
First st. 5 ECoG seizure	81.15 ± 6.34 min
SE	47.22 ± 2.15 min
SE duration	10.12 ± 0.45 h
Rats developing SE	93%

Rats died during or after KA injection	4%
Rats developing “early seizures” after KA treatment	20%
Rats developing SRS	97%
First ECoG SRS	9.96 ± 0.95 days
First convulsive st. 4 or st. 5 ECoG SRS	18.18 ± 2.6 days
First convulsive st. 5 ECoG SRS	21.25 ± 3.04 days

ECoG, electrocorticography; SRS, spontaneous recurrent seizure; st., stage.

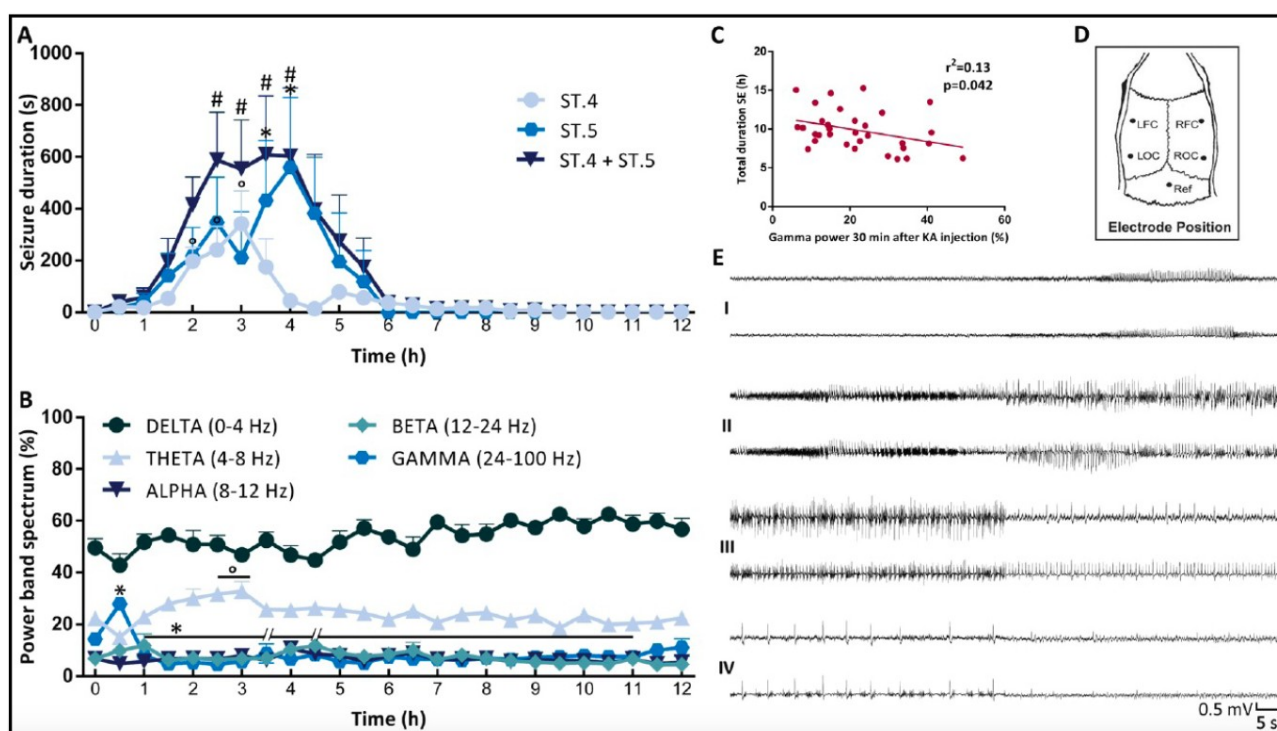


**Fig. 14. Behavioral and electrographic changes observed during status epilepticus (SE).** In A, significant differences in the duration of stage (st.) 4 and 5 convulsive seizures were determined during 12 h after the administration of kainic acid (KA). In B, a relative indication of distribution of power over the frequency, expressed in percentage, was determined during 12 h after the administration of the KA. In C, a linear regression ( $r^2$ ) between the gamma power at 30 min after the administration of KA, and the total duration of SE is illustrated. In D, the position of frontal and occipital electrodes is shown. In E, the development and evolution of SE in the KA model were reported. Particularly, the baseline and then the first nonconvulsive seizure is represented in E.I. The progression from nonconvulsive SE to convulsive SE is reported in E.II. The evolution of SE over time is represented in E.III. The interictal spikes appearing at the end of SE and then the return to baseline are reported in E.IV. Statistical analysis was performed using a one-way repeated measures analysis of variance (ANOVA) followed by multiple comparisons versus control group (Dunnett’s test). Data are shown as mean ± SEM. °  $p < 0.05$  (st. 4), \*  $p < 0.05$  (st. 5), #  $p < 0.05$  (st. 4 + 5); Scale: 0.5 mV/5 s. LFC, left frontal cortex; LOC, left occipital cortex; Ref, reference electrode; RFC, right frontal cortex; ROC, right occipital cortex.

## Neuronal cell damage after SE induction

In contrast to control rats of 8 weeks of age, damaged neurons positive to FJB were found throughout the brain of 8-week-old rats treated with KA (Fig. 20A and B). Particularly, highest densities of FJB-positive cells were found in AOP and MEnt (L.III); intermediate cell damage was in Re, CA3 Py (subregion B), and Sub; lower values characterized the DH (Fig. 15C and D).

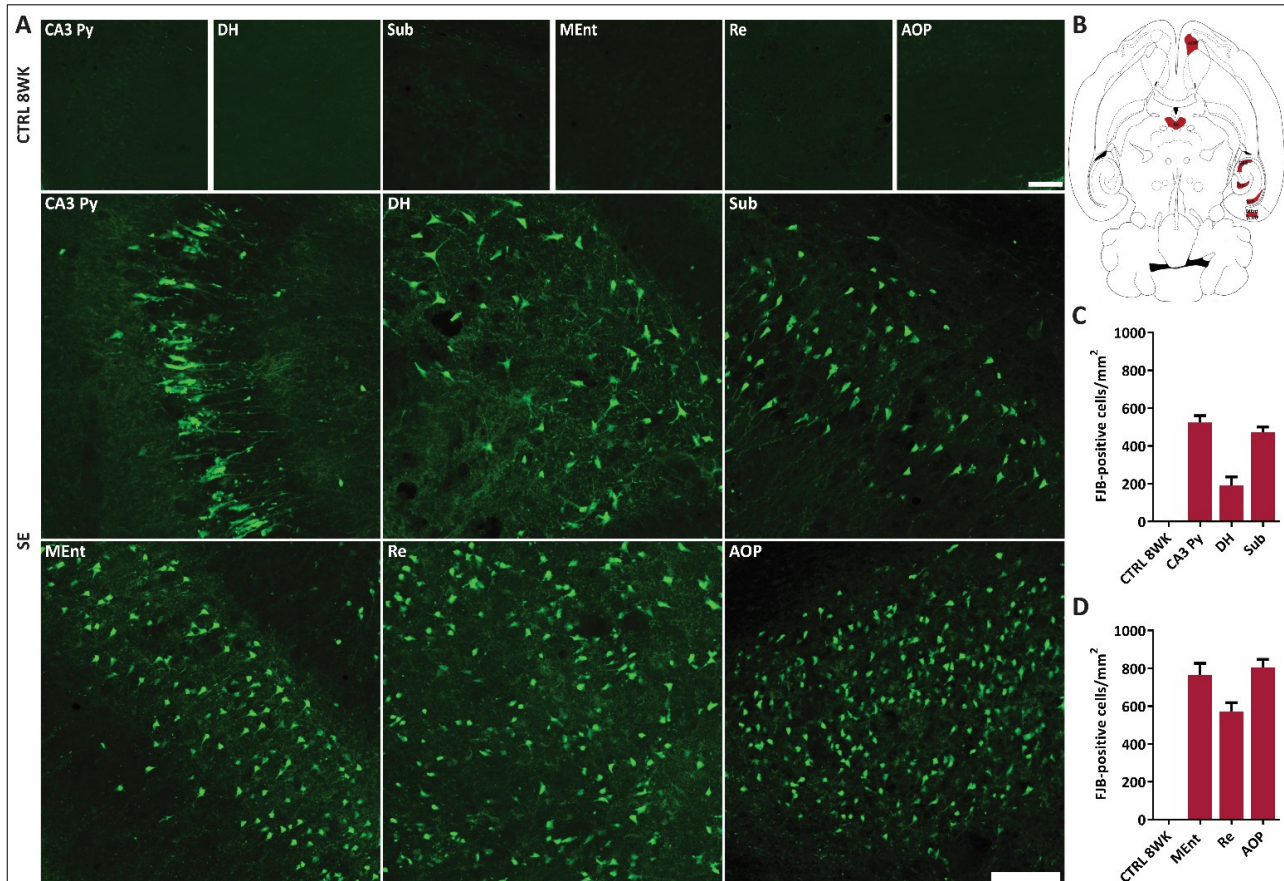


**Fig. 15. Neuronal cell death after induction of status epilepticus (SE) in kainic acid (KA) model.** Sections were stained for Fluoro-Jade B (FJB) to evaluate neuronal cell death (A) in several brain regions (B). The KA treatment induced a significant increase, compared to control group (CTRL) of 8 weeks of age, in FJB staining in the CA3 stratum pyramidalis (CA3 Py, subregion B), hilus of the dentate gyrus (DH) and subiculum (Sub) (C), as well as in layer III of the medial entorhinal cortex (MEnt L.III), nucleus reuniens (Re) and anterior olfactory nucleus (AOP) (D). Quantification was performed using ImageJ. Data are shown as mean  $\pm$  SEM. Scale bar: 100  $\mu$ m. WK, week.

## Neuronal cell survival after induction of SE and development of SRSs

Concerning cell survival (Fig. 15A), neurons were significantly reduced to 56% ( $p < 0.001$ , 3 days post-SE vs age-matched controls; Holm-Sidak test) and, respectively, 72% ( $p < 0.001$ , epileptic animals vs age-matched controls) of control CA3 Py (subregion B) levels (Fig. 15B). In the DH, neurons were reduced to 63% of control rats in rats treated with KA and studied 3 days after the SE ( $p = 0.002$ ). Similarly, in the same brain region,

neurons were reduced to 49% of corresponding controls 64 days post-SE ( $p < 0.001$ ) (Fig. 15C). The Sub was also significantly damaged, as neurons were 62% ( $p < 0.001$ ) of control levels at the earlier time interval, whereas they decreased to 75% of controls at 64 days post-SE ( $p = 0.011$ ) (Fig. 15D). In the MEnt (L.III), neuronal counts were acutely lowered to 56% of control levels ( $p < 0.001$ ), and to 52% of age-matched controls in the epileptic rats ( $p < 0.001$ ) (Fig. 16E). Concerning the Re, neurons decreased to 56% in KA-treated animals vs age-matched controls ( $p = 0.003$ ), and to 40% in epileptic rats ( $p < 0.001$ ) (Fig. 16F). Finally, a similar decrease in neuronal counts was also observed in the AOP, in which cells were 63% of controls ( $p < 0.001$ ) in rats at 3 days after SE, and 50% in epileptic rats ( $p = 0.004$  vs age-matched controls) (Fig. 16G).

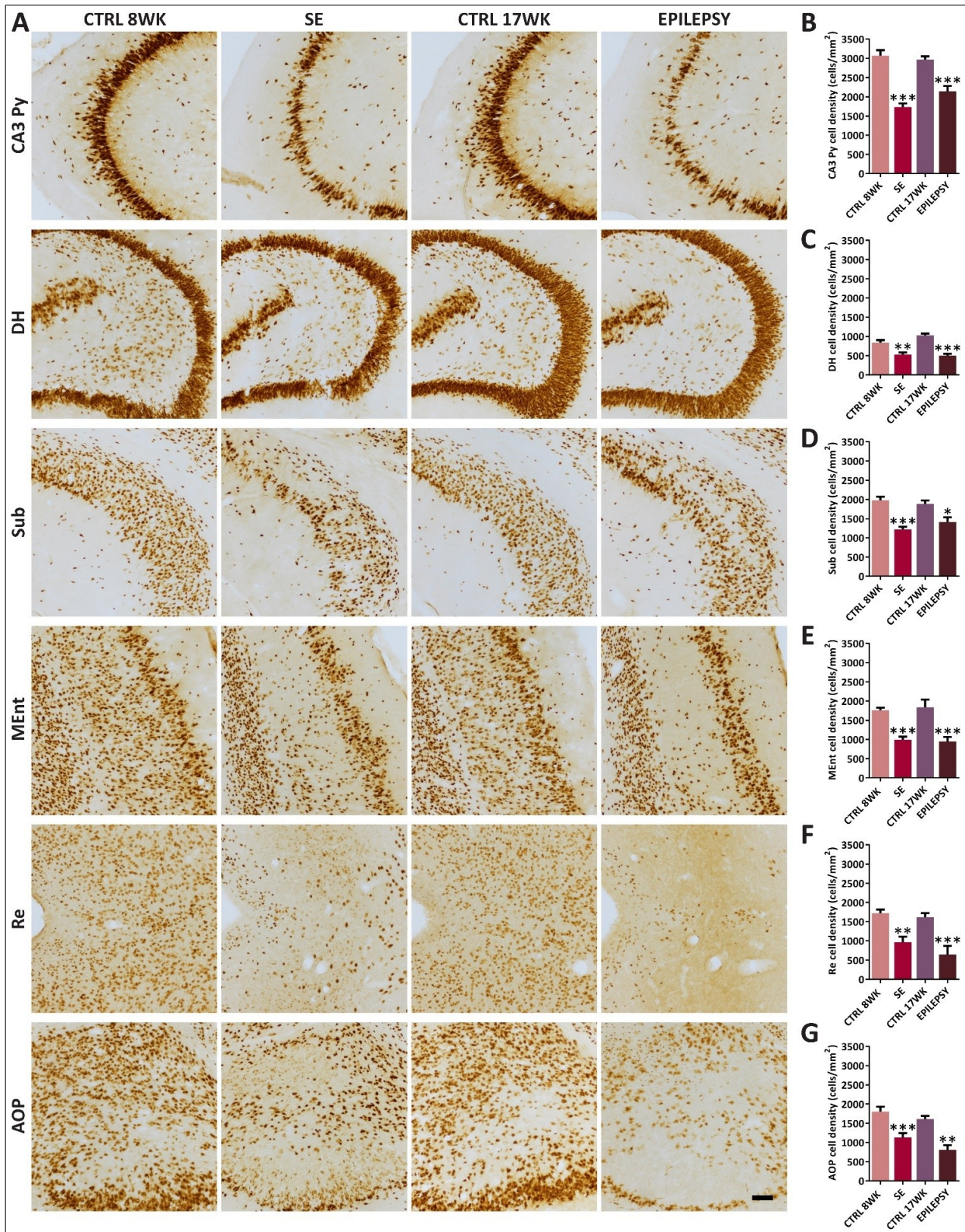


**Fig. 16. Neuronal cell survival after induction of status epilepticus (SE) in the kainic acid (KA) model.** Brain sections were stained against mouse anti-neuron-specific nuclear protein (NeuN) to evaluate neuronal cell survival (A). The KA treatment induced a significant decrease, compared to control group(CTRL), in the number of NeuN-positive cells in the CA3 stratum pyramidalis (CA3 Py, subregion B) (B), hilus of the dentate

gyrus (DH) (C), subiculum (Sub) (D), layer III of the medial entorhinal cortex (MEnt L.III) (E), nucleus reuniens (Re) (F) and anterior olfactory nucleus (AOP) (G). This significant decrease in the number of NeuN- positive cells is present 3 (8 weeks of age) and 64 (17 weeks of age) days after the KA administration. Quantification was performed using ImageJ. Statistical analysis was performed using a one-way ANOVA followed by all pairwise multiple comparison procedures (Holm-Sidak test). Data are shown as mean  $\pm$  SEM. \*  $p < 0.05$ , \*\*  $p < 0.01$ , \*\*\*  $p < 0.001$ ; Scale bar: 100  $\mu$ m. WK, week.

### GFAP-immunonegative areas in the brain after induction of SE

Accordingly to the literature (Gualtieri et al. 2012; Lucchi et al. 2015), when compared to controls (Fig. 17A-B) rats treated with KA presented a mean lesion which respectively was  $0.13 \pm 0.05$  mm<sup>2</sup> in CA3 LMol,  $0.10 \pm 0.02$  mm<sup>2</sup> in Sub,  $0.43 \pm 0.14$  mm<sup>2</sup> in Re and  $0.64 \pm 0.05$  mm<sup>2</sup> in AOP. As shown in Fig. 22C, we also calculated the percentage of the lesion in respect of the total area, evaluated in brain sections stained with NeuN to clearly identify the selected regions. The percentage covered by the lesion respectively was 24% in CA3 LMol, 18% in Sub, 45% in Re and 78% in AOP.

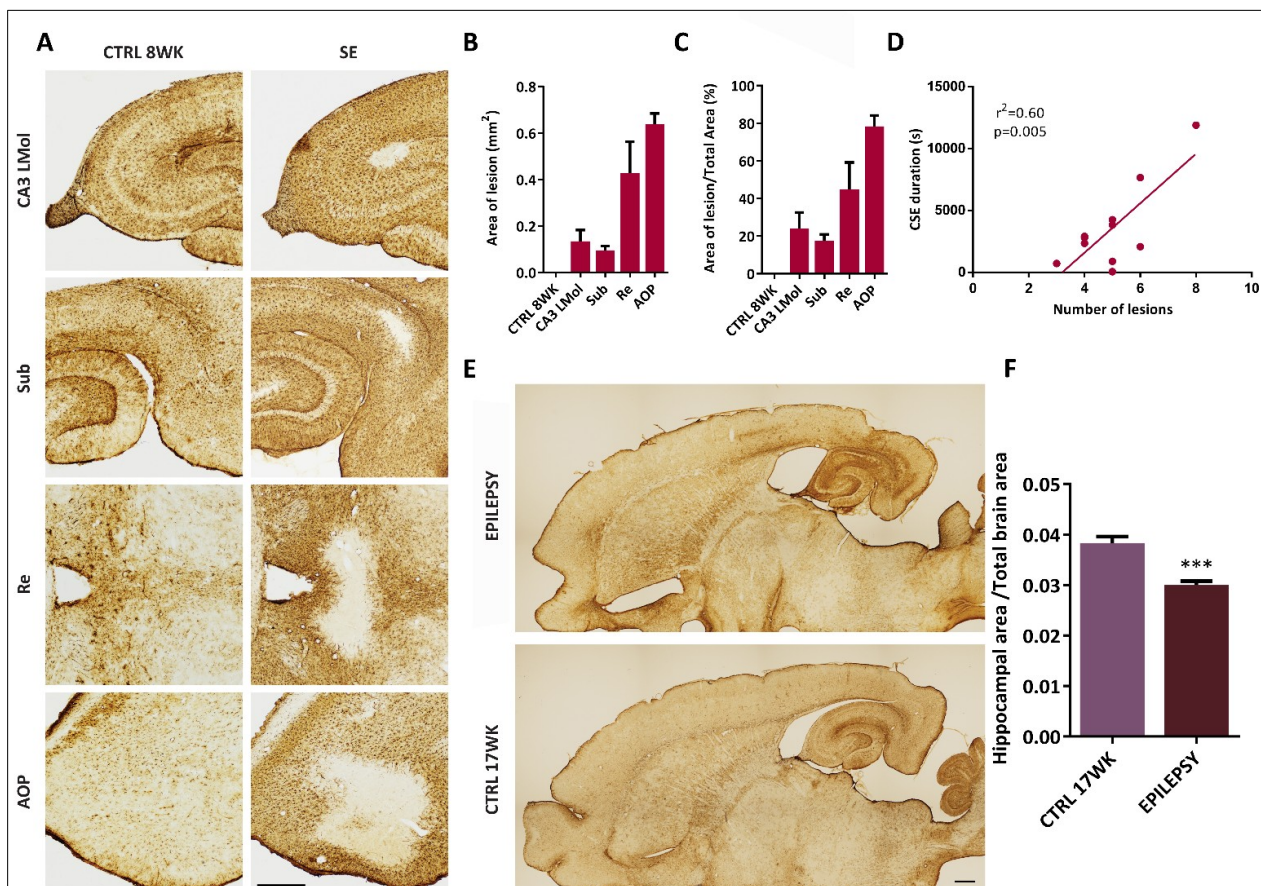


**Fig. 17. Lesioned areas and hippocampal atrophy in kainic acid (KA) model.** Brain sections were stained against mouse anti-glial fibrillary acidic protein (GFAP), a marker of astrocytes, which are absent in lesioned areas (A). Comparing to control group (CTRL) of 8 weeks (WK), the KA treatment induced GFAP-immunonegative areas in CA3 stratum lacunosum-moleculare (CA3 LMol), subiculum (Sub), nucleus reuniens (Re) and anterior olfactory nucleus (AOP) (B). In C, the percentage of lesion area of the total area was also determined in CA3 LMol, Sub, Re and AOP. In D, the linear regression ( $r^2$ ) between the number of damaged brain areas and mean duration of convulsive seizures during status epilepticus (SE) was also determined. The hippocampal atrophy of 64-week-old rats (E) was measured in F. Quantification of the area was performed using the image analysis software NIS-Elements. Statistical analysis was performed using a linear regression analysis and a Student's t-test. Data are shown as mean  $\pm$  SEM. \*\*\* $p < 0.001$ ; Scale bars: 500  $\mu$ m and 1 mm. CSE, convulsive status epilepticus.

### **Relationship between the duration of CSE and the number of damaged areas within the brain**

Three days after SE induction, the percentage of rats presenting lesions revealed by loss of GFAP immunostaining were, respectively, 100% for Sub and AOP, and 64% for CA3 LMol and Re. Additionally, we found that 73% rats were damaged in CA3 Py (subregion B), 27% in CA1 Py, amygdala and entopeduncular nucleus, 9% in CA1 stratum radiatum and substantia nigra. After having calculated the total number of brain lesions for each animal, we tested the relationship between duration of CSE and number of damaged areas, finding a significant relationship between total duration of CSs (stage 4 and stage 5) and the number of damaged areas ( $r^2=0.60$ ,  $p=0.005$ ) (Fig. 17D). At variance, no significant correlation was found between the total duration of SE and the number of damaged areas ( $r^2=0.02$ ,  $p=0.692$ ) (data not shown).

### **Hippocampal atrophy in epileptic rats**

In comparison to the control group, we found that hippocampal atrophy in the epileptic animals corresponds to 25% ( $p < 0.001$ , Student's t-test) (Fig. 17E-F). There was not a significant correlation between hippocampal atrophy and the latency to develop SRSs ( $r^2=0.09$ ,  $p=0.555$ ) (data not shown).

### **Relationship between seizures after the administration of KA and SRSs**

Both nonconvulsive (Fig. 18A-B, on the top) and convulsive SRSs (Fig. 21A-B, on the bottom) were considered in relation to SE progression. We did not find any relationship between: (i) the first stage 0-3 seizures developing after the KA injection and the latency to develop SRSs in chronic epilepsy (Fig. 18C-F); (ii) the latency to develop SE, or alternatively its duration (including the percentage of time spent in convulsive SE over the total SE duration), and the latency to develop SRSs in chronic epilepsy (Fig. 18G-N). In contrast, the latency to develop the first stage 5 CS after KA injection was positively related, respectively, to the latency to

develop the first SRS in chronic epilepsy ( $r^2=0.60$ ,  $p<0.001$ ) (Fig. 18O), and the mean latency to develop the first stage 4-5 SRSs ( $r^2=0.44$ ,  $p<0.001$ ) (Fig. 18P). We also found a relationship between the latency to develop the first SRS and the mean latency to develop the first stage 4-5 SRSs ( $r^2=0.57$ ,  $p<0.001$ ) (Fig. 18Q). Finally, no relationship was found between the duration of SE and the seizure frequency 9 weeks after KA administration ( $r^2=0.14$ ,  $p=0.176$ ) (data not shown).

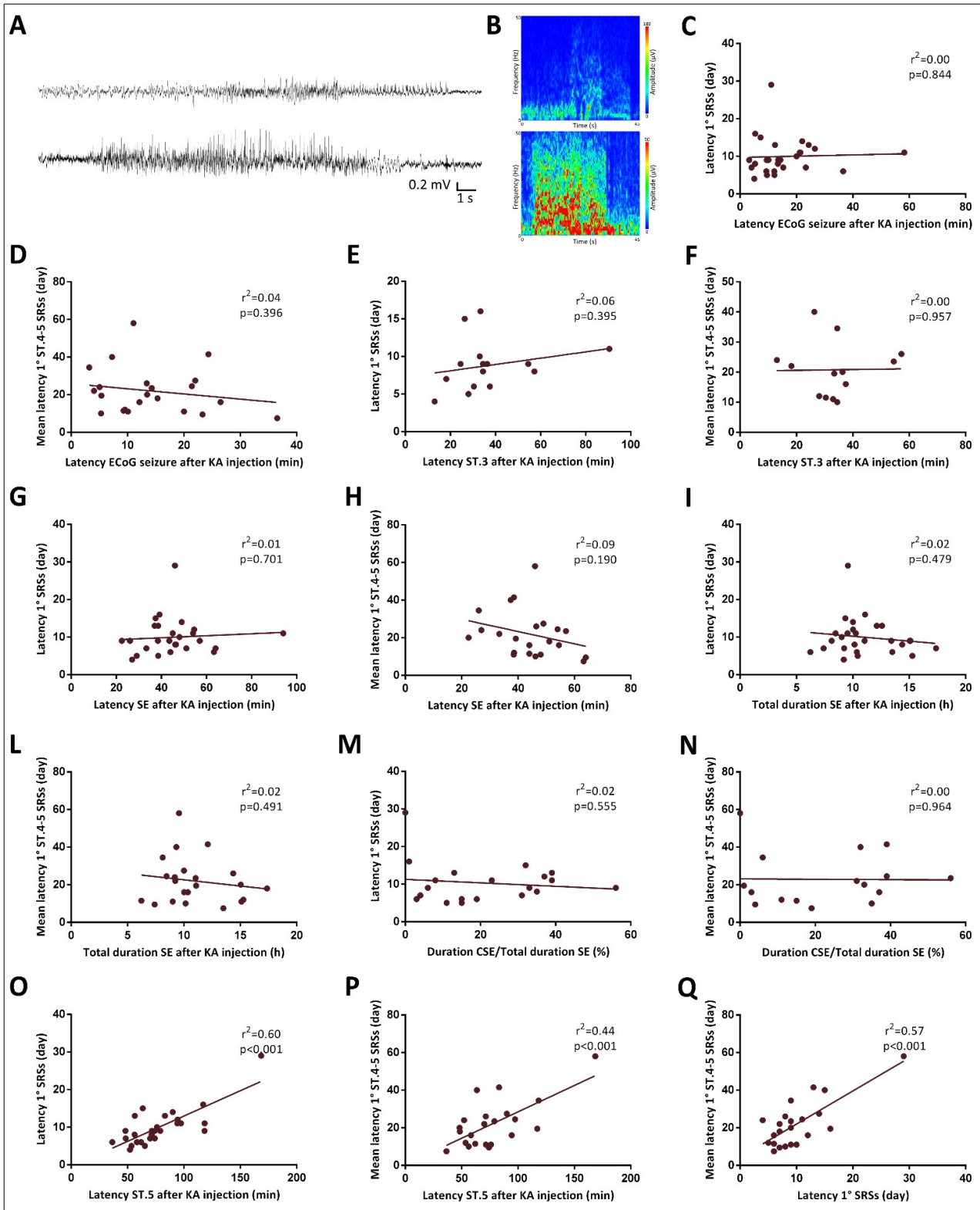


**Fig. 18. Relationship between seizures after the administration of kainic acid (KA) and chronic epilepsy.** In A, the first nonconvulsive (top) and the first convulsive spontaneous recurrent seizures (SRs) (bottom) were reported. In B, the amplitude spectrum maps were shown for the first nonconvulsive (top) and the first convulsive SRs (bottom). Relationships ( $r^2$ ) between the first electrocorticographic seizure after KA injection and SRs were determined in C-D, while relationships between the first stage (st.) 3 seizure after KA injection

and SRSs were determined in E-F. Relationships between the latency to develop status epilepticus (SE) and SRSs were determined in G-H, whereas relationships between the total duration of SE and SRSs were determined in I-L. Similarly, relationships between the percentage of time spent in convulsive SE over the total SE duration and SRSs were determined in M-N. Moreover, relationships between the first st. 5 seizure after KA injection and SRSs were determined in O-P, while the relationship between the latency to develop the first SRS and the mean latency to develop the first convulsive (st. 4-5) SRS was determined in Q. Statistical analysis was performed using a linear regression analysis. Scale: 0.2 mV/1 s. CSE, convulsive status epilepticus; ECoG, electrocorticography.

## DISCUSSION

In the present study, analysis of v-ECoG recordings and lesion extension resulted in the following major findings: i) the early increase of gamma power, which precedes the onset of SE, and the subsequent quick stabilization to under-the-baseline levels until the end of SE, both suggest a predominant role of this ECoG band in determining the overall SE duration; ii) the progressive increase in theta power during SE, reaching the peak in coincidence with the maximal duration of stage 4 CSs and immediately followed by a reduction when stage 5 CSs fully developed, both suggest a role of this band in determining the SE severity; iii) the overall duration of most severe seizures in the course of SE appears to correlate with the brain damage, without affecting the timing of epileptogenesis; iv) the onset of first spontaneous epileptic activity, including both nonconvulsive and convulsive SRSs, is predicted by latency to develop stage 5 CS in the course of SE.

Our main purpose was to re-evaluate the relationship between the lesion extent and the onset of epileptogenesis. To this aim, we first evaluated if the overall duration of CSE and the number of lesions were positively related, finding a significant result. Then, we assumed that a significant relationship should be also found for epileptogenesis, to indicate that a more widespread damage is responsible for an earlier seizure onset in chronic epilepsy. To test this assumption, we evaluated the relationship between overall duration of CSE and onset of SRSs, which was not significant. Although we approached this issue in an indirect manner, our findings are in agreement with evidence obtained in the pilocarpine model showing that rats with a different SE duration, expected to present a different lesion extent (Biagini et al. 2008; Klitgaard et al. 2002), had a similar SRS onset (Bortel 2010; Zhang et al. 2002). However, it would be reasonable to expect that a longer SE might result in earlier appearance of SRSs, but this was not the case in our model. On the other hand, the SE certainly increases the risk to develop epilepsy in adult patients, but the relationship of such risk with the SE duration is not established (Meierkord 2007).

Distribution of lesions caused by KA in our animals was partially consistent with the available knowledge on the model (Lévesque and Avoli 2013; Schwob et al. 1980). For instance, damage to CA3 is commonly observed in KA-treated rats, but it is usually referred to CA3 Py, whereas in the majority of our animals we also found damage in the CA3 LMol, a feature previously reported only in pilocarpine-treated rats (Biagini et

al., 2008). Additionally, we observed that all rats with no exception presented a characteristic lesion in the Sub, in proximity to CA1. This region presents a two-way exchange of information with the Re of the thalamus (McKenna and Vertes 2004; Wouterlood, Saldaña and Witter 1990), which was also damaged in many examined animals. This suggests that the mentioned thalamic-subicular circuit is strongly affected by KA-induced SE so to produce a damage more extensive than that previously found (Drexel et al. 2011). Indeed, a widespread distribution of injuries in KA-treated rats represents a limitation of the model because of the focal nature of lesions found in TLE patients, so to induce the development of other different experimental approaches to model TLE (Schwob et al. 1980; Sloviter and Bumanglag 2013). However, the mentioned alternative approaches did not offer the possibility to address the relationship between SE and epileptogenesis, as instead required by our aims.

According to our aims, we also evaluated the impact of the SE dynamics on onset of SRSs. A growing number of studies suggest that early events occurring already during or immediately after SE could exert long-term morphological and functional effects, thus affecting the onset of seizure activity (Klein et al. 2018). In our experiments, we found that the latency to the first CS with loss of posture in the course of SE was able to predict the onset of SRSs, so the timing of epileptogenesis. This result suggests that any pharmacological intervention able to delay the onset of tonic-clonic seizures during SE could have the potential to delay epileptogenesis. If correct, this means that drugs displaying such an effect may be potentially disclosed for their antiepileptogenic potential in the KA model of SE.

Our findings also indicate that theta and gamma components of cerebral electrical activity can play an important role in determining, respectively, the development of CSE and the overall duration of SE. In our animal model, theta activity might have played a role in promoting stage 4 seizures after SE induction, as its increase in power paralleled the changes in duration of stage 4 seizures and both peaked at the same time. However, when the theta power went back to baseline, CSE became more severe since stage 5 seizures peaked in duration, thus suggesting that a reduction in theta power precedes a full development of CSE. This is in agreement with experiments showing that induction of theta activity in the hippocampus counteracts the development of seizures (Colom et al. 2006; Izadi et al. 2019; Miller, Turner and Gray 1994). Other authors also found a role for theta activity in determining the intensity of SE in knockout mice for the transient receptor potential canonical type 3 channel, in which pilocarpine-induced theta power and seizure scores were both reduced during the pre-ictal phase and SE phase (Phelan et al. 2017). Additionally, the theta band can play a role in the onset of SRSs after the SE, because it was found to be inversely correlated with the latency period and with the power change of the high-gamma rhythm in 3 mouse and 2 rat models of epileptogenesis (Milikovsky et al. 2017).

Gamma activity originates from reciprocal connections of interneurons and principal cells, with a major role played by fast spiking parvalbumin interneurons (Buzsáki and Wang 2012; Wulff et al. 2009). *In vitro* experiments provided evidence for a modulation of gamma oscillations by GABAergic and glutamatergic inputs. Interestingly, GABA type A (GABAA) receptor activation increased the gamma power and, consistently, GABAA receptor antagonism resulted in the opposite finding. Gamma power increased also in presence of GABAB receptor antagonism. Additionally, blockade of the glutamate AMPA receptor reduced the gamma power, which was conversely increased by blocking metabotropic or NMDA glutamatergic receptors (Johnson et al. 2017). Although we did not perform any pharmacological experiment to assess the basis of changes observed in gamma power during the SE in our animals, it is conceivable that a dysfunction in GABAergic inhibitory activity could be responsible for the observed durable reduction in gamma power occurring in the entire course of SE, as suggested by experiments showing an anti-ictogenic role of parvalbumin interneurons during the SE (Lévesque et al. 2019). Conversely, these same experiments revealed a paradoxical capacity to promote seizures of parvalbumin interneurons prior to the SE onset, which could also explain the increase in gamma power anticipating NCSE in our animals.

## **CONCLUSION**

Overall, our study suggests that the analysis of SE dynamics is useful to identify various biomarkers that are predictive of SE progression, the resulting damage, and subsequent epileptogenesis. These biomarkers characterizing the SE dynamics could be useful to disclose new possible targets for more effective therapeutic approaches in TLE.

## **ACKNOWLEDGEMENTS**

Dr. A.M. Costa is recipient of a fellowship from the Fondazione Mariani (Milan, Italy; grant R-19-110 to GB). Dr. C. Lucchi is recipient of a fellowship from the Department of Biomedical, Metabolic and Neural Sciences of the University of Modena and Reggio Emilia ("Progetto Dipartimento di Eccellenza 2018-2022").

## **AUTHOR CONTRIBUTIONS**

A.M.C., C.L., and G.B. designed experiments. A.M.C, C.L., and C.S. collaborated to data acquisition. A.M.C., and G.B. analyzed and interpreted data. A.M.C., and G.B. drafted the article. A.M.C., C.L., C.S, Í.R.L., and G.B. critically revised and finally approved the manuscript.

## **STATEMENT OF ETHICS**

Animal experiments conform to internationally accepted standards and have been approved by the appropriate institutional review body.

## **FUNDING**

This study was supported by the Italian Ministry of Health (grant RF-2011-02350485 to GB), the University of Modena and Reggio Emilia (FAR2018 to GB), and BPER (project “Medicina Clinica e Sperimentale per il Trattamento delle Epilessie” to GB).

## **DISCLOSURE STATEMENT**

The authors have no conflicts of interest to declare.

## Chapter 7

### Summary, conclusion and future perspectives

The findings reported here deepen the understanding about the pathophysiology of MTLE. Together, the data of the present investigation draw attention to the pathology of the amygdala and BF, which has been relatively overlooked in MTLE. Those pathological alterations may be useful as markers for prognosis, or drug response evaluation. Ideally, those alterations should be further explored, for example by means of *in vivo* imaging and single cell omic frameworks. Those approaches could yield deeper insights about the neuroplastic phenomena and how they evolve over the time. This may disclose possible targets of pharmacological intervention directed to regulatory steps of tissue and cellular processes, such as inflammation, cell death, receptor trafficking and so on.

Right now I have rough data to be processed about stereologic measurements of parvalbumin-immunoreactive projection neurons from BF to the amygdala, and parvalbumin-immunoreactive interneurons in amygdala nuclei in epileptic rats. Furthermore, electrophysiological investigations of the effect of proline derivative on the synaptic transmission and its antiepileptic effect are also in course. I hope to complete those manuscripts within some months.

## References

- Abbott, N. Joan. 2013. "Blood-Brain Barrier Structure and Function and the Challenges for CNS Drug Delivery." *Journal of Inherited Metabolic Disease*. J Inherit Metab Dis. <https://doi.org/10.1007/s10545-013-9608-0>.
- Akyuz, Enes, Ayse Kristina Polat, Ece Eroglu, Irem Kullu, Efthalia Angelopoulou, and Yam Nath Paudel. 2020. "Revisiting the Role of Neurotransmitters in Epilepsy: An Updated Review." *Life Sciences*, 118826.
- Alexopoulos, Andreas V. 2013. "Pharmacoresistant Epilepsy: Definition and Explanation." *Epileptology* 1 (1): 38–42. <https://doi.org/10.1016/j.epilep.2013.01.001>.
- Aquino, Pedro Everson Alexandre de, L. C. F. Paes, R. O. Costa, L. A. R. Lima, E. A. Siqueira, M. A. J. Carvalho, T. M. B. Cavalcante, E. R. Silveira, G. S. B. Viana. N-Methyl-trans-4-hydroxy-l-proline isolated from *Sideroxylon obtusifolium* leaves has antioxidant and anticonvulsant activity. In Proceedings of the 2<sup>nd</sup> International Neuroscience Symposium Fortaleza, Brazil, 18 December 2018.
- Aquino, Pedro Everson Alexandre de, Talita Rocha Magalhães, Lucas Antônio Duarte Nicolau, Luzia Kalyne A. Moreira Leal, Nayara Coriolano de Aquino, Sabrina Matias dos Santos, Kelly Rose Tavares Neves, Edilberto Rocha Silveira, and Glauce Socorro de Barros Viana. 2017. "The Anti-Inflammatory Effects of N-Methyl-(2S,4R)-Trans-4-Hydroxy-l-Proline from *Syderoxylon Obtusifolium* Are Related to Its Inhibition of TNF-Alpha and Inflammatory Enzymes." *Phytomedicine* 24 (January): 14–23. <https://doi.org/10.1016/J.PHYMED.2016.11.010>.
- Araujo-Neto, Vitor, Rangel R Bomfim, Valter O. B Oliveira, Ailane M. P. R Passos, Juliana P. R Oliveira, Clésio A Lima, Sandra S Mendes, Charles S Estevam, and Sara M Thomazzi. 2010. "Therapeutic Benefits of *Sideroxylon Obtusifolium* (Humb. Ex Roem. & Schult.) T.D. Penn., Sapotaceae, in Experimental Models of Pain and Inflammation." *Revista Brasileira de Farmacognosia* 20 (6): 933–38. <https://doi.org/10.1590/S0102-695X2010005000043>.
- Arisi, Gabriel M, Megan Ruch, Maira L Foresti, Sanjib Mukherjee, Charles E Ribak, and Lee A Shapiro. 2011. "Astrocyte Alterations in the Hippocampus Following Pilocarpine-Induced Seizures in Aged Rats." *Aging and Disease* 2 (4): 294–300. <https://www.ncbi.nlm.nih.gov/pmc/articles/PMC3295071/pdf/ad-2-4-294.pdf>.
- Aronica, Eleonora, Angelika Mühlebner, Erwin A. van Vliet, and Jan A. Gorter. 2017. *Characterization of Pathology. Models of Seizures and Epilepsy: Second Edition*. Second Edi. Elsevier Inc. <https://doi.org/10.1016/B978-0-12-804066-9.00011-0>.
- Asadi-Pooya, Ali A., S. Mohammad Ali Razavizadegan, Alireza Abdi-Ardekani, and Michael R. Sperling. 2013. "Adjunctive Use of Verapamil in Patients with Refractory Temporal Lobe Epilepsy: A Pilot Study." *Epilepsy & Behavior* 29 (1): 150–54. <https://doi.org/10.1016/J.YEBEH.2013.07.006>.
- Bankstahl, Marion, Jens P. Bankstahl, and Wolfgang Löscher. 2013. "Pilocarpine-Induced Epilepsy

in Mice Alters Seizure Thresholds and the Efficacy of Antiepileptic Drugs in the 6-Hertz Psychomotor Seizure Model.” *Epilepsy Research* 107 (3): 205–16.  
<https://doi.org/10.1016/J.EPLEPSYRES.2013.09.014>.

- Barba, C., G. Barbati, L. Minotti, D. Hoffmann, and P. Kahane. 2007. “Ictal Clinical and Scalp-EEG Findings Differentiating Temporal Lobe Epilepsies from Temporal ‘plus’ Epilepsies.” *Brain* 130 (7): 1957–67. <https://doi.org/10.1093/brain/awm108>.
- Barker-Haliski, Melissa, and H. Steve White. 2017. *Use of Animal Models for Epilepsy Research and Therapy Development. Models of Seizures and Epilepsy: Second Edition*. Second Edi. Elsevier Inc. <https://doi.org/10.1016/B978-0-12-804066-9.00007-9>.
- Bartolomei, Fabrice, Delphine Cosandier-Rimele, Aileen McGonigal, Sandrine Aubert, Jean Régis, Martine Gavaret, Fabrice Wendling, and Patrick Chauvel. 2010. “From Mesial Temporal Lobe to Temporoparietal Seizures: A Quantified Study of Temporal Lobe Seizure Networks.” *Epilepsia* 51 (10): 2147–58. <https://doi.org/10.1111/j.1528-1167.2010.02690.x>.
- Bateman, Alex, Maria Jesus Martin, Claire O’Donovan, Michele Magrane, Emanuele Alpi, Ricardo Antunes, Benoit Bely, et al. 2017. “UniProt: The Universal Protein Knowledgebase.” *Nucleic Acids Research* 45 (D1): D158–69. <https://doi.org/10.1093/nar/gkw1099>.
- Beghi, Ettore. 2016. “Addressing the Burden of Epilepsy: Many Unmet Needs.” *Pharmacological Research* 107: 79–84. <https://doi.org/10.1016/j.phrs.2016.03.003>.
- Behr, C., M. A. Goltzene, G. Kosmalki, E. Hirsch, and P. Ryvlin. 2016. “Epidemiology of Epilepsy.” *Revue Neurologique* 172 (1): 27–36. <https://doi.org/10.1016/j.neurol.2015.11.003>.
- Ben-Ari, Y. 1985. “Limbic Seizure and Brain Damage Produced by Kainic Acid: Mechanisms and Relevance to Human Temporal Lobe Epilepsy.” *Neuroscience* 14 (2): 375–403.  
[https://doi.org/10.1016/0306-4522\(85\)90299-4](https://doi.org/10.1016/0306-4522(85)90299-4).
- Ben-Ari, Y., E. Tremblay, O. P. Ottersen, and B. S. Meldrum. 1980. “The Role of Epileptic Activity in Hippocampal and ‘remote’ Cerebral Lesions Induced by Kainic Acid.” *Brain Research* 191 (1): 79–97. [https://doi.org/10.1016/0006-8993\(80\)90316-9](https://doi.org/10.1016/0006-8993(80)90316-9).
- Ben-Ari, Y., R. E. Zigmond, C. C D Shute, and P. R. Lewis. 1977. “Regional Distribution of Choline Acetyltransferase and Acetylcholinesterase within the Amygdaloid Complex and Stria Terminalis System.” *Brain Research* 120 (3): 435–45. [https://doi.org/10.1016/0006-8993\(77\)90397-3](https://doi.org/10.1016/0006-8993(77)90397-3).
- Bengzon, Johan, Stefan R Hansson, Beth J Hoffman, and Olle Lindvall. 1999. “Regulation of Norepinephrine Transporter and Tyrosine Hydroxylase MRNAs after Kainic Acid-Induced Seizures.” *Brain Research* 842 (1): 239–42.
- Bertoglio, Daniele, Halima Amhaoul, Annemie Van Eetveldt, Ruben Houbrechts, Sebastiaan Van De Vijver, Idrish Ali, and Stefanie Dedeurwaerdere. 2017. “Kainic Acid-Induced Post-Status Epilepticus Models of Temporal Lobe Epilepsy with Diverging Seizure Phenotype and

- Neuropathology.” *Frontiers in Neurology* 8. <https://doi.org/10.3389/FNEUR.2017.00588>.
- Bethmann, Kerstin, Jean-Marc Fritschy, Claudia Brandt, and Wolfgang Löscher. 2008. “Antiepileptic Drug Resistant Rats Differ from Drug Responsive Rats in GABAA Receptor Subunit Expression in a Model of Temporal Lobe Epilepsy.” *Neurobiology of Disease* 31 (2): 169–87. <https://doi.org/10.1016/J.NBD.2008.01.005>.
- Biagini, Giuseppe, Enrica Baldelli, Daniela Longo, Miranda Baccarani Contri, Uliano Guerrini, Luigi Sironi, Paolo Gelosa, Isabella Zini, David S. Ragsdale, and Massimo Avoli. 2008. “Proepileptic Influence of a Focal Vascular Lesion Affecting Entorhinal Cortex-CA3 Connections After Status Epilepticus.” *Journal of Neuropathology and Experimental Neurology* 67 (7): 687–701. <https://doi.org/10.1097/NEN.0b013e318181b8ae>.
- Binder, D.K., and Christian Steinhäuser. 2017. “Role of Astrocyte Dysfunction in Epilepsy.” In *Reference Module in Neuroscience and Biobehavioral Psychology*, 1–7. Elsevier. <https://doi.org/10.1016/B978-0-12-809324-5.00071-7>.
- Binder, Devin K., and Monica J. Carson. 2013. “Glial Cells as Primary Therapeutic Targets for Epilepsy.” *Neurochemistry International* 63 (7): 635–37. <https://doi.org/10.1016/j.neuint.2013.09.004>.
- Birioukova, L M, E Yu Sitnikova, M A Kulikov, and V V Raevsky. 2016. “Compensatory Changes in the Brain Dopaminergic System of WAG/Rij Rats Genetically Predisposed to Absence Epilepsy.” *Bulletin of Experimental Biology and Medicine* 161 (5): 662–65.
- Blümcke, Ingmar, Elisabeth Pauli, Hans Clusmann, Johannes Schramm, Albert Becker, Christian Elger, Martin Merschhemke, et al. 2007. “A New Clinico-Pathological Classification System for Mesial Temporal Sclerosis.” *Acta Neuropathologica* 113 (3): 235–44. <https://doi.org/10.1007/s00401-006-0187-0>.
- Blümcke, Ingmar, Maria Thom, Eleonora Aronica, Dawna D. Armstrong, Fabrice Bartolomei, Andrea Bernasconi, Neda Bernasconi, et al. 2013. “International Consensus Classification of Hippocampal Sclerosis in Temporal Lobe Epilepsy: A Task Force Report from the ILAE Commission on Diagnostic Methods.” *Epilepsia* 54 (7): 1315–29. <https://doi.org/10.1111/epi.12220>.
- Bohni, Nadine, María Lorena Cordero-Maldonado, Jan Maes, Dany Siverio-Mota, Laurence Marcourt, Sebastian Munck, Appolinary R. Kamuhabwa, et al. 2013. “Integration of Microfractionation, QNMR and Zebrafish Screening for the In Vivo Bioassay-Guided Isolation and Quantitative Bioactivity Analysis of Natural Products.” *PLoS ONE* 8 (5): 1–13. <https://doi.org/10.1371/journal.pone.0064006>.
- Borlot, Felipe, Robert G. Wither, Anfal Ali, Nicky Wu, Flavia Verocai, and Danielle M. Andrade. 2014. “A Pilot Double-Blind Trial Using Verapamil as Adjuvant Therapy for Refractory Seizures.” *Epilepsy Research* 108 (9): 1642–51.

<https://doi.org/10.1016/J.EPLEPSYRES.2014.08.009>.

- Bortel, Aleksandra, Maxime Lévesque, Giuseppe Biagini, Jean Gotman, and Massimo Avoli. 2010. "Convulsive Status Epilepticus Duration as Determinant for Epileptogenesis and Interictal Discharge Generation in the Rat Limbic System." *Neurobiology of Disease* 40 (2): 478–89. <https://doi.org/10.1016/J.NBD.2010.07.015>.
- Bouyer, J. J., M.F Montaron, and A Rougeul. 1981. "Fast Fronto-Parietal Rhythms during Combined Focused Attentive Behaviour and Immobility in Cat: Cortical and Thalamic Localizations." *Electroencephalography and Clinical Neurophysiology* 51 (3): 244–52. [https://doi.org/10.1016/0013-4694\(81\)90138-3](https://doi.org/10.1016/0013-4694(81)90138-3).
- Brandt, C., U. Ebert, and W. Löscher. 2004. "Epilepsy Induced by Extended Amygdala-Kindling in Rats: Lack of Clear Association between Development of Spontaneous Seizures and Neuronal Damage." *Epilepsy Research* 62 (2–3): 135–56. <https://doi.org/10.1016/j.eplepsyres.2004.08.008>.
- Brillatz, Théo, Chiara Lauritano, Maxime Jacmin, Supitcha Khamma, Laurence Marcourt, Davide Righi, Giovanna Romano, et al. 2018. "Zebrafish-Based Identification of the Antiseizure Nucleoside Inosine from the Marine Diatom Skeletonema Marinoi." *PLoS ONE* 13 (4): 1–15. <https://doi.org/10.1371/journal.pone.0196195>.
- Brillatz, Théo, Maxime Jacmin, Emerson Ferreira Queiroz, Laurence Marcourt, Ivan Slacanin, Charlotte Petit, Pierre Alain Carrupt, et al. 2020. "Zebrafish Bioassay-Guided Isolation of Antiseizure Compounds from the Cameroonian Medicinal Plant *Cyperus articulatus* L." *Phytomedicine* 70 (December 2019): 153175. <https://doi.org/10.1016/j.phymed.2020.153175>.
- Bronen, Richard A, Robert K Fulbright, Jung H Kim, Susan S Spencer, Dennis D Spencer, and Nayef R F Al-Rodhan. 1995. "Regional Distribution of MR Findings in Hippocampal Sclerosis." *AJNR Am J Neuroradiol*. Vol. 16. <http://www.ajnr.org/content/ajnr/16/6/1193.full.pdf>.
- Buzsáki, György, and Xiao-Jing Wang. 2012. "Mechanisms of Gamma Oscillations." *Annual Review of Neuroscience* 35 (1): 203–25. <https://doi.org/10.1146/annurev-neuro-062111-150444>.
- Callahan, Patrick M., Joseph M. Paris, Cunningham Kathryn A., and Patricia Shinnick-Gallagher. 1991. "Decrease of GABA-Immunoreactive Neurons in the Amygdala after Electrical Kindling in the Rat." *Brain Research* 555 (2): 335–39. [https://doi.org/10.1016/0006-8993\(91\)90361-X](https://doi.org/10.1016/0006-8993(91)90361-X).
- Cameron, Alexandra, Amit Bansal, Tarun Dua, Suzanne R. Hill, Solomon L. Moshe, Aukje K. Mantel-Teeuwisse, and Shekhar Saxena. 2012. "Mapping the Availability, Price, and Affordability of Antiepileptic Drugs in 46 Countries." *Epilepsia* 53 (6): 962–69. <https://doi.org/10.1111/j.1528-1167.2012.03446.x>.
- Camfield, Carol S, Pasquale Striano, and Peter R Camfield. 2013. "Epidemiology of Juvenile Myoclonic Epilepsy." *Epilepsy & Behavior* 28: S15–17. <https://doi.org/https://doi.org/10.1016/j.yebeh.2012.06.024>.

- Canolty, Ryan T, Erik Edwards, Sarang S Dalal, Maryam Soltani, Srikantan S Nagarajan, Heidi E Kirsch, Mitchel S Berger, Nicholas M Barbaro, and Robert T Knight. 2006. "High Gamma Power Is Phase-Locked to Theta Oscillations in Human Neocortex." *Science* 313 (5793): 1626–28.
- Carlsen, Jørn, László Záborszky, and Lennart Heimer. 1985. "Cholinergic Projections from the Basal Forebrain to the Basolateral Amygdaloid Complex: A Combined Retrograde Fluorescent and Immunohistochemical Study." *Journal of Comparative Neurology* 234 (2): 155–67. <https://doi.org/10.1002/cne.902340203>.
- Carlsen, Jørn, and Lennart Heimer. 1986. "A Correlated Light and Electron Microscopic Immunocytochemical Study of Cholinergic Terminals and Neurons in the Rat Amygdaloid Body with Special Emphasis on the Basolateral Amygdaloid Nucleus." *The Journal of Comparative Neurology* 244 (1): 121–36. <https://doi.org/10.1002/cne.902440110>.
- Cavalheiro, E. A., N. F. Santos, and M. R. Priel. 1996. "The Pilocarpine Model of Epilepsy in Mice." *Epilepsia* 37 (10): 1015–19. <https://doi.org/10.1111/j.1528-1157.1996.tb00541.x>.
- Cendes, Fernando, F. Andermann, P. Gloor, A. Evans, M. Jones-Gotman, C. Watson, D. Melanson, et al. 1993. "MRI Volumetric Measurement of Amygdala and Hippocampus in Temporal Lobe Epilepsy." *Neurology* 43 (4): 719–25. <https://doi.org/10.1212/wnl.43.4.719>.
- Cendes, Fernando, F. Andermann, F. Dubeau, P. Gloor, A. Evans, M. Jones-Gotman, A. Olivier, et al. 1993. "Early Childhood Prolonged Febrile Convulsions, Atrophy and Sclerosis of Mesial Structures, and Temporal Lobe Epilepsy: An Mri Volumetric Study." *Neurology* 43 (6): 1083–87.
- Cendes, Fernando, F. Andermann, P. Gloor, I. Lopes-Cendes, E. Andermann, D. Melanson, M. Jones-Gotman, Y. Robitaille, A. Evans, and T. Peters. 1993. "Atrophy of Mesial Structures in Patients with Temporal Lobe Epilepsy: Cause or Consequence of Repeated Seizures?" *Annals of Neurology* 34 (6): 795–801. <https://doi.org/10.1002/ana.410340607>.
- Cendes, Fernando, Americo C. Sakamoto, Roberto Spreafico, William Bingaman, and Albert J. Becker. 2014. "Epilepsies Associated with Hippocampal Sclerosis." *Acta Neuropathologica* 128 (1): 21–37. <https://doi.org/10.1007/s00401-014-1292-0>.
- Cendes, Fernando, François Leproux, Denis Melanson, Romeo Ethier, Alan Evans, Terry Peters, and Frederick Andermann. 1993. "Mri of Amygdala and Hippocampus in Temporal Lobe Epilepsy." *Journal of Computer Assisted Tomography* 17 (2): 206–10. <https://doi.org/10.1097/00004728-199303000-00008>.
- Challal, Soura, Nadine Bohni, Olivia E. Buenafe, Camila V. Esguerra, Peter A.M. De Witte, Jean Luc Wolfender, and Alexander D. Crawford. 2012. "Zebrafish Bioassay-Guided Microfractionation for the Rapid in Vivo Identification of Pharmacologically Active Natural Products." *Chimia* 66 (4): 229–32. <https://doi.org/10.2533/chimia.2012.229>.

- Chen, Zhibin, Martin J. Brodie, Danny Liew, and Patrick Kwan. 2018. "Treatment Outcomes in Patients With Newly Diagnosed Epilepsy Treated With Established and New Antiepileptic Drugs." *JAMA Neurology* 75 (3): 279. <https://doi.org/10.1001/jamaneurol.2017.3949>.
- Chen, Yucai, Jianjun Lu, Hong Pan, Yuehua Zhang, Husheng Wu, Keming Xu, Xiaoyan Liu, et al. 2003. "Association between Genetic Variation of CACNA1H and Childhood Absence Epilepsy." *Annals of Neurology* 54 (2): 239–43. <https://doi.org/https://doi.org/10.1002/ana.10607>.
- Clossen, Bryan L., and Doodipala Samba Reddy. 2017. "Novel Therapeutic Approaches for Disease-Modification of Epileptogenesis for Curing Epilepsy." *Biochimica et Biophysica Acta - Molecular Basis of Disease* 1863 (6): 1519–38. <https://doi.org/10.1016/j.bbadis.2017.02.003>.
- Colom, Luis V., Antonio García-Hernández, Maria T. Castañeda, Miriam G. Perez-Cordova, and Emilio R. Garrido-Sanabria. 2006. "Septo-Hippocampal Networks in Chronically Epileptic Rats: Potential Antiepileptic Effects of Theta Rhythm Generation." *Journal of Neurophysiology* 95 (6): 3645–53. <https://doi.org/10.1152/jn.00040.2006>.
- Commission on Epidemiology and Prognosis., and International League Against Epilepsy. 1993. "Guidelines for Epidemiologic Studies on Epilepsy." *Epilepsia* 34 (4): 592–96. <https://doi.org/10.1111/j.1528-1157.1993.tb00433.x>.
- Committee for the Update of the Guide for the Care and Use of Laboratory Animals. 2011. *GUIDE FOR THE CARE AND USE OF LABORATORY ANIMALS*. Edited by Janet C Garber. 8th ed. Washington, D.C.: The National Academies Press. <http://www.nap.edu>.
- Cornaggia, Cesare Maria, Massimiliano Beghi, Milena Provenzi, and Ettore Beghi. 2006. "Correlation between Cognition and Behavior in Epilepsy." *Epilepsia* 47 (s2): 34–39. <https://doi.org/10.1111/j.1528-1167.2006.00685.x>.
- Coulter, Douglas A., and Christian Steinhäuser. 2015. "Role of Astrocytes in Epilepsy." *Cold Spring Harbor Perspectives in Medicine* 5 (3): 1–12. <https://doi.org/10.1101/cshperspect.a022434>.
- Cronin, James, and F. Edward Dudek. 1988. "Chronic Seizures and Collateral Sprouting of Dentate Mossy Fibers after Kainic Acid Treatment in Rats." *Brain Research* 474 (1): 181–84. [https://doi.org/10.1016/0006-8993\(88\)90681-6](https://doi.org/10.1016/0006-8993(88)90681-6).
- Crunelli, Vincenzo, and Nathalie Leresche. 2002. "Childhood Absence Epilepsy: Genes, Channels, Neurons and Networks." *Nature Reviews Neuroscience* 3 (5): 371–82. <https://doi.org/10.1038/nrn811>.
- Curia, Giulia, Daniela Longo, Giuseppe Biagini, Roland S G Jones, and Massimo Avoli. 2008. "The Pilocarpine Model of Temporal Lobe Epilepsy." *Journal of Neuroscience Methods* 172 (2): 143–57. <https://doi.org/10.1016/j.jneumeth.2008.04.019>.
- D'Ambrosio, Raimondo, and John W Miller. 2010. "What Is an Epileptic Seizure? Unifying Definitions in Clinical Practice and Animal Research to Develop Novel Treatments." *Epilepsy*

*Currents* 10 (3): 61–66. <https://doi.org/10.1111/j.1535-7511.2010.01358.x>.

Dalic, Linda, and Mark J Cook. 2016. “Managing Drug-Resistant Epilepsy: Challenges and Solutions.” *Neuropsychiatric Disease and Treatment* 12: 2605–16. <https://doi.org/10.2147/NDT.S84852>.

De Coteau, William E, Catherine Thorn, Daniel J Gibson, Richard Courtemanche, Partha Mitra, Yasuo Kubota, and Ann M Graybiel. 2007. “Learning-Related Coordination of Striatal and Hippocampal Theta Rhythms during Acquisition of a Procedural Maze Task.” *Proceedings of the National Academy of Sciences of the United States of America* 104 (13): 5644–49. <https://doi.org/10.1073/pnas.0700818104>.

Devinsky, Orrin, and Blanca Vazquez. 1993. “Behavioral Changes Associated with Epilepsy.” *Neurologic Clinics* 11 (1): 127–49. [https://doi.org/10.1016/S0733-8619\(18\)30173-7](https://doi.org/10.1016/S0733-8619(18)30173-7).

Diaz Verdugo, Carmen, Sverre Myren-Svelstad, Ecem Aydin, Evelien Van Hoeymissen, Celine Deneubourg, Silke Vanderhaeghe, Julie Vancraeynest, et al. 2019. “Glia-Neuron Interactions Underlie State Transitions to Generalized Seizures.” *Nature Communications* 10 (1): 1–13. <https://doi.org/10.1038/s41467-019-11739-z>.

Ding, Kan, Puneet K. Gupta, and Ramon Diaz-Arrastia. 2016. *Epilepsy after Traumatic Brain Injury. Translational Research in Traumatic Brain Injury*. Second Edi. Elsevier Inc. <https://doi.org/10.1201/b18959-15>.

Dix, Sophie L., and John P. Aggleton. 1999. “Extending the Spontaneous Preference Test of Recognition: Evidence of Object-Location and Object-Context Recognition.” *Behavioural Brain Research* 99 (2): 191–200. [https://doi.org/10.1016/S0166-4328\(98\)00079-5](https://doi.org/10.1016/S0166-4328(98)00079-5).

Drexel, M., A.P. Preidt, E. Kirchmair, and G. Sperk. 2011. “Parvalbumin Interneurons and Calretinin Fibers Arising from the Thalamic Nucleus Reuniens Degenerate in the Subiculum after Kainic Acid-Induced Seizures.” *Neuroscience* 189 (August): 316–29. <https://doi.org/10.1016/J.NEUROSCIENCE.2011.05.021>.

Drexel, Meinrad, Adrian Patrick Preidt, and Günther Sperk. 2012. “Sequel of Spontaneous Seizures after Kainic Acid-Induced Status Epilepticus and Associated Neuropathological Changes in the Subiculum and Entorhinal Cortex.” *Neuropharmacology* 63 (5): 806–17. <https://doi.org/10.1016/J.NEUROPHARM.2012.06.009>.

Drinovac, Mihael, Helga Wagner, Niruj Agrawal, Hannah R. Cock, Alex J. Mitchell, and Tim J. von Oertzen. 2015. “Screening for Depression in Epilepsy: A Model of an Enhanced Screening Tool.” *Epilepsy and Behavior* 44: 67–72. <https://doi.org/10.1016/j.yebeh.2014.12.014>.

Du, F., T. Eid, E. W. Lothman, C. Kohler, and R. Schwarcz. 1995. “Preferential Neuronal Loss in Layer III of the Medial Entorhinal Cortex in Rat Models of Temporal Lobe Epilepsy.” *Journal of Neuroscience* 15 (10): 6301–13. <https://doi.org/10.1523/jneurosci.15-10-06301.1995>.

Dudek, F. Edward, and Kevin J. Staley. 2017. *Post-Status Epilepticus Models: Systemic Kainic Acid*.

*Models of Seizures and Epilepsy: Second Edition*. Second Edi. Elsevier Inc.  
<https://doi.org/10.1016/B978-0-12-804066-9.00041-9>.

- Dudek, F. Edward, Suzanne Clark, Philip A. Williams, And Heidi L. Grabenstatter. 2006. "Kainate-Induced Status Epilepticus: A Chronic Model of Acquired Epilepsy." In *Models of Seizures and Epilepsy*, 415–32. Elsevier. <https://doi.org/10.1016/B978-012088554-1/50036-0>.
- Dutra Moraes, Márcio Flávio, Orfa Yineth Galvis-Alonso, and Norberto Garcia-Cairasco. 2000. "Audiogenic Kindling in the Wistar Rat: A Potential Model for Recruitment of Limbic Structures." *Epilepsy Research* 39 (3): 251–59. [https://doi.org/10.1016/S0920-1211\(00\)00107-8](https://doi.org/10.1016/S0920-1211(00)00107-8).
- Emre, Murat, Stephan Heckers, Deborah C. Mash, Changiz Geula, and M.-Marsel Mesulam. 1993. "Cholinergic Innervation of the Amygdaloid Complex in the Human Brain and Its Alterations in Old Age and Alzheimer's Disease." *The Journal of Comparative Neurology* 336 (1): 117–34. <https://doi.org/10.1002/cne.903360110>.
- Engel, Jerome. 2006. "ILAE Classification of Epilepsy Syndromes." *Epilepsy Research* 70 Suppl 1 (SUPPL.1): S5-10. <https://doi.org/10.1016/j.eplepsyres.2005.11.014>.
- Epps, S. Alisha, Alexa B. Kahn, Philip V. Holmes, Katherine A. Boss-Williams, Jay M. Weiss, and David Weinshenker. 2013. "Antidepressant and Anticonvulsant Effects of Exercise in a Rat Model of Epilepsy and Depression Comorbidity." *Epilepsy and Behavior* 29 (1): 47–52. <https://doi.org/10.1016/j.yebeh.2013.06.023>.
- Faingold, Carl L. 2013. "Brainstem Networks." In *Jasper's Basic Mechanisms of the Epilepsies*, 257–71. Oxford University Press. <https://doi.org/10.1093/med/9780199746545.003.0020>.
- Feldmann, Maria, Marie-Claude Asselin, Joan Liu, Shaonan Wang, Adam McMahon, José Anton-Rodriguez, Matthew Walker, et al. 2013. "P-Glycoprotein Expression and Function in Patients with Temporal Lobe Epilepsy: A Case-Control Study." *The Lancet Neurology* 12 (8): 777–85. [https://doi.org/10.1016/S1474-4422\(13\)70109-1](https://doi.org/10.1016/S1474-4422(13)70109-1).
- Ferry, Barbara, Damien Gervasoni, and Catherine Vogt. 2014. *Stereotaxic Neurosurgery in Laboratory Rodent - Handbook on Best Practices*. 1<sup>a</sup>. Paris: Springer. <https://doi.org/10.1007/978-2-8178-0472-9>.
- Fisher, Robert S., and Ilo Leppik. 2008. "Debate: When Does a Seizure Imply Epilepsy?" *Epilepsia* 49 (SUPPL. 9): 7–12. <https://doi.org/10.1111/j.1528-1167.2008.01921.x>.
- Fisher, Robert S., Carlos Acevedo, Alexis Arzimanoglou, Alicia Bogacz, J. Helen Cross, Christian E. Elger, Jerome Engel, et al. 2014. "ILAE Official Report: A Practical Clinical Definition of Epilepsy." *Epilepsia* 55 (4): 475–82. <https://doi.org/10.1111/epi.12550>.
- Freund, T F, and A I Gulyás. 1997. "Inhibitory Control of GABAergic Interneurons in the Hippocampus." *Canadian Journal of Physiology and Pharmacology* 75 (5): 479–87. <https://doi.org/10.1139/y97-033>.
- Furtado, M. A., Glaucia K. Braga, José A. C. Oliveira, Flavio Del Vecchio, and Norberto

- Garcia-Cairasco. 2002. "Behavioral, Morphologic, and Electroencephalographic Evaluation of Seizures Induced by Intrahippocampal Microinjection of Pilocarpine." *Epilepsia* 43 (July): 37–39. <https://doi.org/10.1046/j.1528-1157.43.s.5.41.x>.
- Furtado, M.A., O.W. Castro, F. Del Vecchio, J.A. Cortes de Oliveira, and N. Garcia-Cairasco. 2011. "Study of Spontaneous Recurrent Seizures and Morphological Alterations after Status Epilepticus Induced by Intrahippocampal Injection of Pilocarpine." *Epilepsy & Behavior* 20 (2): 257–66. <https://doi.org/10.1016/J.YEBEH.2010.11.024>.
- Galvis-Alonso, O. Y., J. A. Cortes De Oliveira, and N. Garcia-Cairasco. 2004. "Limbic Epileptogenicity, Cell Loss and Axonal Reorganization Induced by Audiogenic and Amygdala Kindling in Wistar Audiogenic Rats (WAR Strain)." *Neuroscience* 125 (3): 787–802. <https://doi.org/10.1016/j.neuroscience.2004.01.042>.
- Gastaut, H. 1970. "Clinical and Electroencephalographical Classification of Epileptic Seizures." *Epilepsia* 11 (1): 102–12. <https://doi.org/10.1111/j.1528-1157.1970.tb03871.x>.
- Geeraedts, L. M.G., R. Nieuwenhuys, and J. G. Veening. 1990. "Medial Forebrain Bundle of the Rat: III. Cytoarchitecture of the Rostral (Telencephalic) Part of the Medial Forebrain Bundle Bed Nucleus." *Journal of Comparative Neurology* 294 (4): 507–36. <https://doi.org/10.1002/cne.902940403>.
- Gfeller, David, Aurélien Grosdidier, Matthias Wirth, Antoine Daina, Olivier Michielin, and Vincent Zoete. 2014. "SwissTargetPrediction: A Web Server for Target Prediction of Bioactive Small Molecules." *Nucleic Acids Research* 42 (W1): 32–38. <https://doi.org/10.1093/nar/gku293>.
- Gfeller, David, Olivier Michielin, and Vincent Zoete. 2013. "Systems Biology Shaping the Interaction Landscape of Bioactive Molecules" 29 (23): 3073–79. <https://doi.org/10.1093/bioinformatics/btt540>.
- Gilioli, Isabella, Aglaia Vignoli, Elisa Visani, Marina Casazza, Laura Canafoglia, Valentina Chiesa, Elena Gardella, et al. 2012. "Focal Epilepsies in Adult Patients Attending Two Epilepsy Centers: Classification of Drug-Resistance, Assessment of Risk Factors, and Usefulness of 'New' Antiepileptic Drugs." *Epilepsia* 53 (4): 733–40. <https://doi.org/10.1111/j.1528-1167.2012.03416.x>.
- Gill, R. S., S. M. Mirsattari, and L. S. Leung. 2017. "Resting State Functional Network Disruptions in a Kainic Acid Model of Temporal Lobe Epilepsy." *Neuroimage Clin* 13: 70–81. <https://doi.org/10.1016/j.nicl.2016.11.002>.
- Giordano, Carmela, Anna Maria Costa, Chiara Lucchi, Giuseppina Leo, Luc Brunel, Jean Alain Fehrentz, Jean Martinez, Antonio Torsello, and Giuseppe Biagini. 2016. "Progressive Seizure Aggravation in the Repeated 6-Hz Corneal Stimulation Model Is Accompanied by Marked Increase in Hippocampal p-ERK1/2 Immunoreactivity in Neurons." *Frontiers in Cellular Neuroscience* 10 (DEC2016): 1–12. <https://doi.org/10.3389/fncel.2016.00281>.

- Giorgi, Filippo Sean, Michela Ferrucci, Gloria Lazzeri, Chiara Pizzanelli, Paola Lenzi, Maria G Alessandrĭ, Luigi Murri, and Francesco Fornai. 2003. "A Damage to Locus Coeruleus Neurons Converts Sporadic Seizures into Self-sustaining Limbic Status Epilepticus." *European Journal of Neuroscience* 17 (12): 2593–2601.
- Goddard, Graham V., Dan C. McIntyre, and Curtis K. Leech. 1969. "A Permanent Change in Brain Function Resulting from Daily Electrical Stimulation." *Experimental Neurology* 25 (3): 295–330. [https://doi.org/10.1016/0014-4886\(69\)90128-9](https://doi.org/10.1016/0014-4886(69)90128-9).
- Goodkin, Howard P., Jwu Lai Yeh, and Jaideep Kapur. 2005. "Status Epilepticus Increases the Intracellular Accumulation of GABA A Receptors." *Journal of Neuroscience* 25 (23): 5511–20. <https://doi.org/10.1523/JNEUROSCI.0900-05.2005>.
- Gorter, Jan A., and Erwin A. Van Vliet. 2017. *Post-Status Epilepticus Models: Electrical Stimulation. Models of Seizures and Epilepsy: Second Edition*. Second Edi. Elsevier Inc. <https://doi.org/10.1016/B978-0-12-804066-9.00044-4>.
- Grabenstatter, Heidi L., Damien J. Ferraro, Philip A. Williams, Phillip L. Chapman, and F. Edward Dudek. 2005. "Use of Chronic Epilepsy Models in Antiepileptic Drug Discovery: The Effect of Topiramate on Spontaneous Motor Seizures in Rats with Kainate-Induced Epilepsy." *Epilepsia* 46 (1): 8–14. <https://doi.org/10.1111/j.0013-9580.2005.13404.x>.
- Grabenstatter, Heidi L., Suzanne Clark, and F. Edward Dudek. 2007. "Anticonvulsant Effects of Carbamazepine on Spontaneous Seizures in Rats with Kainate-Induced Epilepsy: Comparison of Intraperitoneal Injections with Drug-in-Food Protocols." *Epilepsia* 48 (12): 2287–95. <https://doi.org/10.1111/j.1528-1167.2007.01263.x>.
- Grabenstatter, Heidi L., and F. Edward Dudek. 2008. "A New Potential AED, Carisbamate, Substantially Reduces Spontaneous Motor Seizures in Rats with Kainate-Induced Epilepsy." *Epilepsia* 49 (10): 1787–94. <https://doi.org/10.1111/j.1528-1167.2008.01657.x>.
- Greenfield, L. John. 2013. "Molecular Mechanisms of Antiseizure Drug Activity at GABAA Receptors." *Seizure* 22 (8): 589–600. <https://doi.org/10.1016/j.seizure.2013.04.015>.
- Gualtieri, F., G. Curia, C. Marinelli, and G. Biagini. 2012. "Increased Perivascular Laminin Predicts Damage to Astrocytes in CA3 and Piriform Cortex Following Chemoconvulsive Treatments." *Neuroscience* 218 (August): 278–94. <https://doi.org/10.1016/J.NEUROSCIENCE.2012.05.018>.
- Guderian, Sebastian, Björn H. Schott, Alan Richardson-Klavehn, and Emrah Düzel. 2009. "Medial Temporal Theta State before an Event Predicts Episodic Encoding Success in Humans." *Proceedings of the National Academy of Sciences of the United States of America* 106 (13): 5365–70. <https://doi.org/10.1073/pnas.0900289106>.
- Gundersen, H. J. G. 1988. "The Nucleator." *Journal of Microscopy* 151 (1): 3–21. <https://doi.org/10.1111/j.1365-2818.1988.tb04609.x>.
- Gupta, Puneet K., Nasreen Sayed, Kan Ding, Mark A. Agostini, Paul C. Van Ness, Stuart Yablon,

- Christopher Madden, Bruce Mickey, Raimondo D'Ambrosio, and Ramon Diaz-Arrastia. 2014. "Subtypes of Post-Traumatic Epilepsy: Clinical, Electrophysiological, and Imaging Features." *Journal of Neurotrauma* 31 (16): 1439–43. <https://doi.org/10.1089/neu.2013.3221>.
- Hauser, W. Allen, John F. Annegers, and Leonard T. Kurland. 1991. "Prevalence of Epilepsy in Rochester, Minnesota: 1940–1980." *Epilepsia* 32 (4): 429–45. <https://doi.org/10.1111/j.1528-1157.1991.tb04675.x>.
- Hellier, Jennifer L., Peter R. Patrylo, Paul S. Buckmaster, and F. Edward Dudek. 1998. "Recurrent Spontaneous Motor Seizures after Repeated Low-Dose Systemic Treatment with Kainate: Assessment of a Rat Model of Temporal Lobe Epilepsy." *Epilepsy Research* 31 (1): 73–84. [https://doi.org/10.1016/S0920-1211\(98\)00017-5](https://doi.org/10.1016/S0920-1211(98)00017-5).
- Helmstaedter, Christoph, and Edgar Kockelmann. 2006. "Cognitive Outcomes in Patients with Chronic Temporal Lobe Epilepsy." *Epilepsia* 47 (SUPPL. 2): 96–98. <https://doi.org/10.1111/j.1528-1167.2006.00702.x>.
- Henshall, David C. 2017. *Poststatus Epilepticus Models: Focal Kainic Acid. Models of Seizures and Epilepsy: Second Edition*. Second Edi. Elsevier Inc. <https://doi.org/10.1016/B978-0-12-804066-9.00042-0>.
- Hesdorffer, Dale C., Torbjorn Tomson, Emma Benn, Josemir W. Sander, Lena Nilsson, Yvonne Langan, Thaddeus S. Walczak, Ettore Beghi, Martin J. Brodie, and Allen Hauser. 2011. "Combined Analysis of Risk Factors for SUDEP." *Epilepsia*. <https://doi.org/10.1111/j.1528-1167.2010.02952.x>.
- Hiragi, Toshimitsu, Yuji Ikegaya, Ryuta Koyama, Toshimitsu Hiragi, Yuji Ikegaya, and Ryuta Koyama. 2018. "Microglia after Seizures and in Epilepsy." *Cells* 7 (4): 26. <https://doi.org/10.3390/cells7040026>.
- Hitiris, Nikolas, Rajiv Mohanraj, John Norrie, Graeme J. Sills, and Martin J. Brodie. 2007. "Predictors of Pharmacoresistant Epilepsy." *Epilepsy Research* 75 (2–3): 192–96. <https://doi.org/10.1016/J.EPLEPSYRES.2007.06.003>.
- Hogan, Robert Edward. 2001. "Mesial Temporal Sclerosis." *Archives of Neurology* 58 (9): 1484. <https://doi.org/10.1001/archneur.58.9.1484>.
- Hsu, S.-M., L Raine, and H Fanger. 1981. "Use of Avidin-Biotin-Peroxidase Complex (ABC) in Immunoperoxidase Techniques: A Comparison between ABC and Unlabeled Antibody (PAP) Procedures." *J. Histochem. Cytochem.* 29: 577—580.
- Hudak, Anne M, Kavita Trivedi, Caryn R Harper, Kimberly Booker, Rajani R Caesar, Mark Agostini, Paul C Van Ness, and Ramon Diaz-Arrastia. 2004. "Evaluation of Seizure-like Episodes in Survivors of Moderate and Severe Traumatic Brain Injury." *The Journal of Head Trauma Rehabilitation* 19 (4): 290–95. <https://doi.org/10.1097/00001199-200407000-00003>.
- Hudson, Lawrence P., David G. Munoz, Laurie Miller, Richard S. McLachlan, John P. Girvin, and

- Warren T. Blume. 1993. "Amygdaloid Sclerosis in Temporal Lobe Epilepsy." *Annals of Neurology* 33 (6): 622–31. <https://doi.org/10.1002/ana.410330611>.
- Humphrey, William, Andrew Dalke, and Klaus Schulten. 1996. "VMD: Visual Molecular Dynamics." *Journal of Molecular Graphics* 14: 33–38.
- Hung, Te-Yu, Huai-Ying Ingrid Huang, Sheng-Nan Wu, and Chin-Wei Huang. 2020. "Depressive Effectiveness of Vigabatrin ( $\gamma$ -Vinyl-GABA), an Antiepileptic Drug, in Intermediate-Conductance Calcium-Activated Potassium Channels in Human Glioma Cells," May. <https://doi.org/10.21203/RS.3.RS-25157/V1>.
- Izadi, Ali, Aleksandr Pevzner, Darrin J. Lee, Arne D. Ekstrom, Kiarash Shahlaie, and Gene G. Gurkoff. 2019. "Medial Septal Stimulation Increases Seizure Threshold and Improves Cognition in Epileptic Rats." *Brain Stimulation* 12 (3): 735–42. <https://doi.org/10.1016/J.BRS.2019.01.005>.
- Jackson, Michael F., Barbara Esplin, and Radan Čapek. 1999. "Inhibitory Nature of Tiagabine-Augmented GABA(A) Receptor-Mediated Depolarizing Responses in Hippocampal Pyramidal Cells." *Journal of Neurophysiology* 81 (3): 1192–98. <https://doi.org/10.1152/jn.1999.81.3.1192>.
- Janmohamed, Mubeen, Martin J. Brodie, and Patrick Kwan. 2020. "Pharmacoresistance – Epidemiology, Mechanisms, and Impact on Epilepsy Treatment." *Neuropharmacology* 168 (May 2019): 107790. <https://doi.org/10.1016/j.neuropharm.2019.107790>.
- Jardim, Anaclara Prada, Rafael Scarpa da Costa Neves, Luís Otávio Sales Ferreira Caboclo, Carmen Lucia Penteado Lancellotti, Murilo Martinez Marinho, Ricardo Silva Centeno, Esper Abrão Cavalheiro, Carla Alessandra Scorza, and Elza Márcia Targas Yacubian. 2012. "Temporal Lobe Epilepsy with Mesial Temporal Sclerosis: Hippocampal Neuronal Loss as a Predictor of Surgical Outcome." *Arquivos de Neuro-Psiquiatria* 70 (5): 319–24. <https://doi.org/10.1590/s0004-282x2012000500003>.
- Jensen, Ole, and Claudia D. Tesche. 2002. "Frontal Theta Activity in Humans Increases with Memory Load in a Working Memory Task." *European Journal of Neuroscience* 15 (8): 1395–99. <https://doi.org/10.1046/j.1460-9568.2002.01975.x>.
- Johnson, Nicholas W., Mazhar Özkan, Adrian P. Burgess, Emma J. Prokic, Keith A. Wafford, Michael J. O'Neill, Stuart D. Greenhill, Ian M. Stanford, and Gavin L. Woodhall. 2017. "Phase-Amplitude Coupled Persistent Theta and Gamma Oscillations in Rat Primary Motor Cortex in Vitro." *Neuropharmacology* 119 (June): 141–56. <https://doi.org/10.1016/J.NEUROPHARM.2017.04.009>.
- Josephson, Colin B., Mark Lowerison, Isabelle Vallerand, Tolulope T. Sajobi, Scott Patten, Nathalie Jette, and Samuel Wiebe. 2017. "Association of Depression and Treated Depression with Epilepsy and Seizure Outcomes a Multicohort Analysis." *JAMA Neurology* 74 (5): 533–39. <https://doi.org/10.1001/jamaneurol.2016.5042>.

- Kadam, Shilpa D., Raimondo D'Ambrosio, Venceslas Duveau, Corinne Roucard, Norberto Garcia-Cairasco, Akio Ikeda, Marco de Curtis, Aristeia S. Galanopoulou, and Kevin M. Kelly. 2017. "Methodological Standards and Interpretation of Video-Electroencephalography in Adult Control Rodents. A TASK1-WG1 Report of the AES/ILAE Translational Task Force of the ILAE." *Epilepsia* 58: 10–27. <https://doi.org/10.1111/epi.13903>.
- Kahana, Michael J., Robert Sekuler, Jeremy B. Caplan, Matthew Kirschen, and Joseph R. Madsen. 1999. "Human Theta Oscillations Exhibit Task Dependence during Virtual Maze Navigation." *Nature* 399 (6738): 781–84. <https://doi.org/10.1038/21645>.
- Kahane, Philippe, and Fabrice Bartolomei. 2010. "Temporal Lobe Epilepsy and Hippocampal Sclerosis: Lessons from Depth EEG Recordings." *Epilepsia* 51 (February): 59–62. <https://doi.org/10.1111/j.1528-1167.2009.02448.x>.
- Kalilani, Linda, Xuezheng Sun, Barbara Pelgrims, Matthias Noack-Rink, and Vicente Villanueva. 2018. "The Epidemiology of Drug-Resistant Epilepsy: A Systematic Review and Meta-Analysis." *Epilepsia* 59 (12): 2179–93. <https://doi.org/10.1111/epi.14596>.
- Kälviäinen, Reetta, and Tuuli Salmenperä. 2002. "Do Recurrent Seizures Cause Neuronal Damage? A Series of Studies with MRI Volumetry in Adults with Partial Epilepsy." *Progress in Brain Research* 135 (January): 279–95. [https://doi.org/10.1016/S0079-6123\(02\)35026-X](https://doi.org/10.1016/S0079-6123(02)35026-X).
- Kälviäinen, Reetta, Tuuli Salmenperä, Kaarina Partanen, Pauli Vainio, Paavo Riekkinen Sr, and Asla Pitkänen. 1997. "MRI Volumetry and T2 Relaxometry of the Amygdala in Newly Diagnosed and Chronic Temporal Lobe Epilepsy." *Epilepsy Research* 28 (1): 39–50. [https://doi.org/10.1016/S0920-1211\(97\)00029-6](https://doi.org/10.1016/S0920-1211(97)00029-6).
- Kemp, Bob, Teunis van Beelen, Marion Stijl, Paul van Someren, Marco Roessen, and J. Gert van Dijk. 2010. "A DC Attenuator Allows Common EEG Equipment to Record Fullband EEG, and Fits Fullband EEG into Standard European Data Format." *Clinical Neurophysiology* 121 (12): 1992–97. <https://doi.org/10.1016/J.CLINPH.2010.05.006>.
- Kim, Duk-Soo, Ji-Eun Kim, Sung-Eun Kwak, Hui-Chul Choi, Hong-Ki Song, Yeong-In Kim, Soo-Young Choi, and Tae-Cheon Kang. 2007. "Up-Regulated Astroglial TWIK-Related Acid-Sensitive K<sup>+</sup> Channel-1 (TASK-1) in the Hippocampus of Seizure-Sensitive Gerbils: A Target of Anti-Epileptic Drugs." *Brain Research* 1185 (December): 346–58. <https://doi.org/10.1016/J.BRAINRES.2007.09.043>.
- Klee, Rebecca, Claudia Brandt, Kathrin Töllner, and Wolfgang Löscher. 2017. "Various Modifications of the Intrahippocampal Kainate Model of Mesial Temporal Lobe Epilepsy in Rats Fail to Resolve the Marked Rat-to-Mouse Differences in Type and Frequency of Spontaneous Seizures in This Model." *Epilepsy and Behavior* 68: 129–40. <https://doi.org/10.1016/j.yebeh.2016.11.035>.
- Klein, Pavel, Raymond Dingledine, Eleonora Aronica, Christophe Bernard, Ingmar Blümcke, Detlev Boison, Martin J. Brodie, et al. 2018. "Commonalities in Epileptogenic Processes from

Different Acute Brain Insults: Do They Translate?" *Epilepsia* 59 (1): 37–66.  
<https://doi.org/10.1111/epi.13965>.

Klein, Sabine, Jens P. Bankstahl, Wolfgang Löscher, and Marion Bankstahl. 2015. "Sucrose Consumption Test Reveals Pharmacoresistant Depression-Associated Behavior in Two Mouse Models of Temporal Lobe Epilepsy." *Experimental Neurology* 263: 263–71.  
<https://doi.org/10.1016/j.expneurol.2014.09.004>.

Klement, Wendy, Rita Garbelli, Emma Zub, Laura Rossini, Laura Tassi, Benoit Girard, Marine Blaquiere, et al. 2018. "Seizure Progression and Inflammatory Mediators Promote Pericytosis and Pericyte-Microglia Clustering at the Cerebrovasculature." *Neurobiology of Disease* 113 (May): 70–81. <https://doi.org/10.1016/J.NBD.2018.02.002>.

Klimesch, W., M. Doppelmayr, H. Schimke, And B. Ripper. 1997. "Theta Synchronization and Alpha Desynchronization in a Memory Task." *Psychophysiology* 34 (2): 169–76.  
<https://doi.org/10.1111/j.1469-8986.1997.tb02128.x>.

Klitgaard, Henrik, Alain Matagne, Jocelyne Vanneste-Goemaere, and Doru-Georg Margineanu. 2002. "Pilocarpine-Induced Epileptogenesis in the Rat:: Impact of Initial Duration of Status Epilepticus on Electrophysiological and Neuropathological Alterations." *Epilepsy Research* 51 (1–2): 93–107. [https://doi.org/10.1016/S0920-1211\(02\)00099-2](https://doi.org/10.1016/S0920-1211(02)00099-2).

König, Jörg, Fabian Müller, and Martin F Fromm. 2013. "Transporters and Drug-Drug Interactions: Important Determinants of Drug Disposition and Effects." *Pharmacological Reviews* 65 (3): 944–66. <https://doi.org/10.1124/pr.113.007518>.

Kraeuter, Ann-Katrin Katrin, Paul C. Guest, and Zoltán Sarnyai. 2019. "The Y-Maze for Assessment of Spatial Working and Reference Memory in Mice." In *Pre-Clinical Models: Techniques and Protocols, Methods in Molecular Biology*, 1916:105–11. Humana Press, New York, NY.  
[https://doi.org/10.1007/978-1-4939-8994-2\\_10](https://doi.org/10.1007/978-1-4939-8994-2_10).

Krall, R. L., J. K. Penry, B. G. White, H. J. Kupferberg, and E. A. Swinyard. 1978. "Antiepileptic Drug Development: II. Anticonvulsant Drug Screening." *Epilepsia* 19 (4): 409–28.  
<https://doi.org/10.1111/j.1528-1157.1978.tb04507.x>.

Kwan, Patrick, Alexis Arzimanoglou, Anne T. Berg, Martin J. Brodie, W. Allen Hauser, Gary Mathern, Solomon L. Moshé, Emilio Perucca, Samuel Wiebe, and Jacqueline French. 2010. "Definition of Drug Resistant Epilepsy: Consensus Proposal by the Ad Hoc Task Force of the ILAE Commission on Therapeutic Strategies." *Epilepsia* 51 (6): 1069–77.  
<https://doi.org/10.1111/j.1528-1167.2009.02397.x>.

Kwan, Patrick, and Martin J Brodie. 2000. "Epilepsy after the First Drug Fails: Substitution or Add-On?" *Seizure* 9 (7): 464–68. <https://doi.org/10.1053/SEIZ.2000.0442>.

Lancaster, Barrie, and Howard V. Wheal. 1982. "A Comparative Histological and Electrophysiological Study of Some Neurotoxins in the Rat Hippocampus." *The Journal of*

*Comparative Neurology* 211 (2): 105–14. <https://doi.org/10.1002/cne.902110202>.

Lauterborn, Julie C, and Charles E Ribak. 1989. “Differences in Dopamine  $\beta$ -Hydroxylase Immunoreactivity between the Brains of Genetically Epilepsy-Prone and Sprague-Dawley Rats.” *Epilepsy Research* 4 (3): 161–76.

Laxer, Kenneth D., Eugen Trinkka, Lawrence J. Hirsch, Fernando Cendes, John Langfitt, Norman Delanty, Trevor Resnick, and Selim R. Benbadis. 2014. “The Consequences of Refractory Epilepsy and Its Treatment.” *Epilepsy & Behavior* 37 (August): 59–70. <https://doi.org/10.1016/J.YEBEH.2014.05.031>.

Leclercq, Karine, and Rafal M. Kaminski. 2015. “Status Epilepticus Induction Has Prolonged Effects on the Efficacy of Antiepileptic Drugs in the 6-Hz Seizure Model.” *Epilepsy & Behavior* 49 (August): 55–60. <https://doi.org/10.1016/J.YEBEH.2015.06.011>.

Lemos, Tadeu, and Esper A. Cavalheiro. 1995. “Suppression of Pilocarpine-Induced Status Epilepticus and the Late Development of Epilepsy in Rats.” *Exp Brain Res*. Vol. 102. Springer-Verlag. <https://link.springer.com/content/pdf/10.1007/BF00230647.pdf>.

Lévesque, Maxime, and Massimo Avoli. 2013. “The Kainic Acid Model of Temporal Lobe Epilepsy.” *Neuroscience & Biobehavioral Reviews* 37 (10): 2887–99. <https://doi.org/10.1016/J.NEUBIOREV.2013.10.011>.

Lévesque, Maxime, Li-Yuan Chen, Guillaume Etter, Zahra Shiri, Siyan Wang, Sylvain Williams, and Massimo Avoli. 2019. “Paradoxical Effects of Optogenetic Stimulation in Mesial Temporal Lobe Epilepsy.” *Annals of Neurology* 86 (5): 714–28. <https://doi.org/10.1002/ana.25572>.

Lévesque, Maxime, Massimo Avoli, and Christophe Bernard. 2016. “Animal Models of Temporal Lobe Epilepsy Following Systemic Chemoconvulsant Administration.” *Journal of Neuroscience Methods* 260: 45. <https://doi.org/10.1016/J.JNEUMETH.2015.03.009>.

Li, Ruixi, Hisao Nishijo, Quanxin Wang, Teuroko Uwano, Ryoji Tamura, Osamu Ohtani, and Taketoshi Ono. 2001. “Light and Electron Microscopic Study of Cholinergic and Noradrenergic Elements in the Basolateral Nucleus of the Rat Amygdala: Evidence for Interactions between the Two Systems.” *Journal of Comparative Neurology* 439 (4): 411–25. <https://doi.org/10.1002/cne.1359>.

Löscher, Wolfgang, and Heidrun Potschka. 2005. “Drug Resistance in Brain Diseases and the Role of Drug Efflux Transporters.” *Nature Reviews. Neuroscience* 6 (8): 591–602. <https://doi.org/10.1038/nrn1728>.

Löscher, Wolfgang, Heidrun Potschka, Sanjay M Sisodiya, and Annamaria Vezzani. 2020. “Drug Resistance in Epilepsy: Clinical Impact, Potential Mechanisms, and New Innovative Treatment Options.” <https://doi.org/10.1124/pr.120.019539>.

Löscher, Wolfgang, Martin Puskarjov, and Kai Kaila. 2013. “Cation-Chloride Cotransporters NKCC1 and KCC2 as Potential Targets for Novel Antiepileptic and Antiepileptogenic

Treatments.” *Neuropharmacology* 69: 62–74.  
<https://doi.org/10.1016/j.neuropharm.2012.05.045>.

Löscher, Wolfgang. 2011. “Critical Review of Current Animal Models of Seizures and Epilepsy Used in the Discovery and Development of New Antiepileptic Drugs.” *Seizure* 20 (5): 359–68.  
<https://doi.org/10.1016/j.seizure.2011.01.003>.

———. 2017. “The Search for New Screening Models of Pharmacoresistant Epilepsy: Is Induction of Acute Seizures in Epileptic Rodents a Suitable Approach?” *Neurochemical Research* 42 (7): 1926–38. <https://doi.org/10.1007/s11064-016-2025-7>.

Lothman, E W, and R C Collins. 1981. “Kainic Acid Induced Limbic Seizures: Metabolic, Behavioral, Electroencephalographic and Neuropathological Correlates.” *Brain Research* 218 (1–2): 299–318. [https://doi.org/10.1016/0006-8993\(81\)91308-1](https://doi.org/10.1016/0006-8993(81)91308-1).

Lowenstein, Daniel H. 1999. “Status Epilepticus: An Overview of the Clinical Problem.” *Epilepsia* 40 (s1): s3–8. <https://doi.org/10.1111/j.1528-1157.1999.tb00872.x>.

Lucchi, Chiara, Anna M. Costa, Carmela Giordano, Giulia Curia, Marika Piat, Giuseppina Leo, Jonathan Vinet, et al. 2017. “Involvement of PPAR $\gamma$  in the Anticonvulsant Activity of EP-80317, a Ghrelin Receptor Antagonist.” *Frontiers in Pharmacology* 8 (SEP): 1–13.  
<https://doi.org/10.3389/fphar.2017.00676>.

Lucchi, Chiara, Giulia Curia, Jonathan Vinet, Fabio Gualtieri, Elena Bresciani, Vittorio Locatelli, Antonio Torsello, and Giuseppe Biagini. 2013. “Protective but Not Anticonvulsant Effects of Ghrelin and JMV-1843 in the Pilocarpine Model of Status Epilepticus.” *PLoS ONE* 8 (8).  
<https://doi.org/10.1371/journal.pone.0072716>.

Lucchi, Chiara, Jonathan Vinet, Stefano Meletti, and Giuseppe Biagini. 2015. “Ischemic–Hypoxic Mechanisms Leading to Hippocampal Dysfunction as a Consequence of Status Epilepticus.” *Epilepsy & Behavior* 49 (August): 47–54. <https://doi.org/10.1016/J.YEBEH.2015.04.003>.

Lueptow, Lindsay M. 2017. “Novel Object Recognition Test for the Investigation of Learning and Memory in Mice.” *Journal of Visualized Experiments*, no. 126 (August): e55718.  
<https://doi.org/10.3791/55718>.

Łukawski, Krzysztof, Marta Andres-Mach, Mirosław Czuczwar, Jarogniew J. Łuszczki, Krzysztof Kruszyński, and Stanisław J. Czuczwar. 2018. “Mechanisms of Epileptogenesis and Preclinical Approach to Antiepileptogenic Therapies.” *Pharmacological Reports* 70 (2): 284–93.  
<https://doi.org/10.1016/J.PHAREP.2017.07.012>.

Lukoyanov, Nikolai V., Maria J. Sá, M. Dulce Madeira, and Manuel M. Paula-Barbosa. 2004. “Selective Loss of Hilar Neurons and Impairment of Initial Learning in Rats after Repeated Administration of Electroconvulsive Shock Seizures.” *Experimental Brain Research* 154 (2): 192–200. <https://doi.org/10.1007/s00221-003-1658-3>.

Magill, Peter J., Andrew Sharott, J. Paul Bolam, and Peter Brown. 2006. “Delayed Synchronization

- of Activity in Cortex and Subthalamic Nucleus Following Cortical Stimulation in the Rat.” *The Journal of Physiology* 574 (3): 929–46. <https://doi.org/10.1113/jphysiol.2006.110379>.
- Mahringer, Anne, and Gert Fricker. 2016. “ABC Transporters at the Blood–Brain Barrier.” *Expert Opinion on Drug Metabolism & Toxicology* 12 (5): 499–508. <https://doi.org/10.1517/17425255.2016.1168804>.
- Maia, Gisela H, Joana I Soares, Sérgio G Almeida, Juliana M Leite, Helena X Baptista, Alisa N Lukoyanova, Cátia S Brazete, and Nikolai V Lukoyanov. 2019. “Altered Serotonin Innervation in the Rat Epileptic Brain.” *Brain Research Bulletin* 152: 95–106.
- Margerison, J H, and J A N Corsellis. 1966. “EPILEPSY AND THE TEMPORAL LOBES - A CLINICAL, ELECTROENCEPHALOGRAPHIC AND NEUROPATHOLOGICAL STUDY OF THE BRAIN IN EPILEPSY, WITH PARTICULAR REFERENCE TO THE TEMPORAL LOBES,” 499–536. <http://brain.oxfordjournals.org/>.
- Mathern, Gary W., Fredi Cifuentes, Joao P. Leite, James K. Pretorius, and Thomas L. Babb. 1993. “Hippocampal EEG Excitability and Chronic Spontaneous Seizures Are Associated with Aberrant Synaptic Reorganization in the Rat Intrahippocampal Kainate Model.” *Electroencephalography and Clinical Neurophysiology* 87 (5): 326–39. [https://doi.org/10.1016/0013-4694\(93\)90186-Y](https://doi.org/10.1016/0013-4694(93)90186-Y).
- McDonald, A. J., and F. Mascagni. 2010. “Neuronal Localization of M1 Muscarinic Receptor Immunoreactivity in the Rat Amygdala.” *Neuroscience* 215: 37–48. <https://doi.org/10.1016/j.neuroscience.2011.08.032>.
- . 2011. “Neuronal Localization of M2 Muscarinic Receptor Immunoreactivity in the Rat Amygdala.” *Neuroscience* 196: 49–65. <https://doi.org/10.1016/j.neuroscience.2011.08.032>.
- Mcdonald, A. J., J. F. Muller, and F. Mascagni. 2011. “Postsynaptic Targets of Gabaergic Basal Forebrain Projections to the Basolateral Amygdala.” *Neuroscience* 183: 144–59. <https://doi.org/10.1016/j.neuroscience.2011.03.027>.
- McIntyre, Dan C. 2006. “The Kindling Phenomenon.” *Models of Seizures and Epilepsy*, 351–63. <https://doi.org/10.1016/B978-012088554-1/50030-X>.
- McKenna, James Timothy, and Robert P. Vertes. 2004. “Afferent Projections to Nucleus Reuniens of the Thalamus.” *The Journal of Comparative Neurology* 480 (2): 115–42. <https://doi.org/10.1002/cne.20342>.
- Medina-Ceja, Laura, Kenia Pardo-Peña, and Consuelo Ventura-Mejía. 2014. “Evaluation of Behavioral Parameters and Mortality in a Model of Temporal Lobe Epilepsy Induced by Intracerebroventricular Pilocarpine Administration.” *NeuroReport* 25 (11): 875–79. <https://doi.org/10.1097/WNR.000000000000207>.
- Meier, C L, and F E Dudek. 1996. “Spontaneous and Stimulation-Induced Synchronized Burst Afterdischarges in the Isolated CA1 of Kainate-Treated Rats.” *Journal of Neurophysiology* 76

(4): 2231–39.

- Meierkord, Hartmut. 2007. “The Risk of Epilepsy after Status Epilepticus in Children and Adults.” *Epilepsia* 48 (s8): 94–95. <https://doi.org/10.1111/j.1528-1167.2007.01362.x>.
- Ménard, C., G.E. Hodes, and S.J. Russo. 2015. “Pathogenesis of Depression: Insights from Human and Rodent Studies.” *Neuroscience*. <https://doi.org/10.1016/j.neuroscience.2015.05.053>.
- Michael, Michalakis, Damian Holsinger, Candace Ikeda-Douglas, Sam Cammisuli, Janina Ferbinteanu, Cheryl DeSouza, Sandra DeSouza, Jillian Fecteau, Ronald J Racine, and Norton W Milgram. 1998. “Development of Spontaneous Seizures over Extended Electrical Kindling.” *Brain Research* 793 (1–2): 197–211. [https://doi.org/10.1016/S0006-8993\(98\)00155-3](https://doi.org/10.1016/S0006-8993(98)00155-3).
- Midzyanovskaya, I S, A B Shatskova, E MacDonald, ELJM van Luijtelaar, and L M Tuomisto. 2020. “Brain Aminergic Deficiency in Absence Epileptic Rats: Dependency on Seizure Severity and Their Functional Coupling at Rest.”
- Milikovsky, Dan Z, Itai Weissberg, Lyn Kamintsky, Kristina Lippmann, Osnat Schefenbauer, Federica Frigerio, Massimo Rizzi, et al. 2017. “Electrocorticographic Dynamics as a Novel Biomarker in Five Models of Epileptogenesis.” *The Journal of Neuroscience : The Official Journal of the Society for Neuroscience* 37 (17): 4450–61. <https://doi.org/10.1523/JNEUROSCI.2446-16.2017>.
- Miller, John W, Glenna M Turner, and Beverly C Gray. 1994. “Anticonvulsant Effects of the Experimental Induction of Hippocampal Theta Activity.” *Epilepsy Research* 18 (3): 195–204. [https://doi.org/10.1016/0920-1211\(94\)90040-X](https://doi.org/10.1016/0920-1211(94)90040-X).
- Miller, Laurie A., Richard S. McLachlan, M. Susan Bouwer, Lawrence P. Hudson, and David G. Munoz. 1994. “Amygdalar Sclerosis: Preoperative Indicators and Outcome after Temporal Lobectomy.” *Journal of Neurology, Neurosurgery and Psychiatry* 57 (9): 1099–1105. <https://doi.org/10.1136/jnnp.57.9.1099>.
- Morimoto, Kiyoshi, Margaret Fahnestock, and Ronald J Racine. 2004. “Kindling and Status Epilepticus Models of Epilepsy: Rewiring the Brain.” *Progress in Neurobiology* 73 (1): 1–60. <https://doi.org/10.1016/J.PNEUROBIO.2004.03.009>.
- Moshé, Solomon L., Emilio Perucca, Philippe Ryvlin, and Torbjörn Tomson. 2015. “Epilepsy: New Advances.” *The Lancet* 385 (9971): 884–98. [https://doi.org/10.1016/S0140-6736\(14\)60456-6](https://doi.org/10.1016/S0140-6736(14)60456-6).
- Mula, Marco, Josemir W. Sander, Ley Sander, Marco Mula, and Josemir W. Sander. 2016. “Psychosocial Aspects of Epilepsy: A Wider Approach.” *British Journal of Psychiatry Open* 2 (4): 270–74. <https://doi.org/10.1192/bjpo.bp.115.002345>.
- Muller, Jay F., Franco Mascagni, and Alexander J. McDonald. 2011. “Cholinergic Innervation of Pyramidal Cells and Parvalbumin-Immunoreactive Interneurons in the Rat Basolateral Amygdala.” *Journal of Comparative Neurology* 519 (4): 790–805.

<https://doi.org/10.1002/cne.22550>.

- Muller, Jay F., Franco Mascagni, Violeta Zaric, and Alexander J. McDonald. 2013. "Muscarinic Cholinergic Receptor M1 in the Rat Basolateral Amygdala: Ultrastructural Localization and Synaptic Relationships to Cholinergic Axons." *Journal of Comparative Neurology* 521 (8): 1743–59. <https://doi.org/10.1002/cne.23254>.
- Muller, Jay F., Franco Mascagni, Violeta Zaric, David D. Mott, and Alexander J. McDonald. 2016. "Localization of the M2 Muscarinic Cholinergic Receptor in Dendrites, Cholinergic Terminals, and Noncholinergic Terminals in the Rat Basolateral Amygdala: An Ultrastructural Analysis." *Journal of Comparative Neurology* 524 (12): 2400–2417. <https://doi.org/10.1002/cne.23959>.
- Murphy, Niall P., and Nigel T. Maidment. 2002. "Orphanin FQ/Nociceptin Modulation of Mesolimbic Dopamine Transmission Determined by Microdialysis." *Journal of Neurochemistry* 73 (1): 179–86. <https://doi.org/10.1046/j.1471-4159.1999.0730179.x>.
- N’Gouemo, Prosper, Mireille Lerner-Natoli, Gérard Rondouin, Kazuya Watanabe, Françoise Sandillon, Alain Privat, and Michel Baldy-Moulinier. 1990. "Catecholaminergic Systems and Amygdala Kindling Development. Effects of Bilateral Lesions of Substantia Nigra Dopaminergic or Locus Coeruleus Noradrenergic Neurons." *Epilepsy Research* 5 (2): 92–102.
- Na, Meng, Haitao Ge, Chen Shi, Hong Shen, Yu Wang, Song Pu, Li Liu, et al. 2015. "Long-Term Seizure Outcome for International Consensus Classification of Hippocampal Sclerosis: A Survival Analysis." *Seizure* 25: 141–46. <https://doi.org/10.1016/j.seizure.2014.10.006>.
- Nadler, Victor J. 1981. "Kainic Acid as a Tool for the Study of Temporal Lobe Epilepsy." *Life Sciences* 29 (20): 2031–42. [https://doi.org/10.1016/0024-3205\(81\)90659-7](https://doi.org/10.1016/0024-3205(81)90659-7).
- Nadler, Victor J., and Gilbert J. Cuthbertson. 1980. "Kainic Acid Neurotoxicity toward Hippocampal Formation: Dependence on Specific Excitatory Pathways." *Brain Research* 195 (1): 47–56. [https://doi.org/10.1016/0006-8993\(80\)90865-3](https://doi.org/10.1016/0006-8993(80)90865-3).
- Narkilahti, Susanna, Terhi J. Pirttilä, Katarzyna Lukasiuk, Jarkko Tuunanen, and Asla Pitkänen. 2003. "Expression and Activation of Caspase 3 Following Status Epilepticus in the Rat." *European Journal of Neuroscience* 18 (6): 1486–96. <https://doi.org/10.1046/j.1460-9568.2003.02874.x>.
- Naylor, David E., Hantao Liu, and Claude G. Wasterlain. 2005. "Trafficking of GABAA Receptors, Loss of Inhibition, and a Mechanism for Pharmacoresistance in Status Epilepticus." *Journal of Neuroscience* 25 (34): 7724–33. <https://doi.org/10.1523/JNEUROSCI.4944-04.2005>.
- Nerad, Ludek, and Neil McNaughton. 2006. "The Septal EEG Suggests a Distributed Organization of the Pacemaker of Hippocampal Theta in the Rat." *European Journal of Neuroscience* 24 (1): 155–66. <https://doi.org/10.1111/j.1460-9568.2006.04902.x>.
- Nissinen, Jari, Toivo Halonen, Esa Koivisto, and Asla Pitkänen. 2000. "A New Model of Chronic Temporal Lobe Epilepsy Induced by Electrical Stimulation of the Amygdala in Rat." *Epilepsy*

*Research* 38 (2–3): 177–205. [https://doi.org/10.1016/S0920-1211\(99\)00088-1](https://doi.org/10.1016/S0920-1211(99)00088-1).

Nitecka, Liliana, and Michael Frotscher. 1989. “Organization and Synaptic Interconnections of GABAergic and Cholinergic Elements in the Rat Amygdaloid Nuclei: Single- and Double-Immunolabeling Studies.” *Journal of Comparative Neurology* 279 (3): 470–88.

<https://doi.org/10.1002/cne.902790311>.

Pagadala, Nataraj S., Khajamohiddin Syed, and Jack Tuszynski. 2017. “Software for Molecular Docking: A Review.” *Biophysical Reviews* 9 (2): 91–102. <https://doi.org/10.1007/s12551-016-0247-1>.

Panayiotopoulos, C P. 2010. “Principles of Therapy in the Epilepsies.” In *A Clinical Guide to Epileptic Syndromes and Their Treatment*, 173–235. London: Springer London.

[https://doi.org/10.1007/978-1-84628-644-5\\_7](https://doi.org/10.1007/978-1-84628-644-5_7).

Paré, Denis, Dawn R. Collins, and Joe Guillaume Pelletier. 2002. “Amygdala Oscillations and the Consolidation of Emotional Memories.” *Trends in Cognitive Sciences* 6 (7): 306–14.

[https://doi.org/10.1016/S1364-6613\(02\)01924-1](https://doi.org/10.1016/S1364-6613(02)01924-1).

Paré, Denis, and Hélène Gaudreau. 1996. “Projection Cells and Interneurons of the Lateral and Basolateral Amygdala: Distinct Firing Patterns and Differential Relation to Theta and Delta Rhythms in Conscious Cats.” *The Journal of Neuroscience* 16 (10): 3334 LP – 3350.

<https://doi.org/10.1523/JNEUROSCI.16-10-03334>.

Paxinos, G. 2015. *The rat nervous system*. 4<sup>th</sup> ed. San Diego: Elsevier Academic press.

Paxinos, G. F., and Franklin, K. 2003. *The Mouse Brain In Stereotaxic Coordinates*. 3<sup>rd</sup> ed. San Diego: Elsevier Academic Press

Paxinos, George, and Charles Watson. 2005. *The Rat Brain in Stereotaxic Coordinates*. 5<sup>th</sup> ed. San Diego: Elsevier Academic Press.

Phelan, Kevin D., U Thaung Shwe, Michael A. Cozart, Hong Wu, Matthew M. Mock, Joel Abramowitz, Lutz Birnbaumer, and Fang Zheng. 2017. “TRPC3 Channels Play a Critical Role in the Theta Component of Pilocarpine-Induced Status Epilepticus in Mice.” *Epilepsia* 58 (2): 247–54. <https://doi.org/10.1111/epi.13648>.

Pirttila, T. R M, Asla Pitkanen, Jarkko Tuunanen, and Risto A. Kauppinen. 2001. “Ex Vivo MR Microimaging of Neuronal Damage after Kainate-Induced Status Epilepticus in Rat: Correlation with Quantitative Histology.” *Magnetic Resonance in Medicine* 46 (5): 946–54.

<https://doi.org/10.1002/mrm.1281>.

Pitkänen, Asla, Esa Jolkkonen, and Samuli Kemppainen. 2000. “Anatomic Heterogeneity of the Rat Amygdaloid Complex.” *Folia Morphologica* 59 (1): 1–23.

Pitkänen, Asla, Jari Nissinen, Jaak Nairismägi, Katarzyna Lukasiuk, Olli H.J. Gröhn, Riitta Miettinen, and Risto Kappinen. 2002. “Progression of Neuronal Damage after Status Epilepticus and during Spontaneous Seizures in a Rat Model of Temporal Lobe Epilepsy.”

- Progress in Brain Research* 135: 67–83. [https://doi.org/10.1016/S0079-6123\(02\)35008-8](https://doi.org/10.1016/S0079-6123(02)35008-8).
- Pitkänen, Asla, Jarkko Tuunanen, Reetta Kälviäinen, Kaarina Partanen, and Tuuli Salmenperä. 1998. “Amygdala Damage in Experimental and Human Temporal Lobe Epilepsy.” *Epilepsy Research* 32 (1–2): 233–53. [https://doi.org/10.1016/S0920-1211\(98\)00055-2](https://doi.org/10.1016/S0920-1211(98)00055-2).
- Pitkänen, Asla, Jarkko Tuunanen, Reetta Kälviäinen, Kaarina Partanen, and Tuuli Salmenperä. 1998. “Amygdala Damage in Experimental and Human Temporal Lobe Epilepsy.” *Epilepsy Research* 32 (1–2): 233–53. [https://doi.org/10.1016/S0920-1211\(98\)00055-2](https://doi.org/10.1016/S0920-1211(98)00055-2).
- Pitkänen, Asla, Katarzyna Lukasiuk, F Edward Dudek, and Kevin J Staley. 2015. “Epileptogenesis.” *Cold Spring Harbor Perspectives in Medicine* 5 (10): a022822. <https://doi.org/10.1101/cshperspect.a022822>.
- Pitsch, Julika, Albert J. Becker, Susanne Schoch, Johannes Alexander Müller, Marco de Curtis, and Vadym Gnatkovsky. 2017. “Circadian Clustering of Spontaneous Epileptic Seizures Emerges after Pilocarpine-Induced Status Epilepticus.” *Epilepsia* 58 (7): 1159–71. <https://doi.org/10.1111/epi.13795>.
- Puskarjov, Martin, Kristopher T. Kahle, Eva Ruusuvuori, and Kai Kaila. 2014. “Pharmacotherapeutic Targeting of Cation-chloride Cotransporters in Neonatal Seizures.” *Epilepsia* 55 (6): 806–18. <https://doi.org/10.1111/epi.12620>.
- Racine, Ronald J. 1972. “Modification of Seizure Activity by Electrical Stimulation: II. Motor Seizure.” *Electroencephalography and Clinical Neurophysiology* 32 (3): 281–94. [https://doi.org/10.1016/0013-4694\(72\)90177-0](https://doi.org/10.1016/0013-4694(72)90177-0).
- Rainnie, D. G., E. K. Asprodini, and P. Shinnick-Gallagher. 1992. “Kindling-Induced Long-Lasting Changes in Synaptic Transmission in the Basolateral Amygdala.” *Journal of Neurophysiology* 67 (2): 443–54. <https://doi.org/10.1152/jn.1992.67.2.443>.
- Rainnie, Donald Gordon, Irakli Mania, Franco Mascagni, and Alexander Joseph McDonald. 2006. “Physiological and Morphological Characterization of Parvalbumin-Containing Interneurons of the Rat Basolateral Amygdala.” *Journal of Comparative Neurology* 498 (1): 142–61. <https://doi.org/10.1002/cne.21049>.
- Rao, Z R, S Shiosaka, and M Tohyama. 1987. “Origin of Cholinergic Fibers in the Basolateral Nucleus of the Amygdaloid Complex by Using Sensitive Double-Labeling Technique of Retrograde Biotinized Tracer and Immunocytochemistry.” *Journal Fur Hirnforschung* 28 (5): 553–60. <http://www.ncbi.nlm.nih.gov/pubmed/3320200>.
- Ravizza, Teresa, and Annamaria Vezzani. 2018. “Pharmacological Targeting of Brain Inflammation in Epilepsy: Therapeutic Perspectives from Experimental and Clinical Studies.” *Epilepsia Open* 3 (S2): 133–42. <https://doi.org/10.1002/epi4.12242>.
- Remy, Stefan, Bernd W. Urban, Christian E. Elger, and Heinz Beck. 2003. “Anticonvulsant Pharmacology of Voltage-Gated Na<sup>+</sup> Channels in Hippocampal Neurons of Control and

Chronically Epileptic Rats.” *European Journal of Neuroscience* 17 (12): 2648–58.  
<https://doi.org/10.1046/j.1460-9568.2003.02710.x>.

Remy, Stefan, Siegrun Gabriel, Bernd W. Urban, Dirk Dietrich, Thomas N. Lehmann, Christian E. Elger, Uwe Heinemann, and Heinz Beck. 2003. “A Novel Mechanism Underlying Drug Resistance in Chronic Epilepsy.” *Annals of Neurology* 53 (4): 469–79.  
<https://doi.org/10.1002/ana.10473>.

Robel, S., S. C. Buckingham, J. L. Boni, S. L. Campbell, N. C. Danbolt, T. Riedemann, B. Sutor, and H. Sontheimer. 2015. “Reactive Astrogliosis Causes the Development of Spontaneous Seizures.” *Journal of Neuroscience* 35 (8): 3330–45.  
<https://doi.org/10.1523/JNEUROSCI.1574-14.2015>.

Rusina, Evgeniia, Christophe Bernard, and Adam Williamson. 2021. “The Kainic Acid Models of Temporal Lobe Epilepsy.” *Eneuro* 8 (2): ENEURO.0337-20.2021.  
<https://doi.org/10.1523/ENEURO.0337-20.2021>.

Ryley Parrish, R, A J Albertson, S C Buckingham, J J Hablitz, K L Mascia, W Davis Haselden, and F D Lubin. 2013. “Status Epilepticus Triggers Early and Late Alterations in Brain-Derived Neurotrophic Factor and NMDA Glutamate Receptor Grin2b DNA Methylation Levels in the Hippocampus.” *Neuroscience* 248 (September): 602–19.  
<https://doi.org/10.1016/j.neuroscience.2013.06.029>.

Sadleir, L G, K Farrell, S Smith, M B Connolly, and I E Scheffer. 2006. “Electroclinical Features of Absence Seizures in Childhood Absence Epilepsy.” *Neurology* 67 (3): 413 LP – 418.  
<https://doi.org/10.1212/01.wnl.0000228257.60184.82>.

Salmenperä, Tuuli, Reetta Kälviäinen, Kaarina Partanen, and Asla Pitkänen. 2002. “Hippocampal and Amygdaloid Damage in Partial Epilepsy.” *Epilepsy Research* 46 (1): 69–82.  
[https://doi.org/10.1016/s0920-1211\(01\)00258-3](https://doi.org/10.1016/s0920-1211(01)00258-3).

Sander, J W A S, and S D Shorvon. 1996. “Epidemiology of the Epilepsies.” *Journal Of Neurology, Neurosurgery, and Psychiatry*. Vol. 61.  
<https://www.ncbi.nlm.nih.gov/pmc/articles/PMC1074036/pdf/jnnpsyc00011-0003.pdf>.

Sarhan, S, and N Seiler. 1989. “Proline and Proline Derivatives as Anticonvulsants.” *General Pharmacology: The Vascular System* 20 (1): 53–60. [https://doi.org/10.1016/0306-3623\(89\)90060-8](https://doi.org/10.1016/0306-3623(89)90060-8).

Sarter, Martin, Geert Bodewitz, and David N. Stephens. 1988. “Attenuation of Scopolamine-Induced Impairment of Spontaneous Alternation Behaviour by Antagonist but Not Inverse Agonist and Agonist  $\alpha$ -Carbolines.” *Psychopharmacology* 94 (4): 491–95.  
<https://doi.org/10.1007/BF00212843>.

Saunders, Norman R., Mark D. Habgood, Kjeld Møllgård, and Katarzyna M. Dziegielewska. 2016. “The Biological Significance of Brain Barrier Mechanisms: Help or Hindrance in Drug

Delivery to the Central Nervous System?" *F1000Research* 5.  
<https://doi.org/10.12688/F1000RESEARCH.7378.1>.

- Schachter, S. C. 2001. "Pharmacology and Clinical Experience with Tiagabine." *Expert Opinion on Pharmacotherapy* 2 (1): 179–87. <https://doi.org/10.1517/14656566.2.1.179>.
- Schartz, Nicole D, Seth A Herr, Lauren Madsen, Sarah J Butts, Ceidy Torres, Loyda B Mendez, and Amy L Brewster. 2016. "Spatiotemporal Profile of Map2 and Microglial Changes in the Hippocampal CA1 Region Following Pilocarpine-Induced Status Epilepticus." *Scientific Reports* 6 (1): 1–12. <https://doi.org/10.1038/srep24988>.
- Scheffer, Ingrid E., Samuel Berkovic, Giuseppe Capovilla, Mary B. Connolly, Jacqueline French, Laura Guilhoto, Edouard Hirsch, et al. 2017. "ILAE Classification of the Epilepsies: Position Paper of the ILAE Commission for Classification and Terminology." *Epilepsia* 58 (4): 512–21. <https://doi.org/10.1111/epi.13709>.
- Schliebs, Reinhard, Marko Zivin, Jörg Steinbach, and Thomas Rothe. 1989. "Changes in Cholinergic but Not in GABAergic Markers in Amygdala, Piriform Cortex, and Nucleus Basalis of the Rat Brain Following Systemic Administration of Kainic Acid." *Journal of Neurochemistry* 53 (1): 212–18. <https://doi.org/10.1111/j.1471-4159.1989.tb07316.x>.
- Schwob, J.E. E., T. Fuller, J.L. L. Price, and J.W. W. Olney. 1980. "Widespread Patterns of Neuronal Damage Following Systemic or Intracerebral Injections of Kainic Acid: A Histological Study." *Neuroscience* 5 (6): 991–1014. [https://doi.org/10.1016/0306-4522\(80\)90181-5](https://doi.org/10.1016/0306-4522(80)90181-5).
- Scimemi, Annalisa. 2014. "Structure, Function, and Plasticity of GABA Transporters." *Frontiers in Cellular Neuroscience* 8 (JUN): 1–14. <https://doi.org/10.3389/fncel.2014.00161>.
- Scorza, Fulvio Alexandre, Ricardo Mario Arida, Roberta Monterazzo Cysneiros, Carla Alessandra Scorza, Marly de Albuquerque, and Esper Abrão Cavalheiro. 2005. "Estudo Qualitativo Da Formação Hipocampal de Animais Hipertensos Com Epilepsia." *Arquivos de Neuro-Psiquiatria* 63 (2a): 283–88. <https://doi.org/10.1590/S0004-282X2005000200015>.
- Setkovicz, Zuzanna, Emilia Kosonowska, and Krzysztof Janeczko. 2017. "Inflammation in the Developing Rat Modulates Astroglial Reactivity to Seizures in the Mature Brain." *Journal of Anatomy* 231 (3): 366–79. <https://doi.org/10.1111/joa.12636>.
- Shapiro, Lee A., Lulu Wang, and Charles E. Ribak. 2008. "Rapid Astrocyte and Microglial Activation Following Pilocarpine-Induced Seizures in Rats." *Epilepsia* 49 (SUPPL. 2): 33–41. <https://doi.org/10.1111/j.1528-1167.2008.01491.x>.
- Shorvon, Simon D. 2011. "The Etiologic Classification of Epilepsy." *Epilepsia* 52 (6): 1052–57. <https://doi.org/10.1111/j.1528-1167.2011.03041.x>.
- Sisodiya, Sanjay M., Josephine Heffernan, and Marian V. Squier. 1999. "Over-Expression of Pglycoprotein in Malformations of Cortical Development." *NeuroReport* 10 (16): 3437–41.

<https://doi.org/10.1097/00001756-199911080-00032>.

- Sloviter, Robert S., and Argyle V. Bumanglag. 2013. "Defining 'Epileptogenesis' and Identifying 'Antiepileptogenic Targets' in Animal Models of Acquired Temporal Lobe Epilepsy Is Not as Simple as It Might Seem." *Neuropharmacology* 69 (June): 3–15.  
<https://doi.org/10.1016/J.NEUROPHARM.2012.01.022>.
- Smith, Yoland, Jean-François Paré, and Denis Paré. 2000. "Differential Innervation of Parvalbumin-Immunoreactive Interneurons of the Basolateral Amygdaloid Complex by Cortical and Intrinsic Inputs." *Journal of Comparative Neurology* 416 (4): 496–508.  
[https://doi.org/https://doi.org/10.1002/\(SICI\)1096-9861\(20000124\)416:4<496::AID-CNE6>3.0.CO;2-N](https://doi.org/https://doi.org/10.1002/(SICI)1096-9861(20000124)416:4<496::AID-CNE6>3.0.CO;2-N).
- So, Edmund Cheung, King Chuen Wu, Feng Chen Kao, and Sheng Nan Wu. 2014. "Effects of Midazolam on Ion Currents and Membrane Potential in Differentiated Motor Neuron-like NSC-34 and NG108-15 Cells." *European Journal of Pharmacology* 724 (February): 152–60.  
<https://doi.org/10.1016/J.EJP HAR.2013.12.034>.
- Soares, Joana I, Ana R Afonso, Gisela H Maia, and Nikolai V Lukoyanov. 2018. "The Pedunculopontine and Laterodorsal Tegmental Nuclei in the Kainate Model of Epilepsy" 672 (July 2017): 90–95.
- Soares, Joana I, Maria C Valente, Pedro A Andrade, Gisela H Maia, and Nikolai V Lukoyanov. 2017. "Reorganization of the Septohippocampal Cholinergic Fiber System in Experimental Epilepsy," no. October 2016: 2690–2705. <https://doi.org/10.1002/cne.24235>.
- Soares, Joana I., Catarina Da Costa, Maria H. Ferreira, Pedro A. Andrade, Gisela H. Maia, and Nikolai V. Lukoyanov. 2019. "Partial Depletion of Septohippocampal Cholinergic Cells Reduces Seizure Susceptibility, but Does Not Mitigate Hippocampal Neurodegeneration in the Kainate Model of Epilepsy." *Brain Research* 1717 (April): 235–46.  
<https://doi.org/10.1016/j.brainres.2019.04.027>.
- Steward, O, E R Torre, R Tomasulo, and E Lothman. 1991. "Neuronal Activity Up-Regulates Astroglial Gene Expression." *Proceedings of the National Academy of Sciences of the United States of America* 88 (15): 6819–23. <http://www.ncbi.nlm.nih.gov/pubmed/1862105>.
- . 1992. "Seizures and the Regulation of Astroglial Gene Expression." *Epilepsy Research. Supplement 7*: 197–209. <http://www.ncbi.nlm.nih.gov/pubmed/1334663>.
- Sugita, S, N Uchimura, Z G Jiang, and R A North. 1991. "Distinct Muscarinic Receptors Inhibit Release of Gamma-Aminobutyric Acid and Excitatory Amino Acids in Mammalian Brain." *Proceedings of the National Academy of Sciences* 88 (6): 2608 LP – 2611.  
<https://doi.org/10.1073/pnas.88.6.2608>.
- Suzuki, Fumio, Yaeko Makiura, Didier Guilhem, Jens Christian Sørensen, and Brigitte Onteniente. 1997. "Correlated Axonal Sprouting and Dendritic Spine Formation during Kainate-Induced

- Neuronal Morphogenesis in the Dentate Gyrus of Adult Mice.” *Experimental Neurology* 145 (1): 203–13. <https://doi.org/10.1006/exnr.1997.6469>.
- Swinyard, E. A. 1972. “Experimental Models of Epilepsy. a Manual for the Laboratory Worker.” *Raven Press, New York, N.Y.*, 433–58. <https://doi.org/10.1016/B978-0-12-804066-9/00082-1>.
- Szabó, Gergely G, Noémi Holderith, Attila I Gulyás, Tamás F Freund, and Norbert Hájos. 2010. “Distinct Synaptic Properties of Perisomatic Inhibitory Cell Types and Their Different Modulation by Cholinergic Receptor Activation in the CA3 Region of the Mouse Hippocampus.” *European Journal of Neuroscience* 31 (12): 2234–46. <https://doi.org/https://doi.org/10.1111/j.1460-9568.2010.07292.x>.
- Tang, Fei, Anika M.S. Hartz, and Björn Bauer. 2017. “Drug-Resistant Epilepsy: Multiple Hypotheses, Few Answers.” *Frontiers in Neurology* 8 (JUL): 1–19. <https://doi.org/10.3389/fneur.2017.00301>.
- Téllez-Zenteno, Jose F, and Lizbeth Hernández-Ronquillo. 2012. “A Review of the Epidemiology of Temporal Lobe Epilepsy.” *Epilepsy Research and Treatment* 2012: 1–5. <https://doi.org/10.1155/2012/630853>.
- Tescarollo, Fabio C., Diogo M. Rombo, Lindsay K. DeLiberto, Denise E. Fedele, Enmar Alharfoush, Ângelo R. Tomé, Rodrigo A. Cunha, Ana M. Sebastião, and Detlev Boison. 2020. “Role of Adenosine in Epilepsy and Seizures.” *Journal of Caffeine and Adenosine Research* 00 (00): 1–16. <https://doi.org/10.1089/caff.2019.0022>.
- Thom, Maria, and Edward H. Bertram. 2012. “Temporal Lobe Epilepsy.” *Handbook of Clinical Neurology* 107 (January): 225–40. <https://doi.org/10.1016/B978-0-444-52898-8.00014-8>.
- Thurman, David J., Giancarlo Logroscino, Ettore Beghi, W. Allen Hauser, Dale C. Hesdorffer, Charles R. Newton, Fulvio Alexandre Scorza, Josemir W. Sander, and Torbjörn Tomson. 2017. “The Burden of Premature Mortality of Epilepsy in High-Income Countries: A Systematic Review from the Mortality Task Force of the International League Against Epilepsy.” *Epilepsia* 58 (1): 17–26. <https://doi.org/10.1111/epi.13604>.
- Tishler, David M., Kenneth I. Weinberg, David R. Hinton, Nicholas Barbaro, Geralyn M. Annett, and Corey Raffel. 1995. “MDR1 Gene Expression in Brain of Patients with Medically Intractable Epilepsy.” *Epilepsia* 36 (1): 1–6. <https://doi.org/10.1111/j.1528-1157.1995.tb01657.x>.
- Trinka, Eugen, Hannah Cock, Dale Hesdorffer, Andrea O. Rossetti, Ingrid E. Scheffer, Shlomo Shinnar, Simon Shorvon, and Daniel H. Lowenstein. 2015. “A Definition and Classification of Status Epilepticus - Report of the ILAE Task Force on Classification of Status Epilepticus.” *Epilepsia* 56 (10): 1515–23. <https://doi.org/10.1111/epi.13121>.
- Tuunanen, J., and A. Pitkänen. 2000. “Do Seizures Cause Neuronal Damage in Rat Amygdala Kindling?” *Epilepsy Research* 39 (2): 171–76. [https://doi.org/10.1016/S0920-1211\(99\)00123-0](https://doi.org/10.1016/S0920-1211(99)00123-0).
- Tuunanen, J., K. Lukasiuk, T. Halonen, and A. Pitkänen. 1999. “Status Epilepticus-Induced Neuronal

- Damage in the Rat Amygdaloid Complex: Distribution, Time-Course and Mechanisms.” *Neuroscience* 94 (2): 473–95. [https://doi.org/10.1016/S0306-4522\(99\)00251-1](https://doi.org/10.1016/S0306-4522(99)00251-1).
- Tuunanen, J., Toivo Halonen, and Asla Pitkänen. 1996. “Status Epilepticus Causes Selective Regional Damage and Loss of GABAergic Neurons in the Rat Amygdaloid Complex.” *European Journal of Neuroscience* 8 (12): 2711–25. <https://doi.org/10.1111/j.1460-9568.1996.tb01566.x>.
- Tuunanen, Jarkko, Toivo Halonen, and Asla Pitkänen. 1997. “Decrease in Somatostatin-Immunoreactive Neurons in the Rat Amygdaloid Complex in a Kindling Model of Temporal Lobe Epilepsy.” *Epilepsy Research* 26 (2): 315–27. [https://doi.org/10.1016/S0920-1211\(96\)00900-X](https://doi.org/10.1016/S0920-1211(96)00900-X).
- van Elst, L. T., F. G. Woermann, L. Lemieux, P. J. Thompson, and M. R. Trimble. 2000. “Affective Aggression in Patients with Temporal Lobe Epilepsy: A Quantitative MRI Study of the Amygdala.” *Brain* 123 (2): 234–43. <https://doi.org/10.1093/brain/123.2.234>.
- Vinet, Jonathan, Anna-Maria Costa, Manuel Salinas-Navarro, Giuseppina Leo, Lieve Moons, Lutgarde Arckens, and Giuseppe Biagini. 2018. “A Hydroxypyrrone-Based Inhibitor of Metalloproteinase-12 Displays Neuroprotective Properties in Both Status Epilepticus and Optic Nerve Crush Animal Models.” *International Journal of Molecular Sciences* 19 (8): 2178. <https://doi.org/10.3390/ijms19082178>.
- Vinet, Jonathan, Ilia D. Vainchtein, Carlotta Spano, Carmela Giordano, Domenico Bordini, Giulia Curia, Massimo Dominici, Hendrikus W. G. M. Boddeke, Bart J. L. Eggen, and Giuseppe Biagini. 2016. “Microglia Are Less Pro-Inflammatory than Myeloid Infiltrates in the Hippocampus of Mice Exposed to Status Epilepticus.” *Glia* 64 (8): 1350–62. <https://doi.org/10.1002/glia.23008>.
- Vliet, E A van, R van Schaik, P M Edelbroek, R A Voskuyl, S Redeker, E Aronica, W J Wadman, and J A Gorter. 2007. “Region-Specific Overexpression of P-Glycoprotein at the Blood-Brain Barrier Affects Brain Uptake of Phenytoin in Epileptic Rats.” *The Journal of Pharmacology and Experimental Therapeutics* 322 (1): 141–47. <https://doi.org/10.1124/jpet.107.121178>.
- Vliet, E. A. van, E. Aronica, A. Vezzani, and T. Ravizza. 2018. “Review: Neuroinflammatory Pathways as Treatment Targets and Biomarker Candidates in Epilepsy: Emerging Evidence from Preclinical and Clinical Studies.” *Neuropathology and Applied Neurobiology* 44 (1): 91–111. <https://doi.org/10.1111/nan.12444>.
- Vliet, E.A. van, E. Aronica, and J.A. Gorter. 2015. “Blood–Brain Barrier Dysfunction, Seizures and Epilepsy.” *Seminars in Cell & Developmental Biology* 38 (February): 26–34. <https://doi.org/10.1016/J.SEMCDB.2014.10.003>.

- Volk, Holger A., Dimitrula Arabadzisz, Jean-Marc Fritschy, Claudia Brandt, Kerstin Bethmann, and Wolfgang Löscher. 2006. "Antiepileptic Drug-Resistant Rats Differ from Drug-Responsive Rats in Hippocampal Neurodegeneration and GABAA Receptor Ligand Binding in a Model of Temporal Lobe Epilepsy." *Neurobiology of Disease* 21 (3): 633–46. <https://doi.org/10.1016/J.NBD.2005.09.006>.
- Vonderlin, Nadine, Fathima Fischer, Edgar Zitron, Claudia Seyler, Daniel Scherer, Dierk Thomas, Hugo A Katus, and Eberhard P Scholz. 2015. "Anesthetic Drug Midazolam Inhibits Cardiac Human Ether-à-Go-Go-Related Gene Channels: Mode of Action." *Drug Design, Development and Therapy* 9: 867–77. <https://doi.org/10.2147/DDDT.S72765>.
- Walker, Matthew Charles. 2015. "Hippocampal Sclerosis: Causes and Prevention." *Seminars in Neurology* 35 (3): 193–200. <https://doi.org/10.1055/s-0035-1552618>.
- Washburn, M S, and H C Moises. 1992. "Muscarinic Responses of Rat Basolateral Amygdaloid Neurons Recorded in Vitro." *The Journal of Physiology* 449 (1): 121–54. <https://doi.org/https://doi.org/10.1113/jphysiol.1992.sp019078>.
- Wiebe, Samuel, and Nathalie Jette. 2012. "Pharmacoresistance and the Role of Surgery in Difficult to Treat Epilepsy." *Nature Reviews Neurology* 8 (12): 669–77. <https://doi.org/10.1038/nrneurol.2012.181>.
- Wieser, H G. 2000. "Mesial Temporal Lobe Epilepsy versus Amygdalar Epilepsy: Late Seizure Recurrence after Initially Successful Amygdalotomy and Regained Seizure Control Following Hippocampectomy." *Epileptic Disorders : International Epilepsy Journal with Videotape* 2 (3): 141–52. <http://www.ncbi.nlm.nih.gov/pubmed/11022139>.
- Williams, Philip A., Andrew M. White, Suzanne Clark, Damien J. Ferraro, Waldemar Swiercz, Kevin J. Staley, and F. Edward Dudek. 2009. "Development of Spontaneous Recurrent Seizures after Kainate-Induced Status Epilepticus." *Journal of Neuroscience* 29 (7): 2103–12. <https://doi.org/10.1523/JNEUROSCI.0980-08.2009>.
- Woodruff, Alan R, and Pankaj Sah. 2007. "Networks of Parvalbumin-Positive Interneurons in the Basolateral Amygdala." *The Journal of Neuroscience* 27 (3): 553 LP – 563. <https://doi.org/10.1523/JNEUROSCI.3686-06.2007>.
- Woolf, Nancy J., Felix Eckenstein, and Larry L. Butcher. 1984. "Cholinergic Systems in the Rat Brain: I. Projections to the Limbic Telencephalon." *Brain Research Bulletin* 13 (6): 751–84. [https://doi.org/10.1016/0361-9230\(84\)90236-3](https://doi.org/10.1016/0361-9230(84)90236-3).
- Wouterlood, Floris G., Enrique Saldana, and Menno P. Witter. 1990. "Projection from the Nucleus Reuniens Thalami to the Hippocampal Region: Light and Electron Microscopic Tracing Study in the Rat with the Anterograde TracerPhaseolus Vulgaris-Leucoagglutinin." *The Journal of Comparative Neurology* 296 (2): 179–203. <https://doi.org/10.1002/cne.902960202>.

- Wulff, Peer, Alexey A Ponomarenko, Marlene Bartos, Tatiana M Korotkova, Elke C Fuchs, Florian Bähner, Martin Both, et al. 2009. "Hippocampal Theta Rhythm and Its Coupling with Gamma Oscillations Require Fast Inhibition onto Parvalbumin-Positive Interneurons." *Proceedings of the National Academy of Sciences of the United States of America* 106 (9): 3561–66. <https://doi.org/10.1073/pnas.0813176106>.
- Wyatt-Johnson, Season K., Seth A. Herr, and Amy L. Brewster. 2017. "Status Epilepticus Triggers Time-Dependent Alterations in Microglia Abundance and Morphological Phenotypes in the Hippocampus." *Frontiers in Neurology* 8 (DEC): 1–10. <https://doi.org/10.3389/fneur.2017.00700>.
- Xu, Songbai, Qihan Sun, Jie Fan, Yuanyuan Jiang, Wei Yang, Yifeng Cui, Zhenxiang Yu, Huiyi Jiang, and Bingjin Li. 2019. "Role of Astrocytes in Post-Traumatic Epilepsy." *Frontiers in Neurology* 10 (November): 1–10. <https://doi.org/10.3389/fneur.2019.01149>.
- Yajeya, Javier, Antonio De La Fuente, Jose M Criado, Victoria Bajo, Adela Sánchez-Riolobos, and Margarita Heredia. 2000. "Muscarinic Agonist Carbachol Depresses Excitatory Synaptic Transmission in the Rat Basolateral Amygdala in Vitro." *Synapse* 38 (2): 151–60. [https://doi.org/https://doi.org/10.1002/1098-2396\(200011\)](https://doi.org/https://doi.org/10.1002/1098-2396(200011))
- Yang, Fang, Zhi Rong Liu, Jing Chen, Shi Jun Zhang, Qing Yun Quan, Yuan Gui Huang, and Wen Jiang. 2010. "Roles of Astrocytes and Microglia in Seizure-Induced Aberrant Neurogenesis in the Hippocampus of Adult Rats." *Journal of Neuroscience Research* 88 (3): 519–29. <https://doi.org/10.1002/jnr.22224>.
- Zhang, Honghai, Haiting Zhao, Hua-Jun Jun Feng, David J. Thurman, Giancarlo Logroscino, Ettore Beghi, W. Allen Hauser, et al. 2016. "Terminal Seizure Frequency and Its Relation to SUDEP." *Epilepsia* 57 (1): 1–9. <https://doi.org/10.1016/j.yebeh.2017.02.024>.
- Zhang, Xia, Shu-Sen Cui, Amy E. Wallace, Darren K. Hannesson, Larry C. Schmued, Deborah M. Saucier, William G. Honer, and Michael E. Corcoran. 2002. "Relations between Brain Pathology and Temporal Lobe Epilepsy." *Journal of Neuroscience* 22 (14): 6052–61. <https://doi.org/10.1523/JNEUROSCI.22-14-06052.2002>.
- Zhao, Xiaofeng, Yuan Liao, Shannon Morgan, Ramkumar Mathur, Paul Feustel, Joseph Mazurkiewicz, Jiang Qian, et al. 2018. "Noninflammatory Changes of Microglia Are Sufficient to Cause Epilepsy." *Cell Reports* 22 (8): 2080–93. <https://doi.org/10.1016/j.celrep.2018.02.004>.

## **Acknowledgements**

Firstly to The Lord, who is the only one able to bring the good out from the evil.

To the Prof. Giuseppe Biagini, my advisor, for making possible this improvement.

To Dr. Chiara Lucchi and Dr. Anna Maria Costa, for the collaboration at the beginning.

To the Prof. Nikolai V. Lukoyanov, my co-advisor from the University of Porto, for his invaluable collaboration, kind patience, and wise counseling.

To the thesis reviewers, Prof. Amanda Sierra and Prof. Antonio B. Torsello for their relevant feedback.

To Dr. Joana Isa Soares, a restless worker, for the much of work made in concert.

To Dr. Liliana Carvalho, and Mrs. Anabela Costa, for the helpful suggestions, very good ideas, apart from the pleasant talks and togetherness.

To Prof. Glauce S. B. Viana, and Dr. Pedro Everson A. de Aquino for the long-standing and proficuous collaboration.

To Prof. Rodrigo Cunha and his team, from the University of Coimbra, for kindly greeting me to deepen the investigation.

To all my PhD colleagues form the XXXIII Cycle, in special to Dr. Aida Meto for the support over this journey.